DEVELOPMENT OF A GEOTECHNICAL DATABASE FOR THE CITY OF MAYAGÜEZ, PUERTO RICO

By

Carmen Y. Lugo Cintrón

A report submitted in partial fulfillment
of the requirements for the degree of

MASTER IN ENGINEERING

in

Civil Engineering

UNIVERSITY OF PUERTO RICO
MAYAGÜEZ CAMPUS
2007

Approved by:

Ricardo Ramos, Ph.D. — Date
Member, Graduate Committee

Luis E. Suárez, Ph.D. — Date
Member, Graduate Committee

Miguel A. Pando, Ph.D. — Date
President, Graduate Committee

Genock Portela, Ph.D. — Date
Representative of the Graduate School

Ismael Pagán Trinidad, M.S.C.E. — Date
Director of Civil Engineering and
Surveying Department

Abstract

This project focuses in the development of a detailed geotechnical database model of the city of Mayagüez. The database is mainly composed by data gathered from local consulting firms and government agencies as well as geophysical fieldwork performed by various researchers. The model consists of a graphical interface developed in ArcMap© 9.0. The geophysical testing data include Seismic Refraction test performed for this project, Spectral Analysis of Surface Waves (SASW) test by Pérez (2005), and Seismic Refraction and Refraction Microtremor (ReMi) test by Odum et al. (in preparation). Geophysical testing was performed in the west side of Mayagüez based on its seismic hazard vulnerability. The main purpose of the development of this database is for its use as a planning tool for structural and geotechnical engineers to identify areas where liquefaction potential or seismic hazards exist especially for new structural designs or for rehabilitation of existing facilities.

Resumen

Este proyecto está enfocado en el desarrollo de una base de datos geotécnica de la ciudad de Mayagüez. Esta se compone principalmente de información recopilada de firmas consultoras locales y agencias de gobierno así como pruebas geofísicas realizadas por varios investigadores. El modelo consiste en una interfase gráfica desarrollada en ArcMap© 9.0. Las pruebas geofísicas incluyen pruebas de Refracción Sísmica realizadas para este proyecto, pruebas de Análisis Espectral de Ondas Superficiales realizadas por Pérez (2005) y pruebas de Refracción Sísmica y Refracción de Micro-terremotos realizados por Odum et al. (en preparación). Las pruebas geofisicas fueron realizadas en el área oeste de Mayagüez basado en su vulnerabilidad a riegos sísmicos. El propósito principal para el desarrollo de esta base de datos es para su uso como herramienta de planificación para ingenieros estructurales y geotécnicos para identificar áreas donde existe potencial de licuación o riesgo sísmico, especialmente para nuevos diseños estructurales o para rehabilitación de estructuras existentes.

To my family…

Because all of you are the reason of my life and everything I do.

Acknowledgements

I would like to thanks all the members of my graduate committee, Dr. Miguel A. Pando, Dr. Luis E. Suárez and Dr. Ricardo Ramos, for all their help and support through my student career, including as an undergraduate student. Thanks to all, for all their continuous advice and encouragement through this important part of my life. All the lessons learned from you, as an engineer and as a person, will last forever.

Thanks to the USGS for giving me the opportunity of working on this research project and for the economical support. Special thanks to Mr. Jackson Odum, Mr. Robert Williams and Mr. William Stephenson from the USGS Geologic Hazard Team for their collaboration and support provided for this research project.

I would also like to thanks my friends Elvin J. Pérez, Harold J. Irizarry and Professor Eugenio Asencio for all their support during the geophysical test fieldwork. Thanks for your time, the hard work and all the advice provided.

I would like to express my gratitude to the administrator of El Maní Park and Recreational Area Mr. Jimmy Laguna, employee of the Department of Recreation and Sports of Mayagüez, for permitting the use of El Seco Park facilities for the geophysical testing. Thanks for your enthusiasm and your continuous desire to improve the quality of life of your community. Also, to the Matadero and the Abonos Super A supervisors for their support and for also allowing the use of their facilities for this research effort.

Finally, I would like to thank my family, specially my husband Wilmel, for all the love and support provided and for always being there for me whenever I needed them.

Table of Contents

List of Figures

List of Tables

CHAPTER 1 Introduction

1.1 *General Introduction*

This research project was undertaken to generate a geological and geotechnical database for the city of Mayagüez, Puerto Rico. The project attempts to address an important information gap related to the lack of adequate and sufficient information regarding the subsurface soils of the city of Mayagüez. The project also entails carrying out geophysical testing within the city of Mayagüez to further populate the geotechnical database generated as part of this research.

This chapter presents the justification of the developed research project, the objectives, a brief description of the methodology adopted to carryout the research, and a description of the organization of this report.

1.2 *Justification*

The United States (US) commonwealth of Puerto Rico has a population of about 3.8 million (2000 Census), a higher population density than any US state. The island, approximately 160 km from east to west by 50 km from north to south, is surrounded by offshore active faults as shown in Figure 1.1.

The highly seismic environment of Puerto Rico is evident from Figure 1.1. The main sources of seismic activity in the Puerto Rico region are the subduction zone to the north (Puerto Rico Trench), the subduction zone to the south (Muertos Trough), the extension zone to the east (Anegada Trough), and the extension zone to the west (Mona Canyon) (Clinton et al., 2007). All regions have been deemed capable of producing seismic events greater than M7.0, and historical records show evidence that all these seismic sources have generated such magnitude events (e.g., Asencio 1980, Moya and McCann 1992, Macari 1994).

Furthermore, the United States Geological Survey (USGS) seismic hazard maps (Mueller et al., 2004) indicate a seismic hazard similar to high seismic areas of western USA. The current standard building code in Puerto Rico, the 1997 UBC code, assigned Puerto Rico as seismic zone 3. In addition, the island of Puerto Rico has a long history of damaging earthquakes. Major earthquakes have produced damaging ground motions in

Puerto Rico in 1615, 1670, 1751, 1776, 1787 (~ M8.0 Puerto Rico Trench), 1867 (~ M7.3 Anegada Passage), and 1918 (~ M7.3 Mona Passage) (Clinton et al., 2007). Additional to the offshore seismic sources mentioned above, an inland source has recently been identified as capable of generating M7.0 events (Prentice et al., 2000; Prentice and Mann, 2005). This inland fault is identified in Figure 1.1 as SLF for the abbreviation of South Lajas Fault which is located in the south west corner of Puerto Rico.

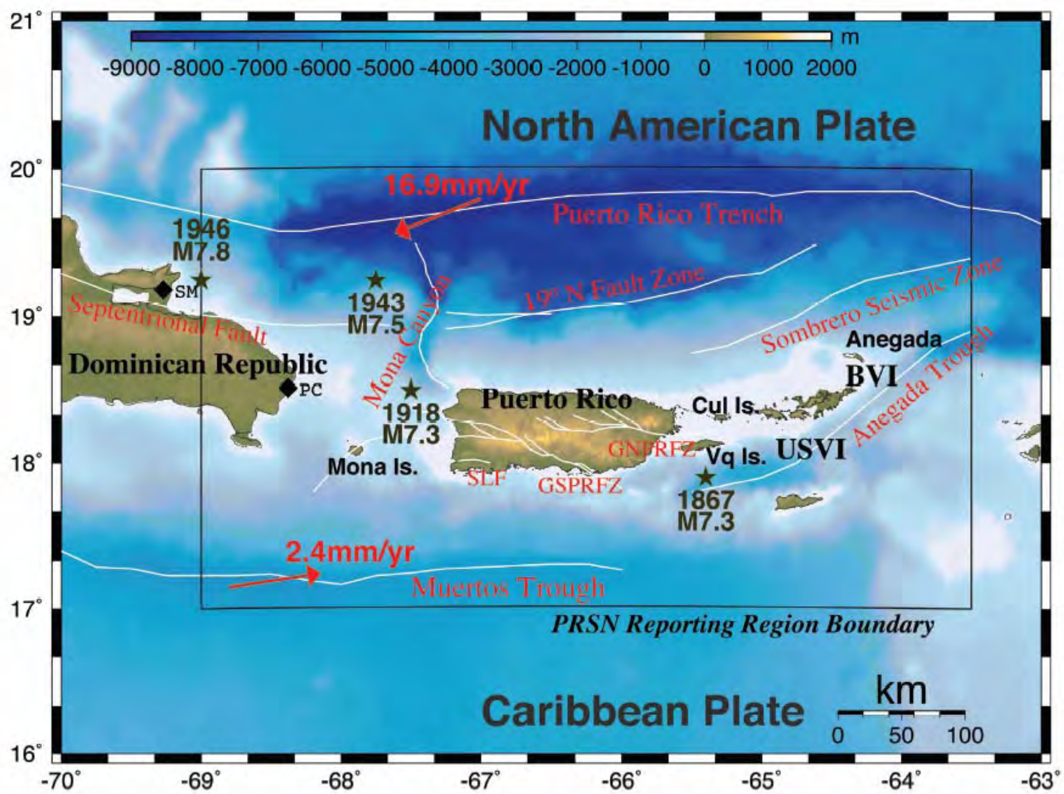

Figure 1.1 Puerto Rico Seismic Settings and Major Faults (From Clinton et. al. 2007)

For the specific area of this research, Mayagüez has been subjected to the 1918 earthquake (Reid and Taber, 1919). This event was generated by the Mona Canyon source with a M7.3 (Pacheco and Sykes, 1992). This event caused substantial structural damage, induced liquefaction near Mayagüez, generated a tsunami, caused about $4 million dollars in damage and killed 116 people (Reid and Taber, 1919; Moya and McCann, 1992; Mercado and McCann, 1998). With the Mayagüez area having a far greater density of population and infrastructure (with most of its infrastructure which has not been tested by strong seismic events since the 1918 earthquake) a similar large seismic event would likely lead to far more severe loss of life and infrastructure (Clinton et al., 2007).

Despite the high seismicity of Mayagüez and its high population density, research to adequately assess and mitigate earthquake hazard lags behind other seismically active region of the United States. Important needs include proper characterization of geotechnical/geological data of the region as well as quantification of expected ground motions. This research project attempts to address the gap of geotechnical/geological data for Mayagüez. The proposed methodology will involve the implementation of a comprehensive geotechnical database using a Geographic Information System (GIS) program.

1.3 *Objectives*

The main objective of this research project is to develop a geotechnical/geological database for the city of Mayagüez, Puerto Rico. More specific objectives of this project are:

- Gather and organize existing geotechnical, geological, geophysical, and hydrological data for the city of Mayagüez.
- Perform geophysical tests (SASW and seismic refraction) to extend the geotechnical information available for Mayagüez, P.R.
- Design and develop a comprehensive geotechnical database using a Geographic Information System (GIS) platform such as ArcView/GIS.

1.4 *General Methodology*

This research project had two main components: development of geotechnical database, and geophysical testing.

The main tasks carried out during the development of the geotechnical database were:

1) Gather existing geotechnical information from local consulting firms, government agencies, published reports and thesis, etc. To a large extent this task was carried out by Llavona (2004).
2) Develop a GIS database within ArcGIS platform. This task included geo-referencing and digitalizing all the available data. General layers were

developed for the model (e.g., topography, surficial geology, flood maps, etc.).

The geophysical testing component of this research project involved:

1) Seismic refraction surveys at six sites within Mayagüez.
2) Spectral Analyses of Surface Waves (SASW) tests at nine sites. This task was mainly carried out by Pérez (2005) as part of a MS thesis.
3) Seismic refraction and refraction microtremor (ReMi) tests at three sites. This task was mainly carried out by Odum et al. (in preparation).

More detailed description of the tasks and the methodology used is provided in the main body of this ME thesis project.

1.5 *Thesis Organization*

This report consists of six chapters: Chapter one gives a general context of the study, including the general description of study area, seismicity and earthquake threats in Puerto Rico, research objectives, and research methodology. Chapter two presents some background information regarding the methods and concepts employed in this research, for example, seismic refraction, NEHRP classification system, and liquefaction susceptibility evaluation. Chapter two also presents a literature review of the most relevant studies previously done in Mayagüez related to geotechnical/geological mapping or characterization, and pertaining seismic evaluations. Chapter three presents a general description of the Mayagüez area, e.g. seismic settings, geology, topography and ground water conditions. Information about geophysical testing performed in the Mayagüez area, including a summary of previous geophysical studies performed on the area, results obtained for this project and a comparison of results with other geophysical tests performed by Pérez (2005) and Odum et al. (in preparation) are presented in Chapter four. Chapter five deals with the generation of the geotechnical database using the program ArcView/GIS 9.0. This chapter includes a guidance section which provides basic guidelines on how to use the basic tools of the program and a brief description of the layers included in the database. Chapter six provides the conclusions resulting from this research project.

CHAPTER 2 Background and Literature Review

2.1 *Introduction*

This chapter presents general background information related to concepts and methods used in this research project. This chapter also presents a literature review of previous studies that were found to involve gathering of geotechnical, geophysical, hydrogeological, geological, and seismic data for the Mayagüez area.

2.2 *Background*

This subsection presents background information and definition for concepts and methods used in this research. The topics presented herein include: seismic refraction method, National Earthquake Hazard Research Program (NEHRP) soil profile classification system, and the general liquefaction susceptibility assessment methodology. The reader familiar with these topics may skip this sub section.

2.2.1 *Seismic Refraction Method*

This section provides a brief description of the seismic refraction methodology and the general background theory of the method. However, it does not provide detailed derivations of the refraction equations since they can be found in most geophysical textbooks (e.g. Burger, 1992 and USACE, 1995). As mentioned before, this material is for the readers who have little or no previous exposure to this geophysical method.

The seismic refraction methodology employed for the geophysical testing of this project has been widely used over the years in many civil engineering applications such as development of subsurface seismic velocity models. Seismic investigations provide the ability to acquire information about the subsurface over a substantial area in a reasonable time frame. Surface seismic methods are used as a less expensive and less invasive alternative (or complement) to traditional borehole studies. While conducting geophysical surveys for civil engineering problems at shallow depth, the higher cost of drilling as compared to geophysical work has to be balanced against the certainty and accuracy of borehole data. The borehole information for the Mayagüez area is of variable quality and in most cases does not provide enough information or lacks the required depth for liquefaction susceptibility assessment. The geophysical testing performed for this project hopes to fill this information gap.

The refraction method consists in measuring the travel times of compressional waves generated by an impulsive energy source, as shown in Figure 2.1. In the process the impulsive energy source generates waves that are detected, amplified, and recorded by sensor detectors (geophones) which are arranged following a certain configuration (see Figure 2.1). The registered data is collected by a special data acquisition equipment. The instant when the energy is released to the ground, known as "zero-time", is registered by the data acquisition device (recording equipment) and used as reference to record arriving pulses. In essence, the recorded raw data consists of travel times and distances where this time-distance information is then manipulated and processed to convert to the format of velocity variations with depth in order to develop a soil velocity profile.

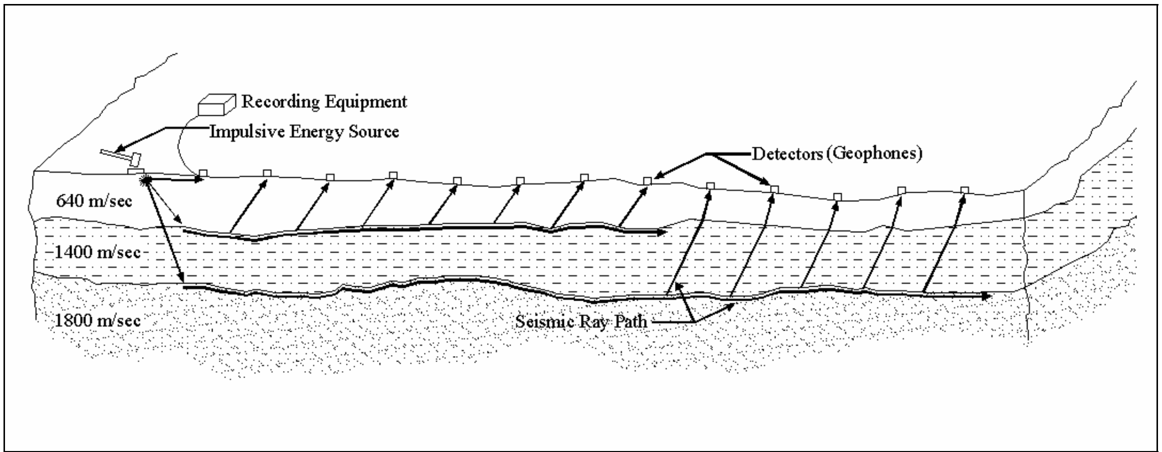

Figure 2.1 Schematic of Seismic Refraction Survey (Modified from Redpath, 1973)

As shown in Figure 2.1, all measurements are made at the surface of the ground, and the layer profiles are inferred from interpretation methods based on energy propagation laws. The propagation of seismic energy through subsurface layers is similar to the propagation of light rays through transparent media. In this method the seismic pulse is refracted or has an angular deviation when it passes from one material to another. The angular deviation depends upon the ratio of the transmission velocities of the materials. Snell's Law is the fundamental law that describes the refraction of light rays which together with the "critical incidence" phenomenon are the physical foundation of seismic refraction surveys.

The principle of Snell's Law along with the ray paths based on the critical angle of incidence is summarized in Figure 2.2. In the refraction method, the incident rays are assumed to travel from a medium with a velocity V_1 to a medium with a higher velocity V_2. The incident rays are refracted until the critical angle of incidence is reached; therefore almost all the compressional energy is transmitted into the higher velocity medium. If the critical angle of incidence is reached, it is assumed that the critically refracted ray travels along the boundary between the two media at the higher of the two velocities. As long as the ray travels along the boundary, it continually generates seismic waves in the lower-velocity layer that depart from the boundary at the angle of critical incidence. As presumed in the refraction method, if the velocities increase with depth, a portion of the energy will eventually be reflected back to the surface where it can be detected. On the other hand, if the critical angle of incidence is exceeded the energy does not refract into the high-speed layer instead the total energy is reflected.

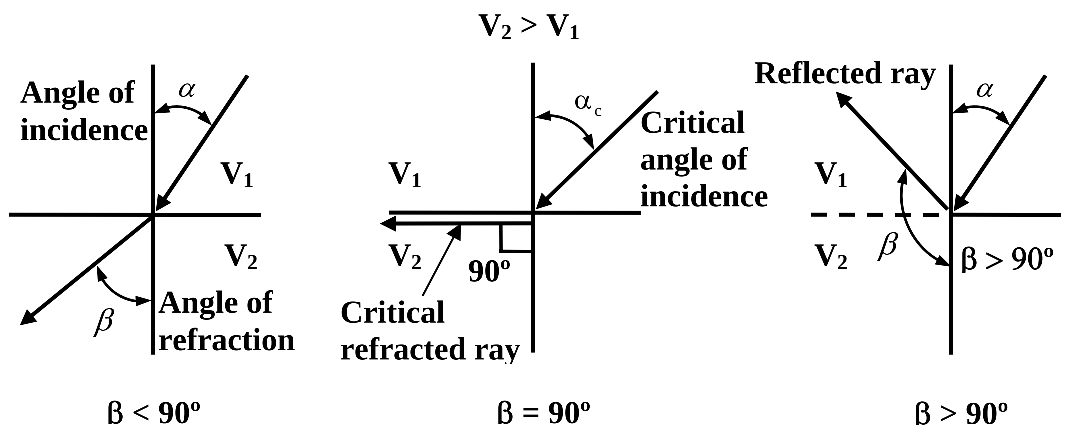

Snell's Law : $\dfrac{\sin\alpha}{\sin\beta} = \dfrac{V_1}{V_2}$

Critical incidence occurs when $\beta = \mathbf{90}^\circ, \therefore \sin\alpha_c = \dfrac{V_1}{V_2}$

Figure 2.2 Refracted and Reflected Compressional Waves as Function of Angle of Incidence.

The seismic refraction methodology is typically suitable for determining depth to the water table or bedrock surface. It is usually not considered suitable for obtaining detailed subsurface characterization or structure. There are two major potential limitations with this method: the phenomenon of "blind zone" and velocity reversal.

The blind zone phenomenon occurs when the refraction seismograph is not able to detect the existences of certain layers because of insufficient velocity contrast or layer thickness. As stated by Soske (1959) this represents a major problem in seismic refraction because it cannot be easily remedied by changing the layout of the detectors (geophones) but can be overcome by changing the impulsive energy source (e.g., energy level). However, this would normally be attempted when the existence of an intermediate layer is known beforehand, usually from other sources of information, such as boreholes. The error associated with the presence of a blind zone is lower computed depths than the true depths.

The velocity reversal issue can occur because of the presence of either a low-velocity layer or a high-velocity layer. In either case, the problem is related to having velocities not increasing progressively with depth and having at some point in the velocity profile a marked decrease due to the presence of a relatively lower velocity layer. Refractions from this layer cannot be detected at the surface; therefore, the existence of this layer cannot be determined from the recorded time-distance curve. As in the blind zone phenomenon the presence of a low-velocity layer will go undetected unless additional information is available, such as boreholes. In contrast to the blind zone, the effect of a low-velocity layer (velocity reversal) is to make the computed depths greater than the actual depths.

2.2.2 *NEHRP Soil Profile Classification System*

Information about this soil classification system is presented because it is commonly used in practice for routine seismic assessments of structures designed following the Uniform Building Code provisions (UBC, 1997). Detailed seismic studies usually depart from this simplified soil profile classification system. Nevertheless, given the scope of this research it is useful to present the basic information regarding the classification system proposed by NEHRP (National Earthquake Hazard Research Program).

The 2000 NEHRP Recommended Provisions for Seismic Regulation for Buildings and Other Structures (NEHRP, 2000) are currently the basis for most earthquake resistant design in the U.S. (Pérez, 2005). They provide criteria for the design and construction of structures to resist earthquake ground motions with the main purposes of:

- Provide minimum design criteria for structures appropriate to their primary function and use considering the need to protect the health, safety, and welfare of the general public by minimizing the earthquake-related risk to life.
- To improve the capability of essential facilities and structures containing substantial quantities of hazardous materials to function during and after design earthquakes.

The NEHRP provisions incorporate local soil site effects in the design of seismic ground motions by means of site amplification factors. These factors are also used in the current UBC provisions (UBC, 1997). The NEHRP or UBC site amplification factors are usually selected based on the site classification system of the project. The site classification system is based on definitions of five site classes which are determined only on the basis of the soil characteristics of the top 30 m. Current provisions disregard soil or rock properties below 30 m. However, this methodology is usually only used for seismic design of non-critical structures. As shown in Table 2.1 the site classification is determined based on the representative average shear-wave velocity (Vs) to a depth of 30 m. This shear wave velocity is not calculated as an arithmetic average of values of Vs down to 30 m, but rather a time-averaged shear-wave velocity to a depth of 30 m, which is obtained by dividing the 30 m length by the travel time calculated using the actual shear wave velocity profile of the 30 m profile. The expression for obtaining the time-averaged shear wave velocity is as follows:

$$\overline{Vs}_{30} = \frac{30}{\sum_{i=1}^{n} \frac{d_i}{Vs_i}} \qquad \textbf{Eq. 2-1}$$

Where:

d_i = thickness (in meters) of layer *i*.

Vs_i = shear-wave velocity (in m/s) of layer *i*.

n = number of layers within the upper 30 meters of site.

As indicated in Table 2.1 there are some exceptions to this equation. For example, a profile with more than 3 m of soft clay is classified as Site Class E, regardless of the average shear-wave velocity of the top 30 m. This modification reflects the importance given to the presence of soft soils within a site, regardless of whether competent soil or rock is encountered within the upper 30 meters.

Table 2.1 NEHRP Soil Profile Classification (adapted from UBC 1997)

Soil Type	Soil Profile Description
A	Hard rock with measured shear wave velocity $v_s > 5{,}000\,ft/s\ (1{,}500m/s)$
B	Rock with shear wave velocity $2{,}500 < v_s \le 5{,}000\ ft/s\ (760 < v_s \le 1{,}500\ m/s)$
C	Very dense soil and soft rock with shear wave velocity $1{,}200 < v_s \le 2{,}500\,ft/s$ $(360 < v_s \le 760m/s)$ or with either standard penetration resistance $N > 50$ or undrained shear strength $S_u \ge 2{,}000\,psf\ (100kPa)$
D	Stiff soil with shear wave velocity $600 < v_s \le 1{,}200\,ft/s\ (180 < v_s \le 360m/s)$ or with either standard penetration resistance $15 \le N \le 50$, or undrained shear strength $1{,}000 \le S_u < 2{,}000\,psf\ (50 \le S_u < 100kPa)$
E	A soil profile with shear wave velocity $v_s < 600\,ft/s\ (180m/s)$ or any profile with more than $10\,ft\ (3m)$ of soft clay, defined as soil with plasticity index $PI > 20$, water content $w \ge 40$ percent and undrained shear strength $S_u < 500\,psf\ (25kPa)$
F	Soils requiring site-specific evaluation: 1. Soils vulnerable to potential failure or collapse under seismic loading; i.e., liquefiable soils, quick and highly sensitive clays, collapsible weakly cemented soils 2. Peat and/or highly organic clay layers more than $10\,ft\ (3m)$ thick 3. Very high-plasticity clay $(PI > 75)$ layers more than $25\,ft\ (8m)$ thick 4. Soft to medium clay layers more than $120\,ft\ (36m)$ thick

The NEHRP site class can also be determined based on a representative average of the Standard Penetration Test (SPT) blow counts obtained at the site. Details on the determination of the NEHRP site class using SPT blow counts can be found in the UBC (1997).

2.2.3 *Liquefaction Susceptibility Assessment*

2.2.3.1 Introduction

The geotechnical database developed in this research project also includes liquefaction susceptibility maps originally developed by Llavona (2004) and updated to some extent in this research project. This section provides definitions and background information relevant to the methodology used to generate these liquefaction maps. The reader familiar with this subject matter may wish to skip this section.

2.2.3.2 General Considerations for Liquefaction Assessment

Soil liquefaction is commonly associated to the significant loss of strength experienced in saturated sandy or cohesionless soils due to the increase of pore water pressures generated during large earthquakes. Sladen et al. (1985) define soil liquefaction in a more precise and general way as follows:

> "Liquefaction is a phenomenon wherein a mass of soil loses a large percentage of its shear resistance, when subjected to monotonic, cyclic, or shock loading, and flows in a manner resembling a liquid until the shear stresses acting on the mass are as low as the reduced shear resistance."

Liquefaction is most commonly observed in shallow, loose, saturated deposits of cohesionless soils when subjected to large magnitude earthquakes. The National Research Council (NRC, 1985) lists the following modes of ground failure associated to liquefaction:

- Sand boils, which usually result in subsidence and relatively minor damage.
- Flow failures of slopes involving very large down-slope movements of a soil mass.
- Lateral spreads resulting from the lateral displacements of gently sloping ground.
- Ground oscillation where liquefaction of a soil deposit beneath a level site leads to back and forth movements of intact blocks of surface soil.
- Loss of bearing capacity causing foundation failures.
- Buoyant rise of buried structures such as tanks.
- Ground settlement, often associated with some other failure mechanism.
- Failure of retaining walls due to increased lateral loads from liquefied backfill soil or loss of support from liquefied foundation soils.

Earthquake-induced liquefaction is most commonly observed in (but not restricted to) the following types of soils: fluvial-alluvial deposits, eolian sands and silts, beach sands, reclaimed land and uncompacted hydraulic fills (Koester, 2000).

Preliminary qualitative liquefaction assessments may often be made to determine whether a given site is clearly likely or not likely to liquefy due to earthquake shaking. This can be based on previous occurrence of liquefaction in site soils, knowledge of embankment placement techniques that have historically performed well or poorly when shaken, the seismicity of the site and degree of saturation are some of the factors that may indicate the potential for future liquefaction (Koester, 2000). The following information is considered essential to perform an initial assessment of the liquefaction potential of a site (Koester, 2000):

- Site topography.
- At any site, minimally, a detailed soil profile, including classification of soil properties and the origin of soils at the site in question.
- Water level records, representative of both current and historical fluctuations.
- Evidence from project records, aerial photographs, or previous investigations of past ground failure at the site or at similar (geological and seismological) nearby areas (including historical records of liquefaction, topographical evidence of landslides, sand boils, effects of ground movement on trees and other vegetation, subsidence, and sand intrusions in the subsurface).
- Seismic history of the site.
- Geologic history of the site, including age and mode of deposition of site soils, glacial preconsolidation or preconsolidation by now-eroded overburden, and lateral extent and continuity of soil deposits.

One important factor that should be considered on the initial liquefaction potential evaluation is the presence of saturated soil. Sites may be considered to pose no potential liquefaction hazard if it can be demonstrated that any potentially liquefiable soil types present at a site are currently unsaturated (above the water table), have not previously been saturated (above the historic high water table), and cannot reasonably be expected to become saturated (Koester, 2000). Table 2.2 summarizes historical data relating water table depth to liquefaction susceptibility presented by Youd (1998). It is important to emphasize that changes in local or regional water patterns, can significantly raise water table elevations. Extrapolation of data regarding water table elevations from adjacent sites will not, by itself, usually suffice to demonstrate the absence of liquefaction hazard in the absence of additional supporting data (Koester, 2000).

Table 2.2 Relative Liquefaction Susceptibility of Natural Deposits as a Function of Groundwater Table Depth (Modified from Youd, 1998)

Ground Water Table	Relative Liquefaction Susceptibility
< 3m (<9.8 ft)	Very High
3m to 6m (9.8 ft to 19.7 ft)	High
6m to 10 m (19.7 ft to 32.8 ft)	Moderate
10 m to 15 m (32.8 ft to 49.2 ft)	Low
> 15 m (> 49.2 ft)	Very Low

Youd and Perkins (1978) provide guidelines to estimate liquefaction resistance based on geologic age, depositional environment, and prior seismic history. These authors found that most liquefaction risk is associated with recent Holocene deposits and uncompacted fills, as progressively older units tend to have progressively higher resistance to liquefaction. Table 2.3 presents a summary of the liquefaction susceptibility assessment provided by Youd and Perkins (1978).

Table 2.3 Estimated Susceptibility of Sedimentary Deposits to Liquefaction During Strong Seismic Shaking based on Geological Age and Depositional Environment (After Youd and Perkins 1978)

		Likelihood that Cohesionless Sediments, When Saturated, Would Be Susceptible to Liquefaction (by Age of Deposit)			
Type of Deposit	**General Distribution of Cohesionless Sediments in Deposits**	**< 500 yr**	**Holocene**	**Pleistocene**	**Pre-Pleistocene**
(a) Continental Deposits					
River channel	Locally variable	Very high	High	Low	Very low
Flood plain	Locally variable	High	Moderate	Low	Very low
Alluvial fan and plain	Widespread	Moderate	Low	Low	Very low
Marine terraces and plains	Widespread	-	Low	Very low	Very low
Delta and fan-delta	Widespread	High	Moderate	Low	Very low
Lacustrine and playa	Variable	High	Moderate	Low	Very low

Table 2.3 Continued					
Colluvium	Variable	High	Moderate	Low	Very low
Talus	Widespread	Low	Low	Very low	Very low
Dunes	Widespread	High	Moderate	Low	Very low
Loess	Variable	High	High	High	Unknown
Glacial till	Variable	Low	Low	Very low	Very low
Tuff	Rare	Low	Low	Very low	Very low
Tephra	Widespread	High	High	?	?
Residual soils	Rare	Low	Low	Very low	Very low
Sebka	Locally variable	High	Moderate	Low	Very low
(b) Coastal Zone					
Delta	Widespread	Very high	High	Low	Very low
Esturine	Locally variable	High	Moderate	Low	Very low
Beach					
High wave energy	Widespread	Moderate	Low	Very low	Very low
Low wave energy	Widespread	High	Moderate	Low	Very low
Lagoonal	Locally variable	High	Moderate	Low	Very low
Fore shore	Locally variable	High	Moderate	Low	Very low
(c) Artificial					
Uncompacted fill	Variable	Very high	-	-	-
Compacted fill	Variable	Low	-	-	-

2.2.3.3 *Quantitative Liquefaction Susceptibility Assessment*

If preliminary qualitative site evaluations indicate likelihood of liquefaction then the resistance of these soils to liquefaction should be evaluated. This subsection provides a summary of the so-called “Revised Simplified Liquefaction Procedure” proposed by Youd et al. (2001). This method is well documented and is commonly used in practice for evaluation of liquefaction potential.

The Revised Simplified Procedure was developed from empirical evaluations of field observations and field and laboratory test data. Data were collected mostly from sites on level to gently sloping terrain, underlain by Holocene alluvial or fluvial sediment at shallow depths (<15 m) as cited by Youd et al. (2001).

On this approach, the liquefaction susceptibility at a site is expressed in terms of a factor of safety (*FS*) against the occurrence of liquefaction. This factor is defined as the ratio between available soil resistance to liquefaction, expressed in terms of the cyclic stresses required to cause soil liquefaction (abbreviated *CRR* for cyclic resistance ratio) and the cyclic stresses generated by the design earthquake (abbreviated *CSR* for cyclic stress ratio). Additional correction factors are applied to the *CRR* ratio, like the Magnitude Scaling Factor (*MSF*), the correction factor to account for confinement stresses (K_σ) and for sloping ground (K_α). The resulting equation for the factor of safety against liquefaction after combining all these factors is the following:

$$FS = \frac{Available\,Soil\,Resistance}{Earthquake\,Induced\,Stresses} = \left(\frac{CRR_{7.5}}{CSR}\right) \times MSF \times K_\sigma \times K_\alpha \qquad \textbf{Eq. 2-2}$$

The *CSR* and *CRR* are computed as follows:

<u>Calculation of Earthquake Induced Stresses or Cyclic Stress Ratio (*CSR*)</u>:

Seed and Idriss (1971) formulated the following simplified equation for estimation of *CSR*:

$$CSR = \left(\frac{\tau_{cyc}}{\sigma'_{vo}}\right) = 0.65 \times \frac{a_{\max}}{g} \times \frac{\sigma_{vo}}{\sigma'_{vo}} \times r_d \qquad \textbf{Eq. 2-3}$$

Where:

τ_{cyc} = equivalent cyclic shear stress
$a_{\max}$ = peak horizontal acceleration at the ground surface generated by the earthquake
g = acceleration of gravity
σ_{vo} = total vertical overburden stress
σ'_{vo} = effective vertical overburden stress
r_d = stress reduction coefficient which accounts for flexibility of the soil profile

To calculate the cyclic stress ratio the estimation of the peak horizontal acceleration, which is used to characterize the intensity of the ground shaking, is required. For the Simplified Procedure, Youd et al. (2001) recommend the following methods for estimating $a_{\max}$, in order of preference:

- Based on empirical correlations of $a_{\max}$ with earthquake magnitude, distance from the seismic energy source, and local site conditions. Selection of an attenuation relationship should be based on such factors as region of the country, type of faulting, and site condition.

- a_{max} may be estimated from local site response analyses using computer programs like SHAKE or QUAD4. This method requires input ground motions in the form of recorded accelerograms or synthetic records.
- The use of amplification factors. These factors use a multiplier or ratio by which bedrock outcrop motions are amplified to estimate surface motions at soil sites.

As the liquefaction evaluation for this project is a continuation and extension of the work done by Llavona (2004) the methodology and the values used for design variables were kept the same. Llavona (2004) used the third method for estimating a_{max} due to the lack of available information for the city of Mayagüez. Furthermore, his project was part of a study funded by the Puerto Rico Insurance Commissioner which required a recurrence period of 250 years. Therefore, for his study he estimated the peak horizontal acceleration based on recommendations provided by Mueller et al. (2003) and a design earthquake magnitude of M = 7.0 which was also recommended by Mueller et al. (2003). Llavona (2004) selected a_{max} for Mayagüez based on the seismic hazard curves shown in Figure 2.3. These curves were provided by Mueller et al. (2003) for the Mayagüez area which considered the different seismic zones affecting the region of Mayagüez. The resulting a_{max} for a 250 years recurrence period (Exceedance/Years = 0.004) obtained using the curve titled “all modeled sources” which represents the probabilistic contribution of each of the modeled sources. The resulting value for peak ground acceleration, corresponding to a rock site, for Mayagüez from this curve is 0.2g.

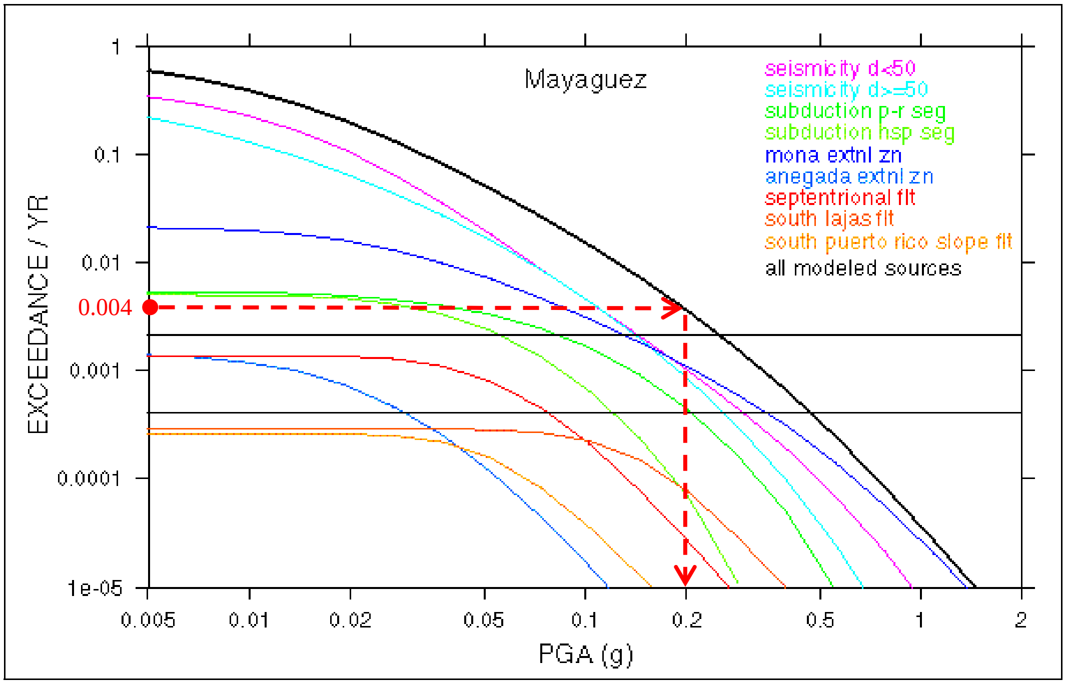

Figure 2.3 PGA Hazard Curves for Mayagüez (from Mueller et al., 2003)

Once the peak ground acceleration (PGA) on rock was determined the peak ground acceleration on the ground surface (a_{max}) for a soil site was calculated using the appropriate NEHRP (or UBC97) amplification factor. The amplification factor can be estimated as the ratio of seismic coefficients (Ca) recommended by UBC 97. The value of Ca will depend on the soil type as shown in Table 2.4. These seismic coefficients are equivalent to the effective maximum acceleration on the surface ground, depending on the soil type and the seismic zone factor (Z) which is equivalent to the peak ground acceleration on the rock, which in this case was determined to be 0.2.

Table 2.4 Seismic Coefficients (Ca) According to UBC 97

Soil Type	**Seismic Zone Factor, Ca**				
	Z=0.075	**Z=0.15**	**Z=0.2**	**Z=0.3**	**Z=0.4**
S_A	0.06	0.12	0.16	0.24	0.32Na
S_B	0.08	0.15	0.20	0.30	0.40Na
S_C	0.09	0.18	0.24	0.33	0.40Na
S_D	0.12	0.22	0.28	0.36	0.44Na
S_E	0.19	0.30	0.34	0.36	0.36Na
S_F	Specific geotechnical investigations and dynamic analysis required				

The next parameter that needs to be determined is the stress reduction coefficient (r_d). Youd et al. (2001) recommended the following equations:

$$r_d = 1.0 - 0.00765 \times z \qquad \text{For } z \leq 9.15 \text{ m} \qquad \textbf{Eq. 2-4}$$

$$r_d = 1.174 - 0.0267 \times z \qquad \text{For } 9.15 \text{ m} < z < 23 \text{ m} \qquad \textbf{Eq. 2-5}$$

Where:
z = depth below ground surface in meters

Calculation of Available Soil Resistance or Cyclic Resistance Ratio ($CRR_{7.5}$):

The method based on the SPT value, presented by Youd et al. (2001), is commonly used to determine the available soil resistance to liquefaction. This method is described because it was the one used by Llavona (2004). *CRR* values are based on the analysis of historic cases of sites impacted by earthquakes with magnitudes of 7.5 or close to 7.5. For these sites the corresponding cyclic stress ratio (*CSR*) was calculated. Knowing the *CSR* values that induced liquefaction and the Standard Penetration Test (SPT) data at the site graphs were generated relating SPT $(N_1)_{60}$ versus *CSR* as shown in Figure 2.4. In this plot, $(N_1)_{60}$ is defined as the SPT blow count normalized to an overburden pressure of approximately 100 kPa (1 ton/sq ft) and a hammer energy ratio or hammer efficiency of 60%. Figure 2.4 shows curves for sites with sands having fines contents of 5% or less, 15%, and 35%. As the *CRR* curves in the graph are valid only for magnitude 7.5 earthquakes, magnitude scaling factors have to be used to adjust *CRR* values to other earthquake magnitudes.

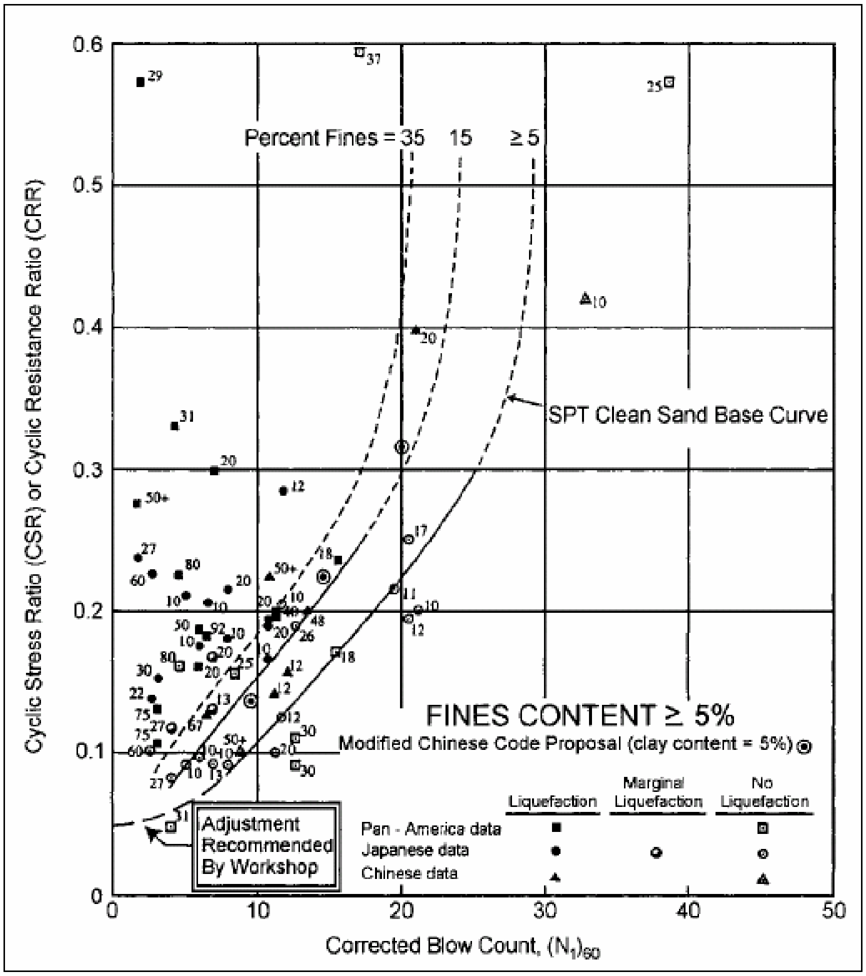

Figure 2.4 Youd et al. Recommended Graphs to Obtain $CRR_{7.5}$ depending on Fines Content (From Youd et al., 2001)

Equation 2-6 is the approximation obtained to estimate the $CRR_{7.5}$ for the 5% fines content curve, also known as Simplified Base Curve. This equation is valid for $(N_1)_{60} < 30$. If $(N_1)_{60} > 30$, clean granular soils are considered too dense to liquefy and are classed as non-liquefiable.

$$\mathrm{CRR}_{7.5} = \frac{\mathbf{1}}{\mathbf{34} - (\mathrm{N}_1)_{60}} + \frac{(\mathrm{N}_1)_{60}}{\mathbf{135}} + \frac{\mathbf{50}}{[\mathbf{10} \cdot (\mathrm{N}_1)_{60} + \mathbf{45}]^2} - \frac{\mathbf{1}}{\mathbf{200}} \qquad \textbf{Eq. 2-6}$$

The SPT $(N_1)_{60}$ can be calculated using the following expression:

$$(N_1)_{60} = N_m \cdot C_N \cdot C_E \cdot C_B \cdot C_R \cdot C_S \qquad \textbf{Eq. 2-7}$$

Where:

N_m = measured standard penetration resistance (SPT-N)
C_N = normalize N_m to a common reference effective overburden stress (1 atm)
C_E = correction for hammer energy ratio (ER) (normalized to 60% of theoretical SPT energy
C_B = correction factor for borehole diameter
C_R = correction factor for rod length
C_S = correction for samplers with or without liners

Table 2.5 provides the values for each of the correction factors.

Table 2.5 $(N_1)_{60}$ Correction Factors (From Youd et al. 2001)

Correction Factor	Equipment Variable	Term	Correction
Overburden pressure	----	C_N	$(P_a/\sigma'_{vo})^{0.5}$
Overburden pressure	----	C_N	$C_N \leq 1.7$
Energy ratio	Donut Hammer	C_E	0.5 – 1.0
Energy ratio	Safety Hammer	C_E	0.7 – 1.2
Energy ratio	Automatic-trip Donut-type Hammer	C_E	0.8 – 1.3
Borehole diameter	65 – 115 mm	C_B	1.0
Borehole diameter	150 mm	C_B	1.05
Borehole diameter	200 mm	C_B	1.15
Rod length	<3 m	C_R	0.75
Rod length	3 – 4 m	C_R	0.80
Rod length	4 – 6 m	C_R	0.85
Rod length	6 – 10 m	C_R	0.95
Rod length	10 – 30 m	C_R	1.0
Sampling method	Standard Sampler	C_S	1.0
Sampling method	Sampler without liner	C_S	1.1 – 1.3

The $(N_1)_{60}$ of a certain site can also be converted to an equivalent $(N_1)_{60}$ of a clean sand condition $[(N_1)_{60cs}]$ as follows:

$$(N_1)_{60cs} = \alpha + \beta (N_1)_{60} \qquad \textbf{Eq. 2-8}$$

Where α and β are coefficients that depend on the fines content and are determined from the following relationships:

$$\alpha = 0 \qquad for\ FC \leq 5\% \qquad \textbf{Eq. 2-9}$$

$$\alpha = \exp\left[1.76 - (190/FC^2)\right] \qquad for\ 5\% < FC < 35\% \qquad \textbf{Eq. 2-10}$$

$\alpha = 5$ $for\ FC \leq 35\%$ **Eq. 2-11**

$\beta = 1.0$ $for\ FC \leq 5\%$ **Eq. 2-12**

$\beta = \left[0.99 + \left(FC^{1.5} / 1000\right)\right]$ $for\ 5\% < FC < 35\%$ **Eq. 2-13**

$\beta = 1.2$ $for\ FC \leq 35\%$ **Eq. 2-14**

Where:
FC = fines content (% of particles smaller than 75 microns)

In the absence of grain size tests, the fines content can be estimated based on the ASTM D422 guidelines for visual description of soils shown in Table 2.6.

Table 2.6 Fines Content based on the Visual Classification of ASTM D422

Soil Description	*FC* (%)
silt or clay	> 35 %
and silt or and clay	> 35 %
silty or clayey	20 % - 35 %
some silt or some clay	10 % - 20 %
trace of silts, trace of clays	1 % - 10 %

<u>Calculation of Magnitude Scaling Factor (MSF)</u>:

As mentioned before, the *CRR* values obtained from Figure 2.4 correspond to magnitude 7.5 earthquakes ($CRR_{7.5}$). To obtain the *CRR* for other earthquake magnitudes, the *CRR* values from Figure 2.4 must be adjusted using a Magnitude Scaling Factor (*MSF*). The *MSF* is directly applied to the Factor of Safety Equation (Eq. 2-2). For this project, the *MSF* values used were based on recommendations provided by Youd et al. (2001), as follows:

$$MSF_{ave} = \frac{MSF_{Andrus-Stokoe} + MSF_{Idriss}}{2} \quad For\ MSF \leq 7.5 \qquad \textbf{Eq. 2-15}$$

$$MSF_{ave} = MSF_{Idriss} \quad For\ MSF > 7.5 \qquad \textbf{Eq. 2-16}$$

Where:

$$MSF_{Andrus-Stokoe} = \left[\frac{M_w}{7.5}\right]^{-3.3} \quad \textbf{Eq. 2-17}$$

$$MSF_{Idriss} = \frac{10^{2.24}}{M_w^{\ 2.56}} \quad \textbf{Eq. 2-18}$$

<u>Correction for Confining Stresses (K_σ) and Sloping Ground (K_α):</u>

Although correction factors for confining stresses (K_σ) and sloping ground (K_α) are suggested (e.g. Seed 1983), for this project these were not considered given that most potentially liquefiable areas in Mayagüez are in coastal deposits with relatively horizontal ground conditions. For simplicity K_σ and K_α were not considered in this preliminary screening.

<u>Liquefaction Potential Index (LPI):</u>

After using the simplified procedure to calculate the factor of safety to liquefaction at different depths for a soil profile, it is necessary to obtain or assign a value which can be representative of the total liquefaction potential for the site. For this purpose, the Liquefaction Potential Index (LPI) method proposed by Iwasaki et al. (1982) was used.

The Liquefaction Potential Index is a parameter for prediction of occurrence of liquefaction. The LPI value is proportional to the thickness and the factor of safety explained previously. The LPI uses a depth weighting factor function to assign more weight to liquefiable layers present at shallow depths compared to deep layers. This way a site will have a higher index if liquefiable layers are near the surface and not penalize unnecessarily a site if there is only a thin liquefiable layer at a considerable depth. Iwasaki et al. (1982) concluded that when the LPI of a site was greater than 15, severe liquefaction was likely to occur. For LPI<5 no evidence of liquefaction was observed. Table 2.7 presents the estimated damage as a function of the LPI value obtained for the site.

Table 2.7 Level of Damage as a Function of the LPI Value (Iwasaki et al., 1982)

LPI	Liquefaction Potential	Estimated Damage
0	Extremely low	No Damage
0 - 5	Low	Minor Damage
5 - 15	Moderate	Moderate Damage
> 15	High	Mayor Damage

The LPI index is computed using the following equations:

$$LPI = \int_0^z F * w(z)dz \qquad \textbf{Eq. 2-19}$$

$$F = 1 - FS \qquad For FS \leq 1 \qquad \textbf{Eq. 2-20}$$

$$F = 0 \qquad For FS > 1 \qquad \textbf{Eq. 2-21}$$

$$w(z) = 10 - 0.5 * z \qquad \textbf{Eq. 2-22}$$

Where:

FS = safety factor calculated using the simplified procedure
z = depth in meters
w(z) = depth weighting factor, which assigns more importance to safety factors of layers closer to the surface and also establish the limit depth for the application of the LPI method to 20 meters

To perform the Liquefaction Potential Index analyses the program LicuadoPR developed by Sosa and Pando (2004) was used. This program was developed for the Puerto Rico Strong Motion Program of the Civil Engineering Department of the University of Puerto Rico, Mayagüez Campus. The program is based on the Simplified Procedure discussed previously. Some of the information required to be input to the program is the following: maximum acceleration at the ground surface, earthquake magnitude, information of the equipment used to perform the SPT test (borehole diameter, sampling method, hammer type and hammer efficiency), and the information of the soil profile obtained from the SPT test, like depth of profile, blow counts for each layer, unit weight of the soils, fines content, and description of the soil. More details can be found in Sosa and Pando (2004).

2.3 *Literature Review*

This subsection presents a summary of the most relevant studies previously done for Mayagüez related to mapping or characterization (geotechnical, geological, geophysical, hydrogeological, liquefaction, etc.) or pertaining seismic evaluations.

2.3.1 *Reid and Taber 1919*

Reid and Taber (1919) performed a detailed study of the effects of the 1918 earthquake to the islands of Puerto Rico, Vieques, and St. Thomas. They described the island of Puerto Rico as extremely mountainous, with no large areas of flat land and with narrow alluvial plains in places along the coasts which extend for several miles up the larger valleys. The October 11, 1918 Earthquake was estimated to be approximately 15 km off the coast of the Aguadilla-Mayagüez Region. Reid and Taber (1919) described the earthquake as beginning with a pronounced vertical vibration, which was followed by horizontal oscillations. A tsunami created by the earthquake hit the western portion of Puerto Rico soon after the shaking had ceased. Mayagüez, having a population of 17,000 at the time of the quake, received an intensity of shock VIII and IX on the revised Rossi-Forel scale (Reid and Taber 1919).

On their report they mentioned that the apparent intensity was always greater on the alluvial soils than at corresponding points on rock or residual soil, and this effect was most noticeable on alluvial soils where the ground water stood close to the surface. As the city of Mayagüez is mostly built on alluvial soils, which in some places are saturated with water, this was believed to be one of the main factors that contributed to the large property damage and loss of life. Damage to Mayagüez described by Reid and Taber (1919) included severe cracking in brick, masonry, and concrete structures. Much of the infrastructure; including bridges, railroad lines, pipelines, and utility cables; were damaged in the Mayagüez area and throughout Puerto Rico.

2.3.2 *McCann 1986*

In 1986 McCann studied all the sources of earthquake activity for western Puerto Rico and estimated the recurrence intervals of earthquakes having shock intensities greater than VII in the Modified Mercalli Intensity (MMI) for each of the sources. He found that most of the recurrence periods are between 29 to 68 years for the MMI of VII and that there is a high probability that a major earthquake (MMI > VII) will occur in

Puerto Rico in the near future because he defined that the period of recurrence for such events is, on average, as frequently as the great earthquakes in the Puerto Rico Trench. Thus, he concluded that the main earthquake hazard on the Mayagüez area come not from great earthquakes to the north of the island, but rather from major earthquakes occurring closer to the area.

2.3.3 *Moya et al. 1992*

Moya et al. (1992) studied the seismic vulnerability of the Mayagüez area. They found that three major earthquake sources must be taken in consideration when designing near the Mayagüez area. These sources are the Puerto Rico Trench, the Mona Canyon and the Mayagüez or Cordillera Fault. In addition to this, they employed a methodology that classify the sites according to the geologic characteristics of the materials (like kind of rock or sediment and age) to estimate the level of earthquake susceptibility. Table 2.8 presents the different classification zones they defined associated with their respective amplification, liquefaction potential, and potential for soil failure. The location of different zones can be observed on Figure 2.5. They also estimated that the tsunami threat in Mayagüez is limited to the coastal area within 300 to 400 meters of the coast and elevations 2 to 6 meters above sea level. They concluded that the coastal zone of Mayagüez is the most prone to suffer severely during a major earthquake.

Table 2.8 Zone Classification of the Mayagüez Area based on Geological Aspects Associated to Seismic Susceptibility (Moya and McCann, 1992).

Zone	Soil Amplification	Liquefaction Potential	Soil Failure Potential
A - 1	Non Significant	Low	Very Low
A - 2	Non Significant	Low - Moderate	Low
A - 3	Non Significant - Low	Moderate - High	High - Where materials are not laterally confined and have moderate slope
A - 3 - S	High	High - On soil deposits covered by sand	High - On soil deposits covered by sand
B - 1	Non Significant	None	Very low
B - 2	Moderate - Very High	High - Where materials are not laterally confined	High - Along rivers Lateral Slide

Table 2.8 Continued			
B - 3	High	High - Especially on loose sand deposits	High - Lateral Slide
C - 1	Non Significant	None	Low
C - 2	Non Significant	None	Moderate - High
C - 3	Non Significant	None	High

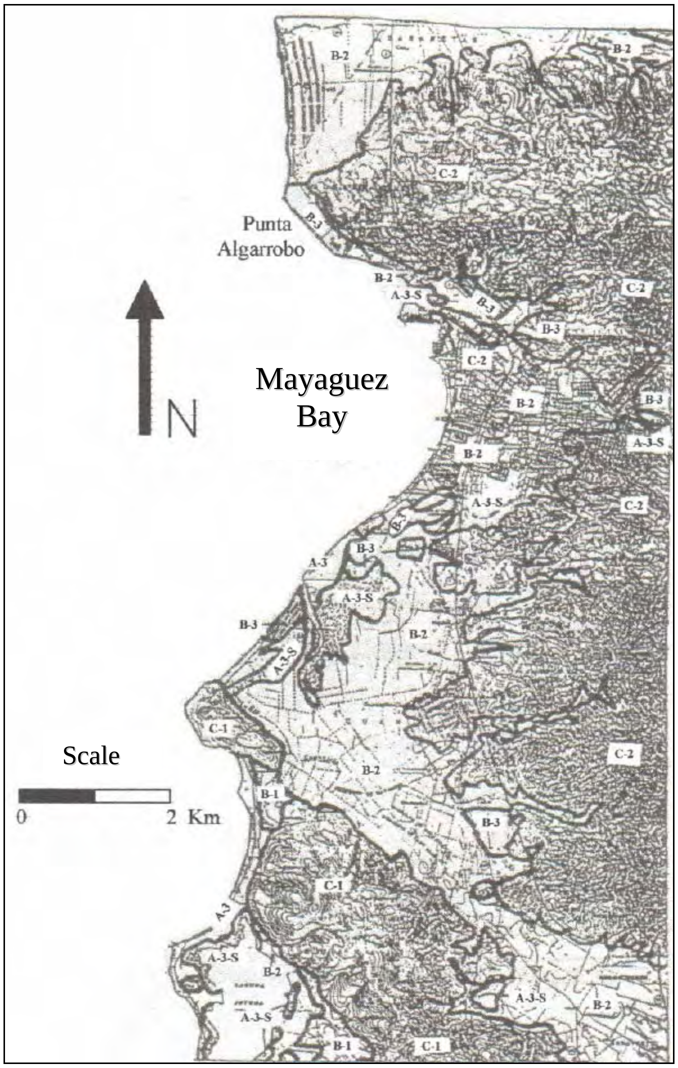

Figure 2.5 Zone Classification Map according to Moya et. al. (1992) [See Table 2.8]

2.3.4 *Macari 1994*

In 1994 Macari performed a series of geophysical test using the procedure of Spectral Analysis of Surface Waves (SASW) as well as Piezocone Penetration (CPT) test in the island of Puerto Rico. As mentioned by Pérez (2005), he obtained the shear wave velocity and shear strength characteristics at eight sites in western Puerto Rico including locations within Mayagüez. Macari (1994) tested three sites in downtown Mayagüez: the Athletic Field at the UPR-Mayagüez, the India Brewery in front of the UPR-Mayagüez campus, and a site adjacent to the PR-2 highway near the Darlington building. The SASW tests revealed these sites are composed of deep soil deposits with a relatively low shear wave velocity. He found shear wave values starting at 91.4 m/s near the ground surface and increasing with depth to almost 213.3 m/s in the upper 15 m. The SASW test did not help determine the total depth of the soil deposit, but it was inferred to extend beyond 30 m depth. In addition to these sites, Macari also studied a site at the Guanajibo valley, located adjacent to the Mayagüez Bay and the Guanajibo River. He found that the shear wave velocity increases quickly with depth reaching values of 610 m/s to 914 m/s at 9 m depth. This study indicates that these high shear wave velocities values are associated with soft rock and sandstone. The shear wave velocity profiles and CPT soundings are included in the geotechnical database created for this research project.

2.3.5 *Macari 1997*

In 1997 Macari performed a seismic hazard and risk analyses for the western part of Puerto Rico. In this study he evaluated the liquefaction potential based on the Liquefaction Potential Index (LPI) method for a maximum credible earthquake (M=7.5) and several Peak Ground Accelerations (PGA) values varying from 0.05g to 0.15g. Using LPI and this range of PGA’s he developed a series of Liquefaction Hazard Maps that help identify regions of low (LPI<5), moderate (5<LPI<15) and high (LPI>15) liquefaction potential. Figure 2.6 presents one of the liquefaction maps developed in this study which shows contours of liquefaction potential for a PGA of 0.15g. This figure shows how several areas were identified as having high liquefaction potential. However the author recommended a more thorough investigation that was based on a larger data set of soil properties.

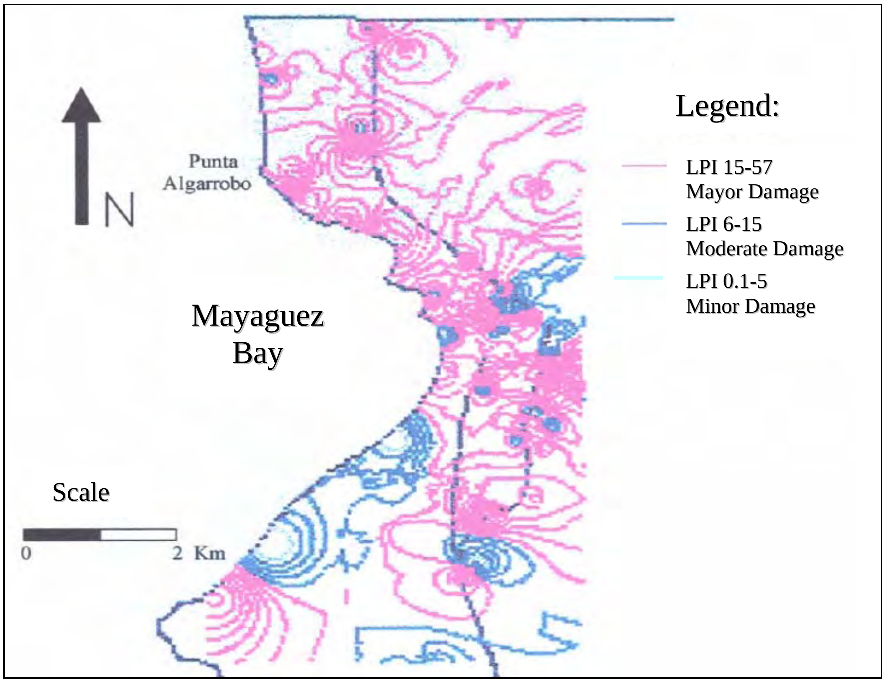

Figure 2.6 Liquefaction Hazard Map Developed by Macari (1997)

2.3.6 *UPRM Master in Engineering Thesis by Llavona 2004*

Llavona (2004) gathered geotechnical information from local agencies, including sources from the public and private sector. The main goal of this study was to identify NEHRP zones and to perform a study of the liquefaction hazard for the Mayagüez area. The project was funded by the Puerto Rico Insurance Commission Office. He developed soil classification maps for the Mayagüez area based on the 1997 Uniform Building Code Provisions (UBC 97) for soil classification and liquefaction maps based on LPI values obtained for each site. Llavona (2004) collected all the required information from available boring logs, such as soil types, standard penetration test (SPT) N values, and the depth of the water table, among other properties. He based his site classification on the SPT N values. The liquefaction hazard analyses were performed following the recommendations presented by Youd et al. (2001) regarding the simplified procedure for evaluation liquefaction resistance of soils which was summarized in section 2.2.3.3.

For his study, Llavona used the seismic coefficients Ca recommended in the UBC-97 for site classification to estimate the peak ground acceleration at the surface induced by an earthquake. With the use of the LPI values determined for each site Llavona (2004) found that starting at the northwest part of Mayagüez, following through the coast and ending in the city limits in the southwest part of Mayagüez, the soil profile is classified as S_F. He classified most of the central and eastern part of Mayagüez as soil profile S_D with some areas in the downtown area classified as S_E. Llavona (2004) developed a liquefaction map for the Mayagüez city based on LPI values. This map is presented in Chapter 5. More detailed information on this study can be found in Llavona (2004). It is important to mention that Llavona (2004) identified that most of the Mayagüez urban area is located inside the liquefaction susceptible zone. The work done by Llavona (2004) was the basis for most of the information used in the development of the geotechnical database completed for this project.

2.3.7 *UPRM Master in Science Thesis by Pérez 2005*

In 2005 Pérez carried out one dimensional seismic response analyses for fifteen sites in the Mayagüez area. In order to obtained information required for these analyses he performed a series of geophysical test based on the Spectral Analysis of Surface Waves (SASW) at nine sites in the Mayagüez area. To obtain the information for the remaining sites he correlated the shear wave velocity and N values from the Standard Penetration Tests obtained from previous studies. As a result of the SASW tests, Pérez (2005) obtained shear wave velocity profiles for each site. Some of the tested sites are composed primarily of alluvial soils, e.g., the Abonos and 341HWY sites, other sites are located within coastal deposits like the Maní Park, Maní, Seco Park, Isidoro García, and Ramírez de Arellano sites whereas the Sultanita and Civil sites are located within residual soils. More detailed information on the test results by Pérez (2005) are provided in Chapter 4.

Using the computer program SHAKE2000, Pérez performed equivalent linear analyses using the SASW data obtained and complementing it with available geotechnical information. For these analyses he considered four artificial accelerograms compatible with the UBC-97 design response spectrum for seismic zone 3 in rock and a real acceleration record. From this analyses, the soil profile fundamental period, peak acceleration, and ground response spectrum at the surface was obtained for each site. Pérez (2005) concluded that sites located in the Añasco Valley and part of the downtown area resulted in relatively higher spectral accelerations than the recommended in the UBC-97 for the same soil type.

2.3.8 *Odum et al. (in preparation)*

During the summer of 2003, Odum et al., from the United States Geological Survey carried out geophysical test at three sites in the Mayagüez area in collaboration with the Puerto Rico Seismic Network and the Puerto Rico Strong Motion Program. These tests consisted of seismic refraction and refraction microtremor (ReMi) tests. The sites in the Mayagüez area, included: El Seco Park, the UPRM track field, and the Candelaria site. From these tests, they obtained shear wave velocity profiles for each site and they classified the sites according to the NEHRP provisions. All sites were classified as NEHRP soil type S_D. They found that the stratigraphic section and seismic velocity columns for the Candelaria and El Seco sites are very similar. Both sites have a similar upper layer of weathered bedrock (Vs=340 and 355 m/s). In addition, the depth from the surface to the boundary between saprolite and less weathered bedrock was essentially the same for both sites, approximately at 20 and 18 m respectively. More detailed information on these tests results are provided in Chapter 4.

CHAPTER 3 General Description of the Mayagüez Area

3.1 *Introduction*

A general description of Mayagüez city and vicinity is presented in this chapter. The description is divided into seismic settings, general geology, topography, and ground water conditions of the area.

3.2 *Seismic Settings*

The island of Puerto Rico is located in a very active and complex tectonic region in the northeastern Caribbean Sea. Most of the seismic activity of the area is produced by the convergence and lateral translation of the North American and Caribbean Plates beneath the Puerto Rico Platelet (Tuttle et al., 2005) as shown in Figure 3.1.

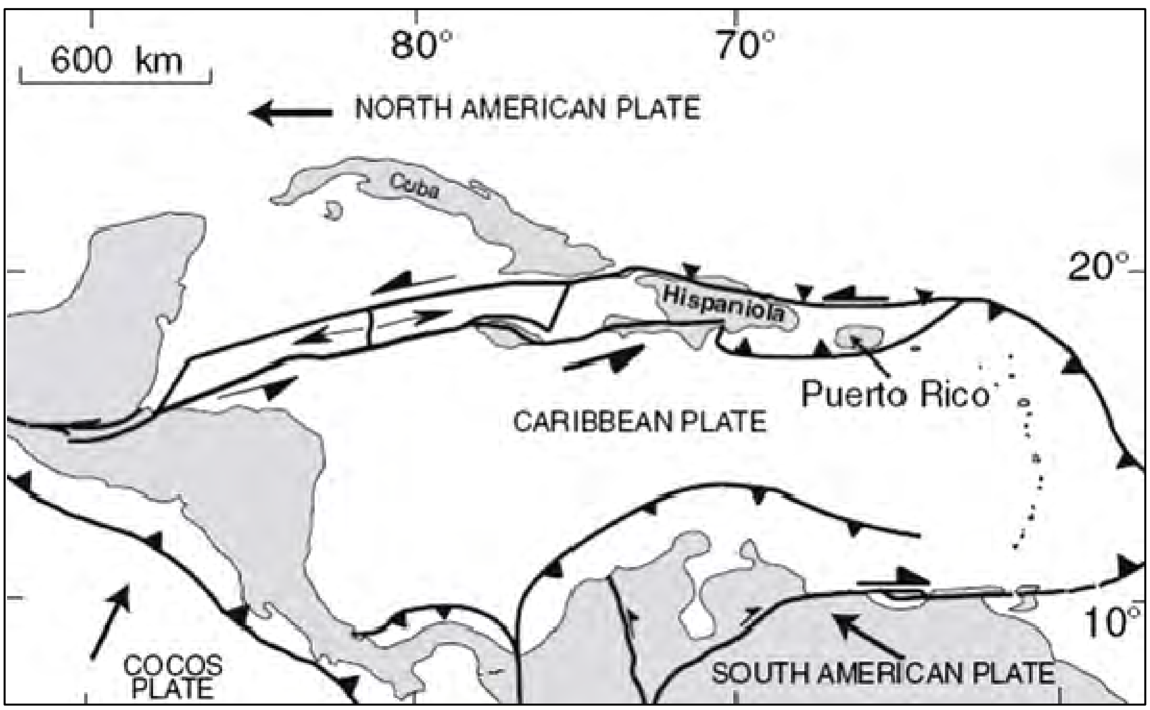

Figure 3.1 Tectonic Plates Settings for the Caribbean Region (From Tuttle et al., 2005)

Figure 3.2 shows how Puerto Rico is surrounded by offshore active faults which are considered the major sources of seismic activity on the island. The Mona Canyon and the Anegada Passage are extension zones located to the west and east side of the island, respectively. There are two subduction zones to the north and south side of Puerto Rico called the Puerto Rico Trench and Muertos Trough respectively. Also there are segments of the Great Southern Puerto Rico Fault Zone (GSPRFZ) and Great Northern Puerto Rico Fault Zone (GNPRFZ) that cross the island from northwest to southeast. Additional to the offshore seismic sources mentioned above, an inland source has recently been identified as capable of generating M7.0 events (Prentice et al., 2000; Prentice and Mann, 2005). This inland fault is identified in Figure 3.2 as SLF for the abbreviation of South Lajas Fault which is located in the south west corner of Puerto Rico.

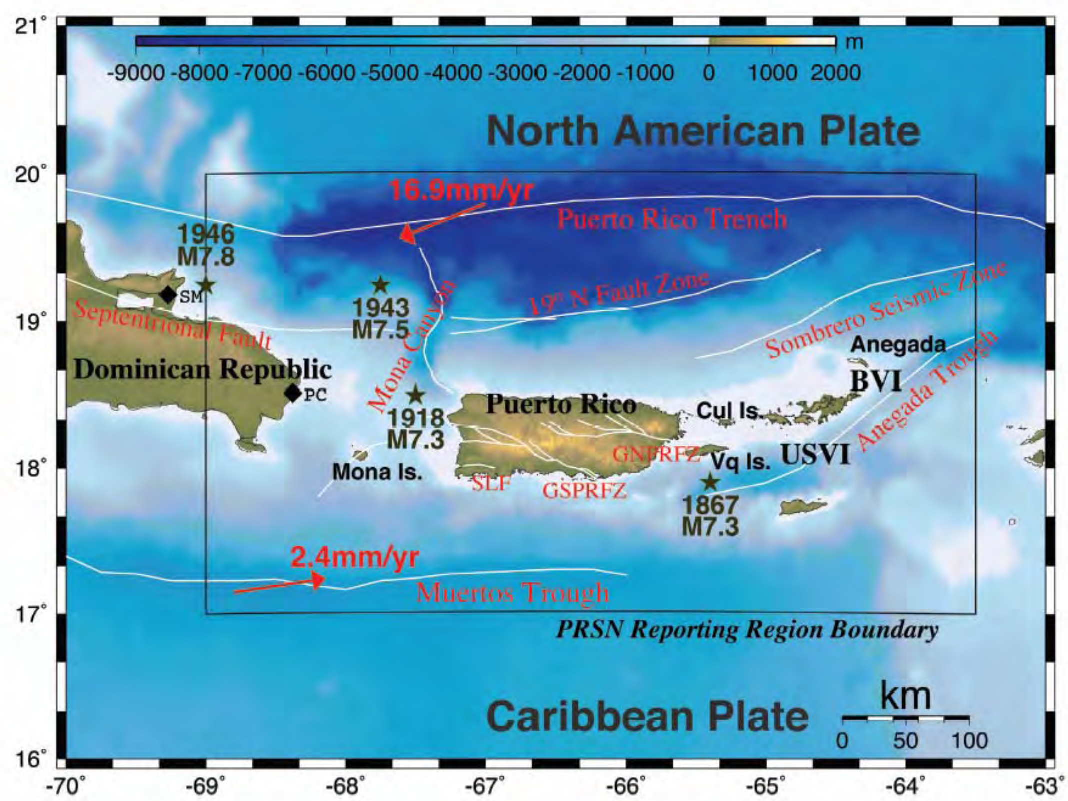

Figure 3.2 Seismic Settings and Major Faults (From Clinton et. al., 2007)

The most important seismic potential sources for the Mayagüez area are the Puerto Rico Trench, the Muertos Trough and the Mona Passage (McCann, 1987). Historic records demonstrate that strong earthquakes have occurred in the Puerto Rico Trench in the past (Sykes et al., 1982 and McCann et al., 1993). It is believed that the Puerto Rico Trench is capable of generating maximum events of M ~ 8.0 as there is evidence that in 1943 it produced an event of M ~7.75 (McCann, 1987). Also, according to McCann (1987) the Muertos Trough is considered to be capable of producing events of M ~7.5 to 8.0. However, the seismicity produced by the Mona Passage is considered the most threatening for the west coast due to the proximity to the area. This zone is capable of generating shocks of M ~ 7.5 to 8.0 (McCann, 1987). In 1918, this zone generated the most damaging event for the Mayagüez area with an estimated magnitude of 7.5. Approximately 116 people died due to this event and $4 million in property damage was estimated (Reid and Taber, 1919).

3.3 *General Geology*

The general geology for the Mayagüez area has been mapped by Curet (1986). Figure 3.3 shows the different geologic units identified by Curet (1986) and Table 3.1 provides a brief description of these units. In general, the Mayagüez area lies between the contact of two different geologic units: the Sierra Bermeja Complex and a volcanic complex (Moya and McCann, 1992). The Sierra Bermeja Complex is composed mainly by volcanic and metamorphic rocks of pre-Cretaceous to Early Cretaceous age and is considered as the oldest rock formation in the island (Moya and McCann, 1992). The volcanic complex is a folded sequence of sedimentary and volcanic rocks of Late Cretaceous to Early Tertiary age that overlays the Sierra Bermeja Complex (Moya and McCann, 1992).

Table 3.1 Geologic Stratigraphic Table for the Mayagüez Area (After Curet, 1986)

Age	Stratigraphy	Description
Holocene	Qal alluvium	Sand, silt and gravels, includes rock falls and landslide deposits
Early Tertiary Maestrictian (Maest.)	TKpb Basalts	Basalts and basalts weathered
	TKpa Andesite-diorite	Porphyritic andesite- diorite
	TKpaa Andesite-diorite	Altered porphyritic andesite-diorite
	TKhp Diorite	Porphyritic hornblende diorite (massive)
	TKab Basalt	Porphyritic augite basalt (massive)
Maestrictian and Campanian	Kmr Maricao Formation	Massive breccia, conglomerate sandstone and limestone
	Ky Yauco Formation	Calcareous volcanoclastic sandstone, siltstone, claystone, limestone, breccia, conglomerate
Maestrictian and Turonian	Ksg Sábana Grande Formation	Massive breccia, conglomerate sandstone, siltstone, claystone and limestone
Pre. Late Kimmeridgian	Jse Serpentinite	Massive and weathered serpentinite

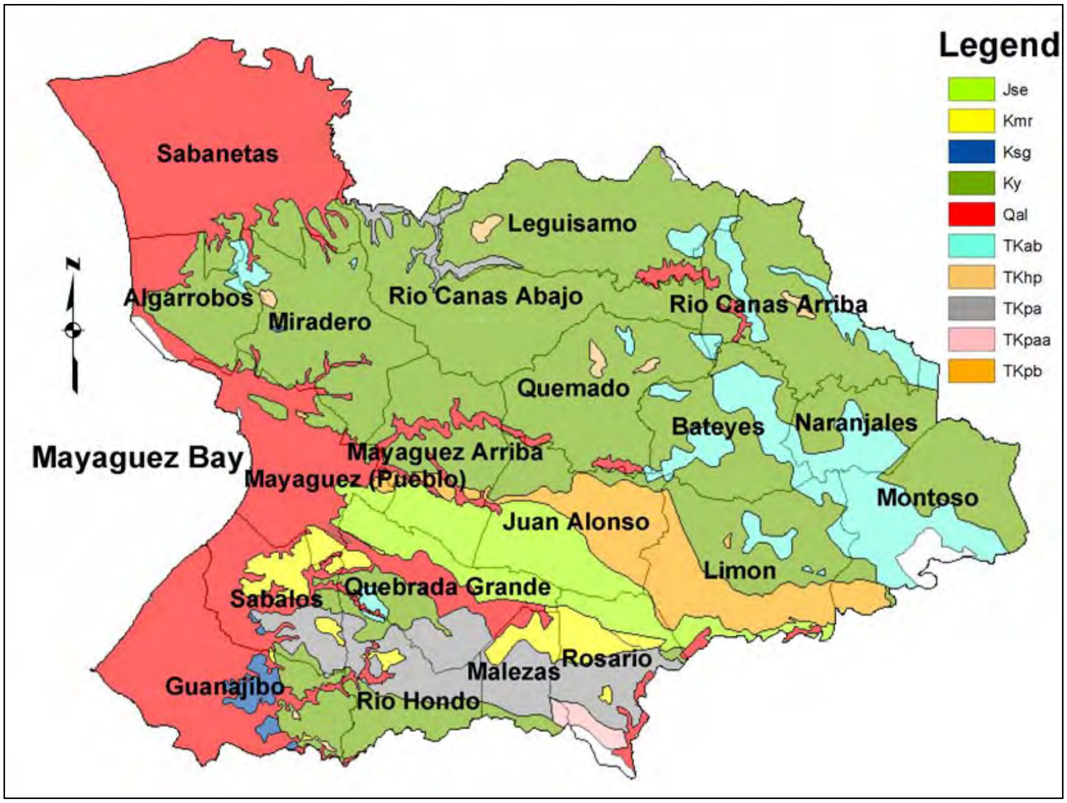

Figure 3.3 Mayagüez Geologic Map (After Curet, 1986)

The areas near the shoreline are to a large extent sand beach deposits characteristic of coastal environments. These sands are composed mainly by quartz sands formed in the Holocene and are described as mainly rounded, moderately to well sort sands with minor gravel sizes (Moya and McCann, 1992). Near the rivers (e.g., Guanajibo River) the soils are alluvial deposits from the Late Pleistocene and Holocene. They are described as poorly to moderately sorted, moderately to well-bedded sand, silt, and cobble or boulder gravel (Moya and McCann, 1992). At the Guanajibo River, the thickness of the alluvium deposits range from 50 to 100 ft (Colón-Dieppa et al., 1985). In the Añasco river flood plain the deposits are typically more than 100 ft thick (Colón-Dieppa et al., 1985). In the vicinity of the Yagüez River alluvial soils were found to extend to the final depth investigated of 120 ft (Capacete and Herrera, 1972) and are believed to extend from 170 ft to up to 300 ft in the Mayagüez alluvial plains (McGuinness, 1946; Rodríguez and Capacete, 1988). The Sabanetas and Downtown districts of Mayagüez are mostly comprised of alluvial soils. The Algarrobos, Miradero, Sábalos, and Guanajibo neighborhoods of Mayagüez also have alluvial deposits but to smaller extents since they are predominantly residual soils. The residual soils in the

Mayagüez area are typically located in the mountainous terrain away from rivers and creeks.

Rodríguez-Martínez et al. (2004) divided Mayagüez into five hydrogeologic terranes according to the hydrogeologic and topographic characteristics and the ground-water resource development potential. The aerial extent of these terranes is shown in Figure A-1 of Appendix A.

The first terrane identified by Rodríguez-Martínez et al. (2004), Mayagüez Hydrologic Terrane 1 (MayHT1), is restricted to lowlands, including the coastal areas and alluvial terraces along rivers and creeks in the mountainous interior. This terrane is subdivided into upper zone and lower zone. The upper zone is composed mostly of Quaternary alluvium and to a lesser extent, Quaternary mangrove and swamp deposits. According to Rodríguez-Martínez et al. (2004) the alluvium zone on this terrane is predominantly fine grained material, with high contents of silt and clay and minor amounts of sand. Minor deposits of gravel and sand of considerable thickness are highly localized and can be found mostly on the vicinity of ancient and present river channels deposits. This study estimated that the thickness of the upper zone generally ranges from 50 to 100 ft. The lower zone, underlying the upper zone, consists of pre-Quaternary fluvial and marine sandstones and Late Cretaceous and Early Tertiary-age volcaniclastics (sandstones, siltstones, claystone, and breccia) and limestones. The lower zone is underlain by Middle and Late Cretaceous-age serpentinite and intrusive igneous rocks (Curet, 1986). The thickness of the lower zone is unknown. The volcaniclastics rocks found on this zone were originated either from the deposition of volcanic eruption materials directly to the sea or from erosion and final deposition of existing volcanic rocks (Curet, 1986).

The second terrane defined by Rodríguez-Martínez et al. (2004) is labeled MayHT2. It consists of volcaniclastic rocks intruded by intrusive igneous rocks. This terrane is located on the barrios (neighborhoods) of Río Cañas Abajo, Montoso, Bateyes, and Naranjales. The volcaniclastic and intrusive rocks are Cretaceous and Tertiary in age (Curet, 1986). The volcaniclastic units founded on this zone in order of decreasing aerial extent are the Yauco Formation and the Maricao Formation (Curet, 1986). The Yauco Formation is mainly composed of interbedded and calcareous volcaniclastic sandstone, siltstone, mudstone, claystone, limestone, and subordinate breccia and conglomerate while the Maricao Formation consists mostly of breccia with minor amounts of conglomerate, volcaniclastic sandstone, and limestone.

Rodríguez-Martínez et al. (2004) defined the third hydrogeologic terrane, MayHT3, as consisting primarily of the Yauco Formation, subordinate amounts of the Maricao Formation, and minor intrusive igneous rocks of basaltic and dioritic composition (Curet, 1986). The MayHT2 and MayHT3 hydrogeologic terranes are continuous and separated by a poorly defined transitional zone, mainly in the Barrios of Leguísamo, Río Cañas Abajo, and Quemado (Rodríguez-Martínez et al., 2004).

The hydrogeologic terrane MayHT4, is located in the southern part of Mayagüez and is restricted to the Cerro de Las Mesas upland. It consists mostly of serpentinite, a rock consisting mostly of the mineral serpentine, and other minor intrusive igneous rocks presumed to be of Early to Middle Tertiary age. Rodríguez-Martínez et al. (2004) indicates that in large areas of the MayHT4 hydrogeologic terrane the serpentinite bedrock is directly exposed with no soil cover.

The last hydrogeologic terrane defined by Rodríguez-Martínez et al. (2004), MayHT5, consists of intrusive igneous rocks of Tertiary and Cretaceous age (Curet, 1986). These igneous rocks are of basaltic and dioritic composition, similar to the MayHT2 and MayHT3 hydrogeologic terranes.

3.4 *Topography*

Mayagüez is located on one of the coastal valleys of the west side of the Puerto Rico Island. The topography of the Mayagüez area can be described as mild to flat sloped terrain on coastal deposits of Holocene age and alluvial valleys, and mountainous terrain, on the east and northeast part of the city.

The coastal deposits are found along the coast of the Mayagüez Bay. The other low lying areas of the region, which are the alluvial valleys, are found on the lands surrounding the principal rivers of the area, called Yagüez and Guanajibo Rivers, as they were formed by the deposition of alluvial deposits from these rivers. The widest portion of the coastal plain or flatland is located at the mouth of the Guanajibo River, which is located at the south part of the Mayagüez city. On the other hand, the central range of mountains is located on the east part of the city starting near the coastal area and rapidly rising to 350 meters above mean sea level.

The study by Rodríguez-Martínez et al. (2004) also described the topographic characteristics of the five Mayagüez hydrogeologic terranes mentioned on the previous section. MayHT1 is described as flat and lowlands. MayHT2 are sloping grounds with variable slopes with most exceeding 15 degree slope angles. In the MayHT3 the land slopes are also variable, but the portion with slopes equal to or less than 15 degrees is higher than in MayHT2. In the case of MayHT4 and MayHT5, land slopes range from less than 15 to more than 45 degrees.

The importance of the differentiation of the Mayagüez region into flatlands areas or mountain areas comes when assessing the liquefaction susceptibility of the region. It is widely referenced that structures founded on unconsolidated materials and shallow water table, like coastal deposits and alluvial plains, are more frequently susceptible to damage when subjected to seismic loadings than structures located on competent soil or consolidated soils. As the coastal deposits of the Mayagüez area are characterized by low slopes, this area is considered most likely to be susceptible to liquefaction.

A topographic profile was created as part of this study using the topographic map included on the ArcMap 9.0© database developed for the Mayagüez area. The topographic profile was generated in the north to south direction as shown on Figure 3.4. The topographic profile is shown on Figure 3.5. From this figure it can be inferred that the Sabanetas and the Mayagüez Pueblo (downtown) areas can be classified as low lying lands in which the elevation ranges mostly between 2 m and 15 m above mean sea level. As mentioned on the previous section, these two regions are mainly composed of alluvial deposits which may be considered prone to liquefaction.

According to the U.S. Census Bureau (2000), almost 33 percent of the Mayagüez population lives in the Mayagüez Pueblo (downtown) area with a total of 38 percent of the Mayagüez housing units located on this area. On the other hand, only 2.7 percent of the population and 2.5 percent of the total housing units are located on the Sabanetas area. Population and Housing Units values for the other regions that were intersected by the topographic cross section of Figure 3.5 are shown on Table 3.2.

Table 3.2 Population Facts for Areas along the N-S Topographic Profile[1]

N-S Profile Geographic Area	Estimated Population	Housing Units	% Total Population	% Total Housing Units
Sabanetas	2,645	985	2.7	2.5
Miradero	5,510	2,155	5.6	5.5
Mayagüez (Pueblo)	32,043	14,932	32.6	37.9
Sábalos	10,271	3,773	10.4	9.6
Guanajibo	7,165	2,754	7.3	7.0

After comparing the population distribution of the regions along the topographic profile, it can be appreciated that the Mayagüez (Pueblo) region is a densely populated area. With a large part of the Mayagüez population living in this area and considering the geologic settings of the region, it can be inferred that the effects of a major earthquake, like the October 11, 1918, could be more devastating today than at that time.

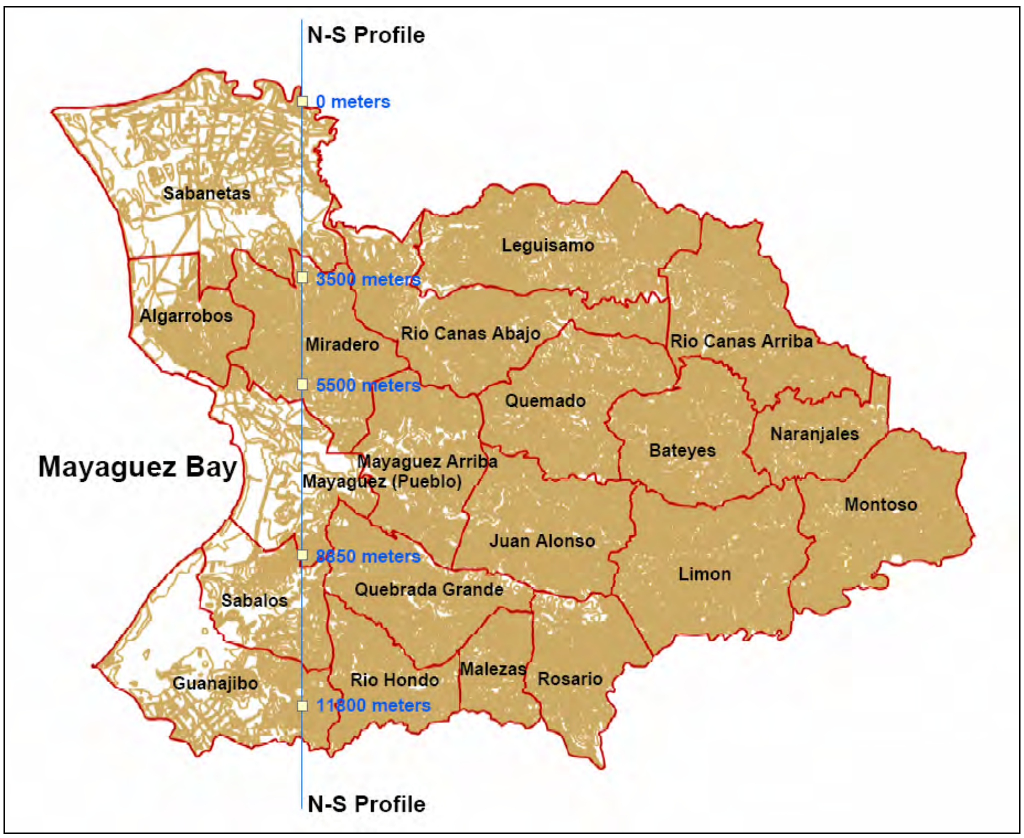

Figure 3.4 Location of N-S Topographic Profile

[1] Source: U.S. Census Bureau, Census 2000 Summary File 1

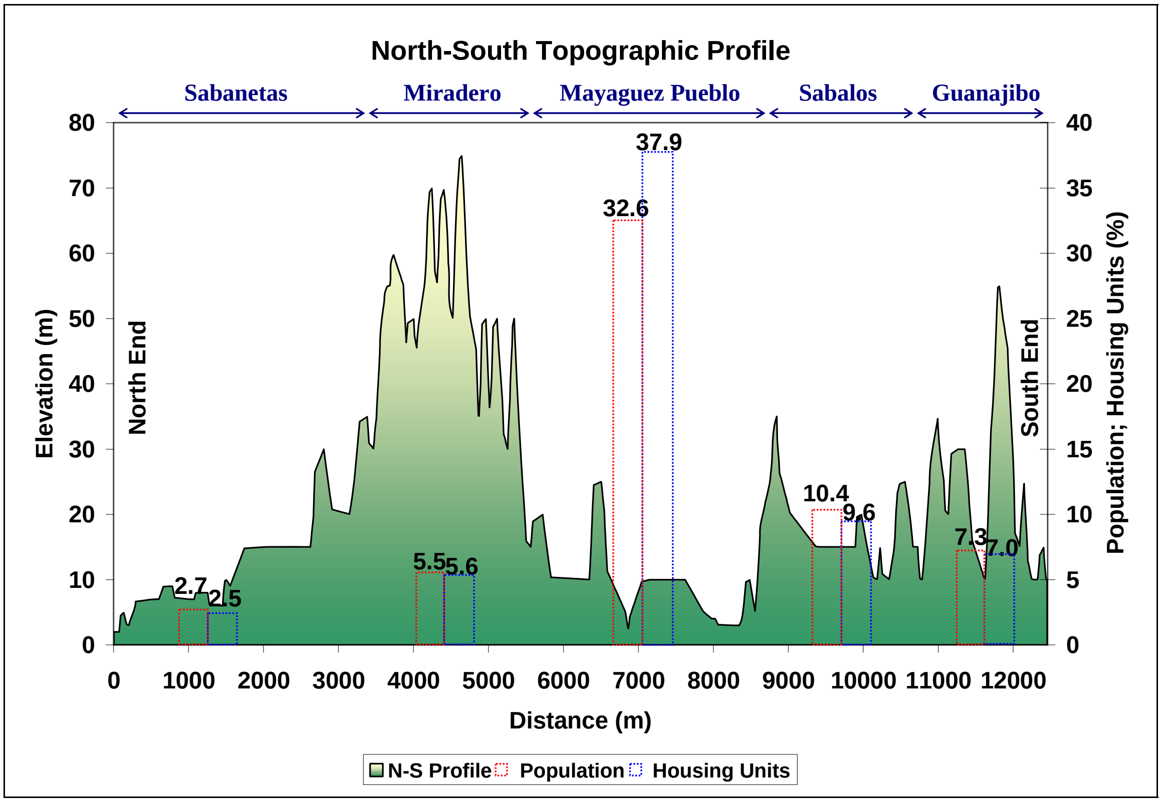

Figure 3.5 North–South Direction Topographic Profile

3.5 *Ground Water Conditions*

As mentioned before (Section 2.2.3.2) ground water conditions play a major role on the evaluation of liquefaction potential. Furthermore, when performing a site characterization for a liquefaction potential assessment it is important to consider the groundwater level conditions using historical records representative of current and historical fluctuations.

For this project, the USGS Ground Water Levels database was used to obtain historical information regarding the ground water levels conditions for the Mayagüez area. For the Mayagüez County, a total of 142 groundwater wells were found on the USGS database (www.usgs.gov). Very few of these wells provided enough historical data to determine a ground water level pattern by means of probabilistic information. However, after evaluating all available data, it was found that the “Autoridad de los Puertos” Well had an adequate amount of information to estimate the average ground water level depth of the site. The “Autoridad de los Puertos” Well is located on the North side of Mayagüez on the Sabanetas area. This well is located on one of the flatland areas of Mayagüez and it is located at an approximate elevation of 6 meters above mean sea level. Figure 3.6 presents the data of ground water level below land surface (in feet) plotted against the month of the year in which it was recorded for a total of 16 years ranging from 1967 to 1984.

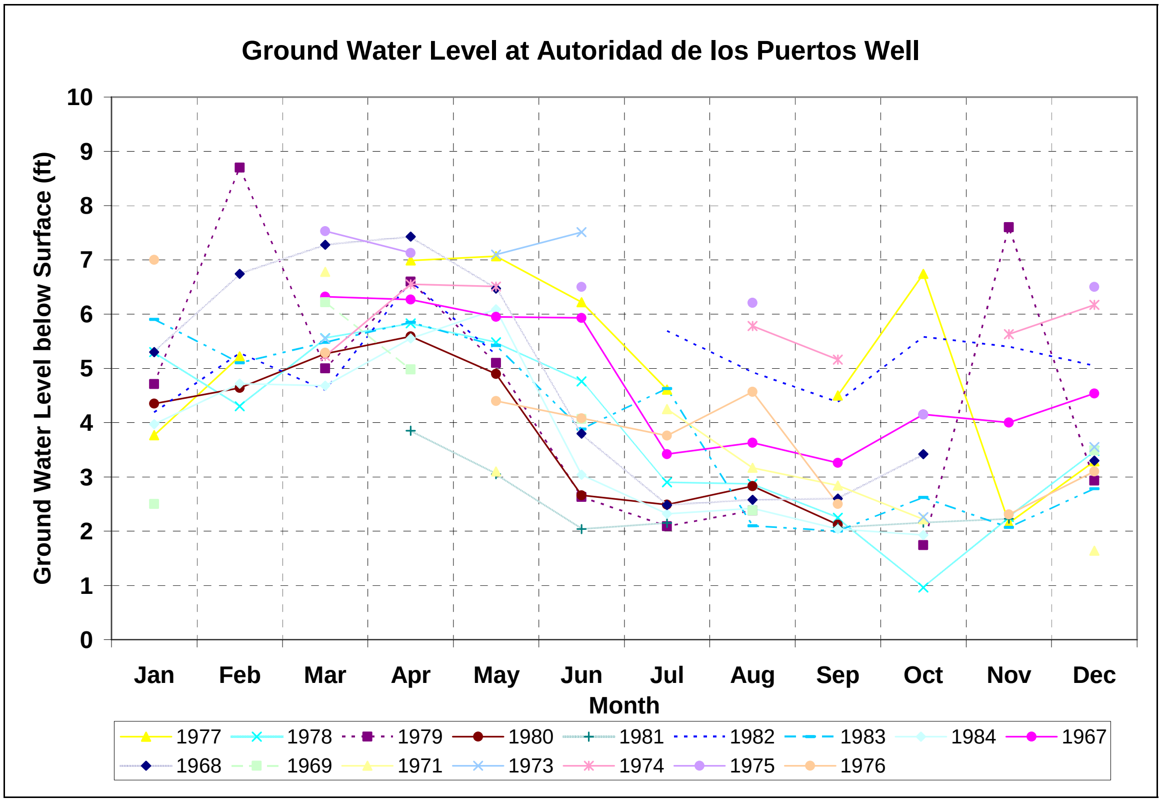

Figure 3.6 Ground Water Level at the "Autoridad de los Puertos" Well

The mean monthly ground water level was calculated with this data as well as the trend lines with ± one standard deviation, as shown on Figure 3.7. This graph indicates ground water levels fluctuate from 5 to 9 ft depth in the dry season from January to July, and from 4 to 6 ft in the rainy season from July to November. Figure 3.7 also shows average monthly rainfall quantities for 1971 to 2000. Figure 3.7 confirms that ground water level fluctuations follow an inverse pattern with the rainfall fluctuations.

Even though this behavior may be representative of the ground water conditions through the Mayagüez area, it cannot be extrapolated to other sites of interest due to other factors that can affect the ground water depth. Some examples of these factors are the distance to water bodies and topographic conditions.

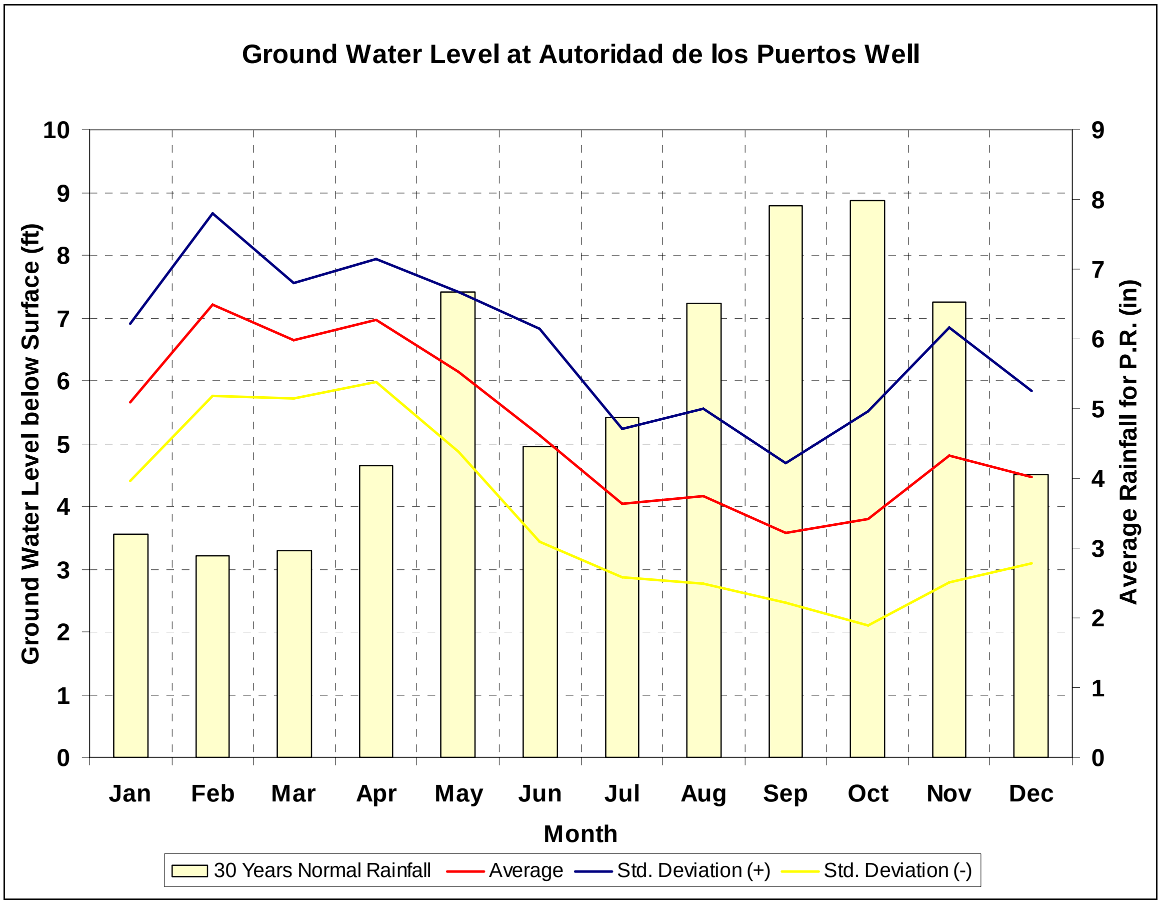

Figure 3.7 Ground Water Level combined with Average Rainfall in PR

Rodríguez-Martínez et al. (2004) defined generalized relations between depth to water and topographic relief for the Mayagüez area based on historic water-level measurements. The relations defined by Rodríguez-Martínez et al. (2004) are the following:

- The water level at wells located in the coastal plain generally is less than 10 ft below land surface.
- The depths to water at wells located in a river valley are most likely greater than 10 ft but equal to or less than 15 ft below land surface.
- In slopes with varying degrees, the depth to water generally lies between 15 and 40 ft below land surface.
- In wells installed in hilltops, the water level generally is greater than 40 ft but equal to or less than 110 ft below land surface (depending on elevation).

CHAPTER 4 Geophysical Testing in the Mayagüez Area

4.1 *Introduction*

As part of the development of a detailed geotechnical database for the city of Mayagüez available geophysical data was collected and compiled. This research project also included carrying out additional geophysical tests to further populate the developed database.

This chapter summarizes available geophysical data obtained by others as well as the data generated as part of this research.

4.2 *Previous Geophysical Studies*

4.2.1 *Data from Pérez (2005)*

The study conducted by Pérez (2005) consisted in a series of SASW field tests at nine locations within the city of Mayagüez boundaries. Site selection criteria were based on sites where geotechnical information was limited or insufficient to perform ground response analyses and other seismic studies. Figure 4.1 displays the locations of the sites tested on a Mayagüez map and Table 4.1 lists their respective geographic coordinates. According to Pérez (2005), the Abonos and 341HWY sites are composed primarily of alluvial soils, the Maní Park, Maní, Seco Park, Isidoro García, and Ramírez de Arellano sites are located within coastal deposits, and the Sultanita and Civil sites are located within residual soils.

This section presents the results obtained by Pérez (2005) using the Spectral Analysis of Surface Wave (SASW) tests. The results are presented in the form of the shear wave velocity profiles and the resulting site classification interpretation based on the NEHRP site classification system presented in Chapter 2.

Figure 4.1 Location of SASW tests by Pérez (2005)

Table 4.1 Coordinates for SASW Test Sites by Pérez (2005)

Site	Geographic Coordinates
Abonos	18º 16' 01N / 67º 09' 44W
341HWY	18º 15' 50N / 67º 10' 35W
Maní	18º 13.79N / 67º 10.33W
Maní Park	18º 14.81N / 67º 10.46W
Seco Park	18º 12.76N / 67º 09.57W
Isidoro García	18º 11' 24N / 67º 09' 14W
Ramírez de Arellano	18º 11.34N / 67º 09.59W
Sultanita	18º 12.81N / 67º 08.65W
Civil	18º 12.81N / 67º 08.39W

<u>Abonos Site:</u>

Pérez (2005) found relatively low shear wave velocities for this site. He described the first layer on the velocity profile as a compacted fill material with an estimated thickness of 2.5 meters. Below this fill, he found relative loose soft materials with wave velocities increasing with depth from 150 m/s to 328 m/s. The average shear wave velocity in the upper 30 meters depth calculated by Pérez (2005) was 196.9 m/s and the site was classified as soil type S_D according to the NEHRP site classification system. Figure 4.2 presents the velocity profile obtained from the SASW test. This figure also includes a table with the specific thickness and shear wave velocities for each layer found from the SASW inversion for this site.

Velocity Profile	Profile Values

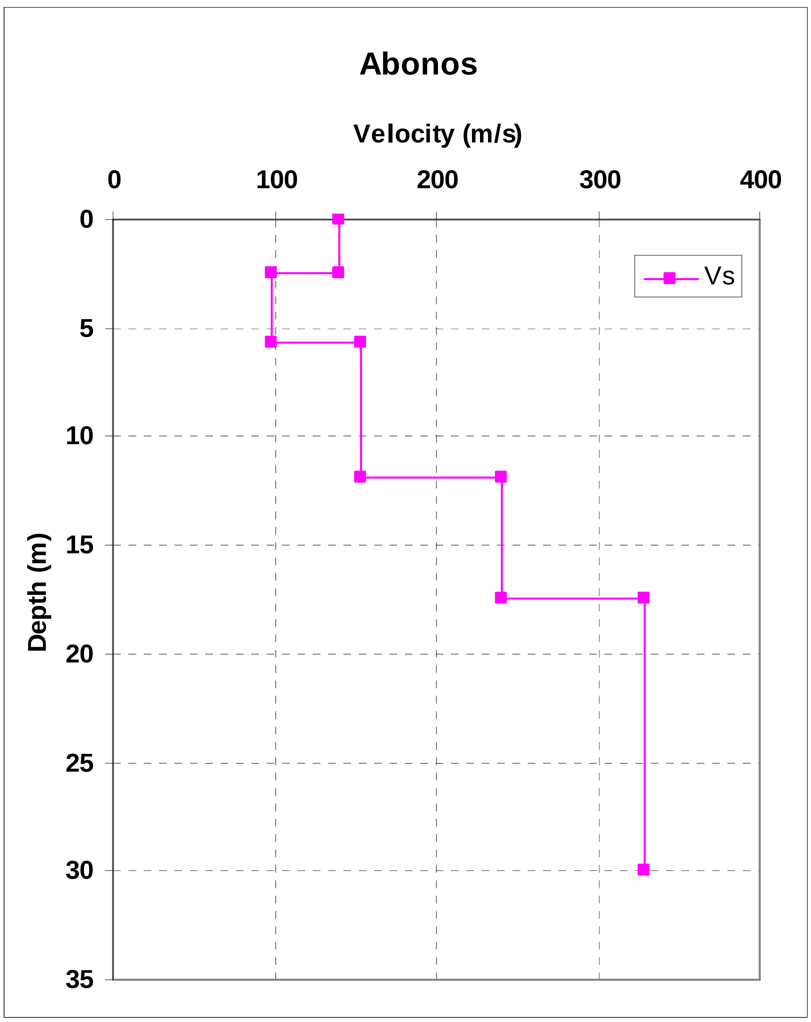

Abonos	
Velocity Profile	
h	Vs
(m)	(m/s)
2.5	140.3
3.2	97.6
6.2	153.3
5.6	240.4
12.5	328.8
Vs30 (NEHRP) =	196.9
Soil Type =	D

Figure 4.2 SASW Velocity Profile for Abonos Site (from Pérez , 2005)

<u>341 HWY Site:</u>

The 341HWY site is located to the west of the Abonos site in the Añasco Valley next to highway PR-341. Pérez (2005) found similar geological conditions to the Abonos site with the difference that a relatively stiff layer was found at a depth of 15 meters. He calculated that the average shear wave velocity in the upper 30 meters depth was 203.3 m/s and thus its NEHRP site classification is S_D. Figure 4.3 presents the velocity profile obtained from the SASW test. This figure also includes a table with the interpreted thickness and shear wave velocities for each layer found at this site.

Velocity Profile	Profile Values

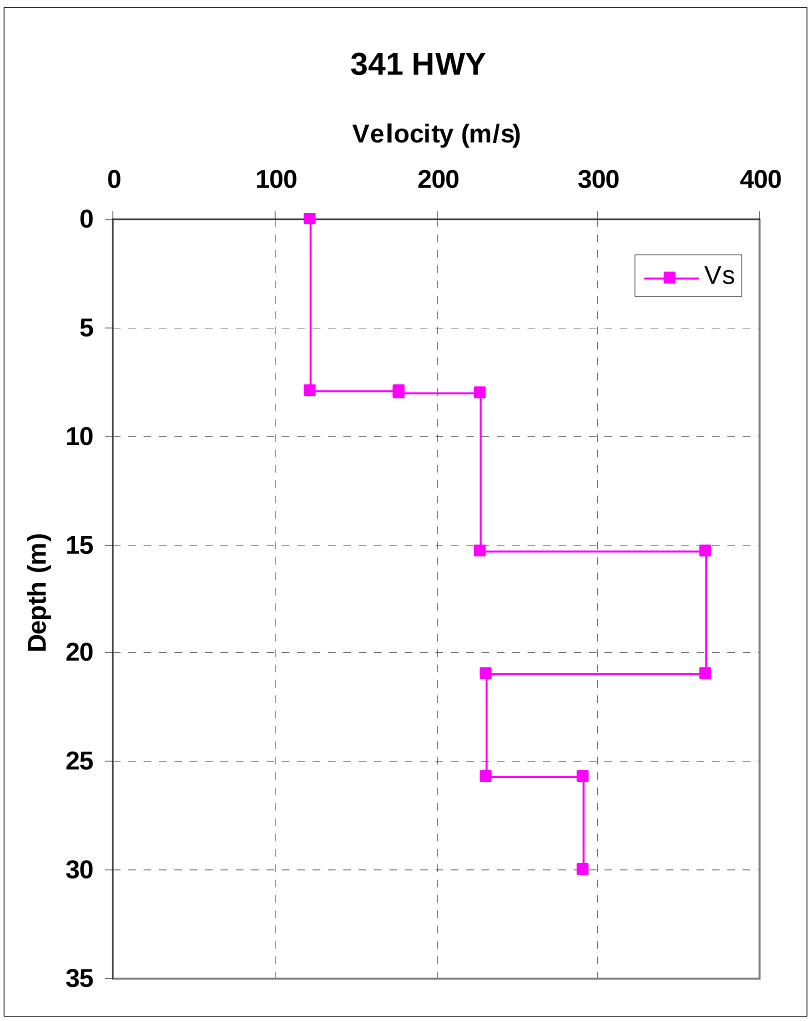

341HWY	
Velocity Profile	
h	Vs
(m)	(m/s)
7.9	122.9
0.1	177.0
7.3	227.7
5.7	366.8
4.7	231.2
4.3	290.9
Vs30 (NEHRP) =	203.3
Soil Type =	D

Figure 4.3 SASW Velocity Profile for 341 HWY Site (from Pérez , 2005)

Maní Site:

El Maní site is located in the PR-341 highway in the neighborhood of Mayagüez known as El Maní near to the coastal area. Pérez (2005) described the site as having leveled ground surface located adjacent to the Maní beach. The upper 10 meters had shear wave velocities close to 300 m/s. Below 10 m the shear wave velocity was inferred to be much higher in the order of 1200 m/s or higher. He inferred that this high shear wave velocity contrast was related to the presence of weathered rock, but he concluded that this finding did not necessary represent the typical geological conditions of the coast of Mayagüez but rather a particular feature of this site. This site was classified as S_C with an average shear wave velocity in the upper 30 meters depth of 504.1 m/s. Figure 4.4 presents the velocity profile obtained from the SASW test and it also includes a table with the interpreted thickness and shear wave velocities for each layer found from the test at this site.

Velocity Profile | **Profile Values**

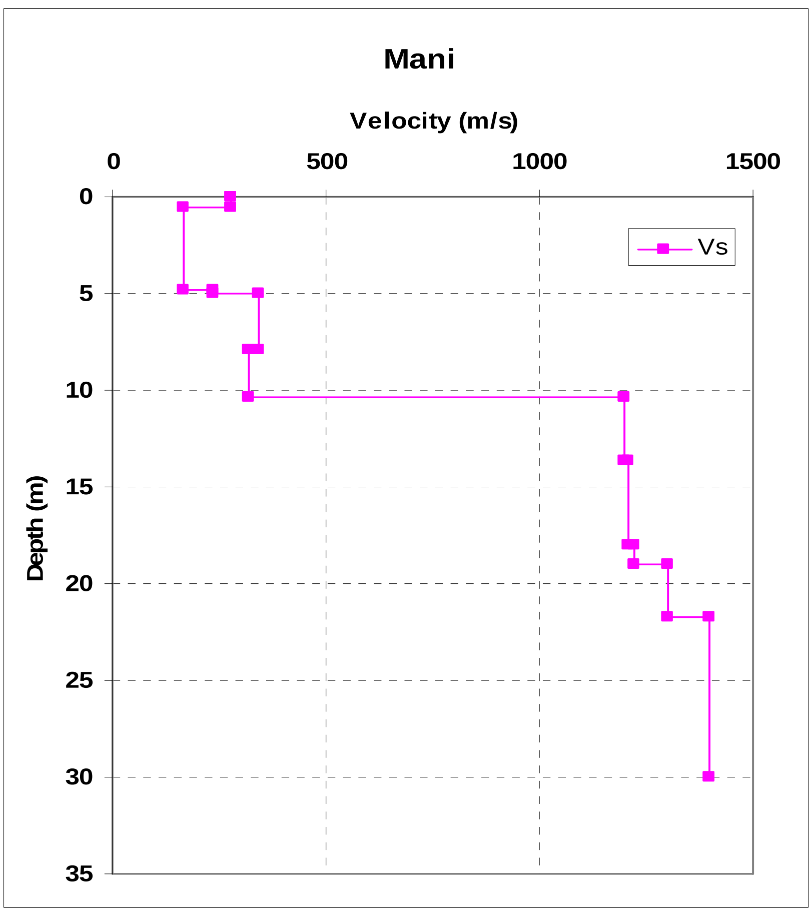

Mani	
Velocity Profile	
h	Vs
(m)	(m/s)
0.5	279.6
4.3	168.5
0.2	238.1
2.9	344.5
2.5	320.0
3.2	1200.0
4.4	1210.0
1.0	1220.0
2.7	1300.0
8.3	1400.0
Vs30 (NEHRP) =	504.1
Soil Type =	C

Figure 4.4 SASW Velocity Profile for Maní Site (from Pérez , 2005)

Maní Park:

The Maní Park is a baseball park located in the end of highway PR-341 highway in the neighborhood of Mayagüez known as El Maní near to the coastal area. This site can be described also as a flat surface ground at the side of the beach. The upper 15 meters had a relatively low shear wave velocity (about 200 m/s), as shown in Figure 4.5. Velocities below 15 meters increased from 290 m/s to 778 m/s at 30 meters depth. This site was classified as S_D with an average shear wave velocity of 273.8 m/s. The thicknesses of each layer along with the corresponding shear wave velocity are listed in a table located on the same figure.

Velocity Profile	Profile Values

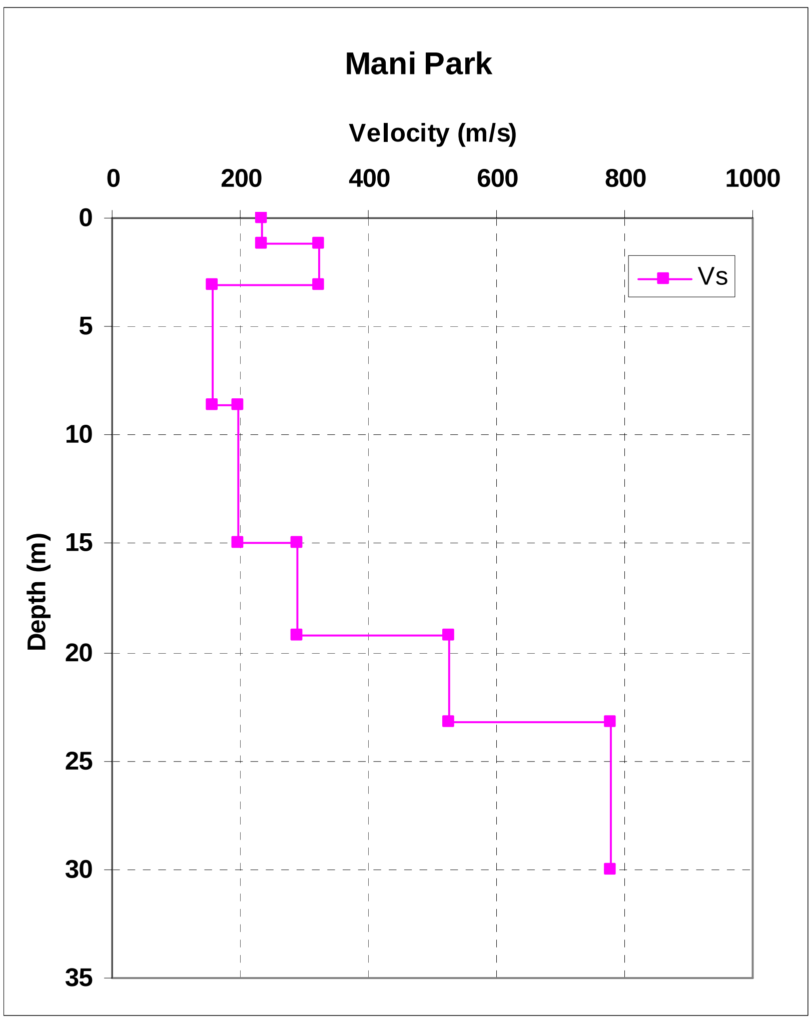

Mani Park	
Velocity Profile	
h	Vs
(m)	(m/s)
1.2	234.7
1.9	323.4
5.5	155.8
6.4	197
4.2	290.5
4	525.9
6.8	778.9
Vs30 (NEHRP) =	273.8
Soil Type =	D

Figure 4.5 SASW Velocity Profile for Maní Park Site (from Pérez , 2005)

Seco Park:

For the Seco Park Site, Pérez (2005) found a pattern of shear wave velocity profile similar to the Maní Park site. The Seco Park site is a baseball park located in the coast of Mayagüez to the south of the Maní Park site in PR-62 highway in the neighborhood known as El Seco. The shear wave velocity of the upper 8.6 m was found to be about 230 m/s. Below 8.6 meters depth the shear wave velocity decreased to 150 m/s to a depth of 10 meters. Below 10 meters, the shear wave velocity increased gradually with depth until reaching a value of 458 m/s at 30 meters. The average shear wave velocity calculated by Pérez (2005) for the upper 30 meters of this site was 243.8 m/s which classifies as a soil profile type S_D per the NEHRP site classification system. Figure 4.6 presents the velocity profile obtained from the SASW test and it also includes a table with the interpreted thickness and shear wave velocities for each layer found at this site.

Velocity Profile

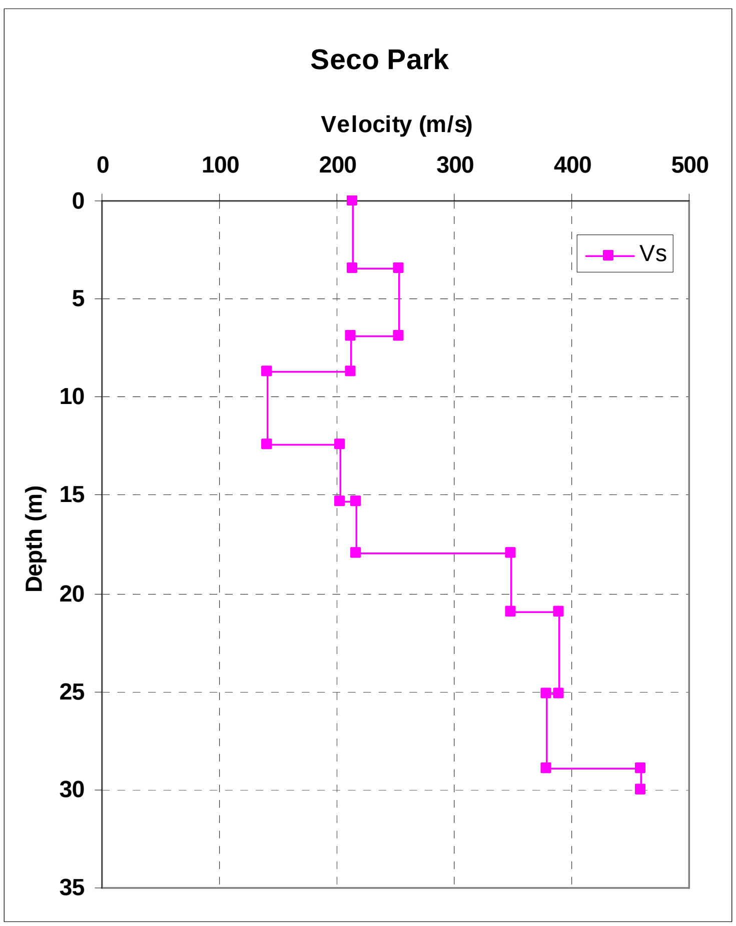

Profile Values

Seco Park	
Velocity Profile	
h	Vs
(m)	(m/s)
3.4	212.9
3.5	253.2
1.7	212.6
3.8	140.7
2.9	202.3
2.6	216.1
3.1	349.0
4.1	389.8
3.9	379.5
1.0	458.6
Vs30 (NEHRP) =	243.8
Soil Type =	D

Figure 4.6 SASW Velocity Profile for SecoPark Site (from Pérez , 2005)

Isidoro Garcia Site:

The Isidoro García site tested by Pérez (2005) is located to the south of the Mayagüez downtown near the coast of Mayagüez at the side of the PR-102 highway. He described the field test area as a flat ground surface outside the Isidoro Garcia Baseball Park. On this site he found a low shear wave velocity layer of 140 m/s that extend to a depth of 13.5 meters. Below this depth the velocity increased up to 430 m/s at a depth of 30 meters. The average shear wave velocity calculated by Pérez (2005) for this site was 211.6 m/s which corresponded to a soil profile type S_D according to the NEHRP site classification system. Figure 4.7 presents the velocity profile obtained from the SASW test and it also includes a table with the interpreted thickness and shear wave velocities for each layer found at this site.

Velocity Profile

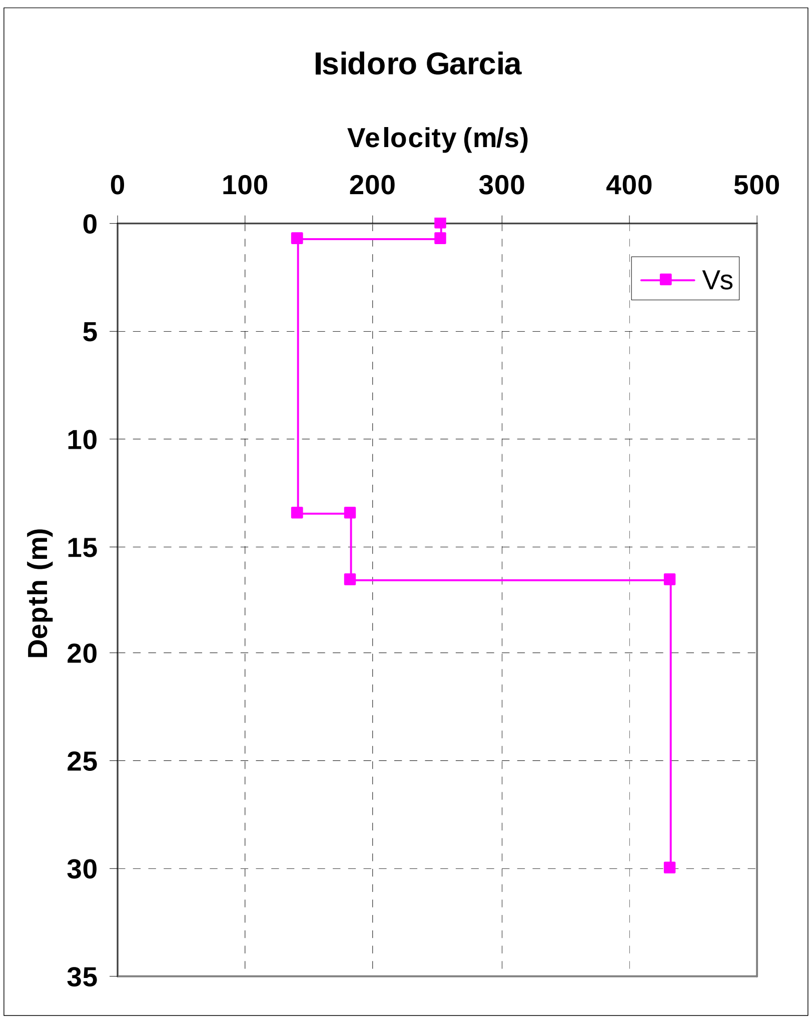

Profile Values

Isidoro Garcia Velocity Profile	
h (m)	Vs (m/s)
0.7	253.5
12.8	140.6
3.1	183.2
13.4	432.1
Vs30 (NEHRP) =	211.6
Soil Type =	D

Figure 4.7 SASW Velocity Profile for Isidoro Garcia Site (from Pérez , 2005)

Ramírez de Arellano Site:

This site is located at the south of the city of Mayagüez. Pérez (2005) described this site as a flat surface ground that is located between the Ramírez de Arellano residential buildings and the PR-102 at the side of the beach. He found relatively low shear wave velocities in the upper 15 meters. This is consistent with the observations found at other sites located near the shoreline. Beyond 15 meters depth the velocity profile varied from 265 m/s to 452 m/s at a depth of 30 meters. The average shear wave velocity for the upper 30 meters of this site calculated by Pérez (2005) was 244 m/s. This value corresponds to a site classified as soil type S_D according to the NEHRP site classification system. Figure 4.8 presents the velocity profile obtained from the SASW test and a table with the interpreted thickness and shear wave velocities for each layer found from this test at this site.

Velocity Profile

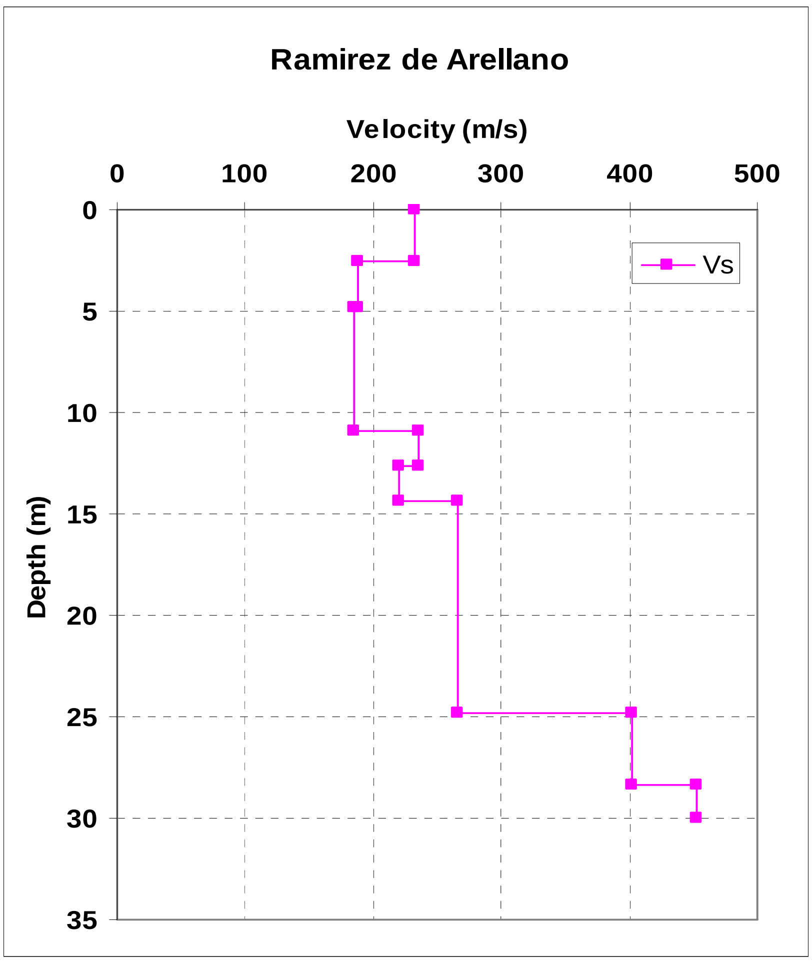

Profile Values

Ramirez de Arellano Velocity Profile	
h	Vs
(m)	(m/s)
2.5	232.7
2.3	188.7
6.1	185.3
1.8	235.3
1.7	219.5
10.5	265.5
3.5	401.9
1.7	452.4
Vs30 (NEHRP) =	244.1
Soil Type =	D

Figure 4.8 SASW Velocity Profile for Ramirez de Arellano Site (from Pérez , 2005)

Sultanita Site:

The Sultanita site is located in a baseball park of the Sultanita sector located on the west side of Mayagüez in the Sábalos neighborhood. This site is in higher elevation than the other sites and is located in hilly terrain believed to be composed of residual soils. Pérez (2005) found a high shear wave velocity contrast of 1097 m/s at 21 meters depth. He inferred that this high velocity layer was mainly composed of weathered rock. Figure 4.9 presents the velocity profile obtained from the SASW test and a table with the interpreted thickness and shear wave velocities for each layer found at this site. Pérez (2005) classified this site as soil profile type S_D because the calculated average shear wave velocity for the upper 30 meters was 270.6 m/s.

Velocity Profile

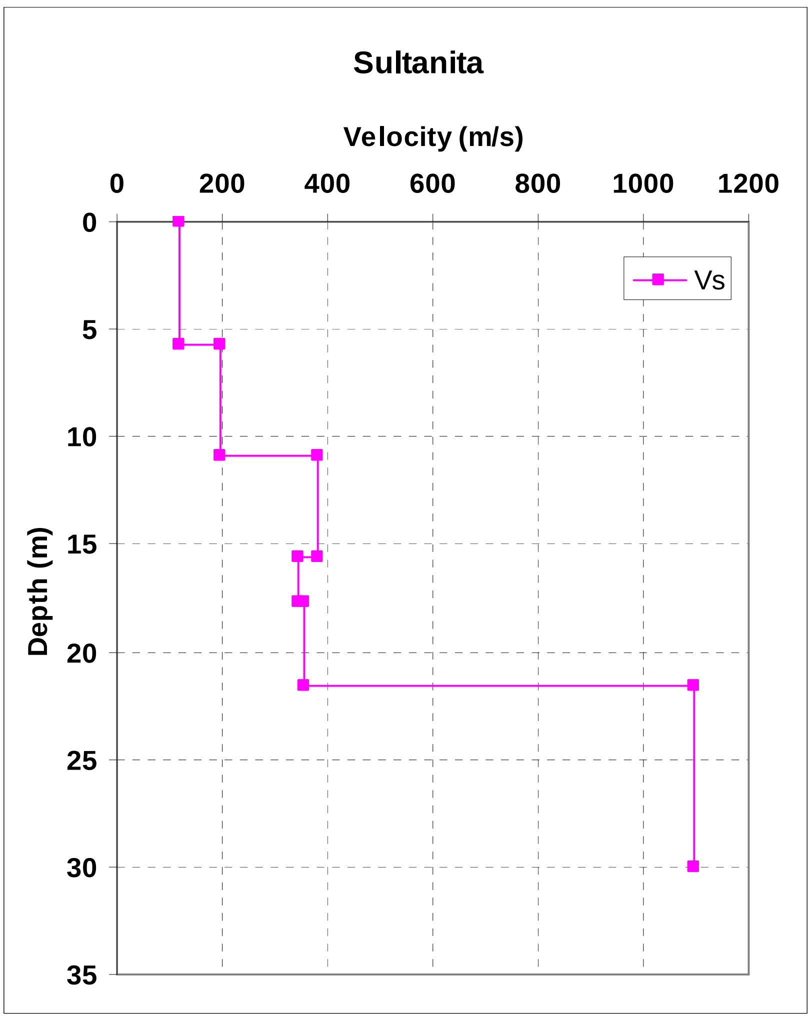

Profile Values

Sultanita Velocity Profile	
h	Vs
(m)	(m/s)
5.7	120.0
5.2	197.7
4.7	381.7
2.1	343.3
3.9	355.7
8.4	1097.4
Vs30 (NEHRP) =	270.6
Soil Type =	D

Figure 4.9 SASW Velocity Profile for Sultanita Site (from Pérez , 2005)

<u>Civil Engineering Site:</u>

The last site tested by Pérez (2005) in the Mayagüez area was located next to the building of the Civil Engineering Department of the University of Puerto Rico, Mayagüez Campus. At this site he obtained a shear wave velocity profile that increased with depth as shown on Figure 4.10. He found a low shear wave velocity layer near the surface, but it quickly increased with depth reaching 935 m/s below a depth of 14 meters. Pérez (2005) classified this site as soil profile type S_C with an average shear wave velocity of 457.1 m/s up to 30 meters depth. As mentioned before, Figure 4.10 presents the velocity profile obtained from the SASW test and a table with the interpreted thickness and shear wave velocities for each layer found at this site.

Velocity Profile | **Profile Values**

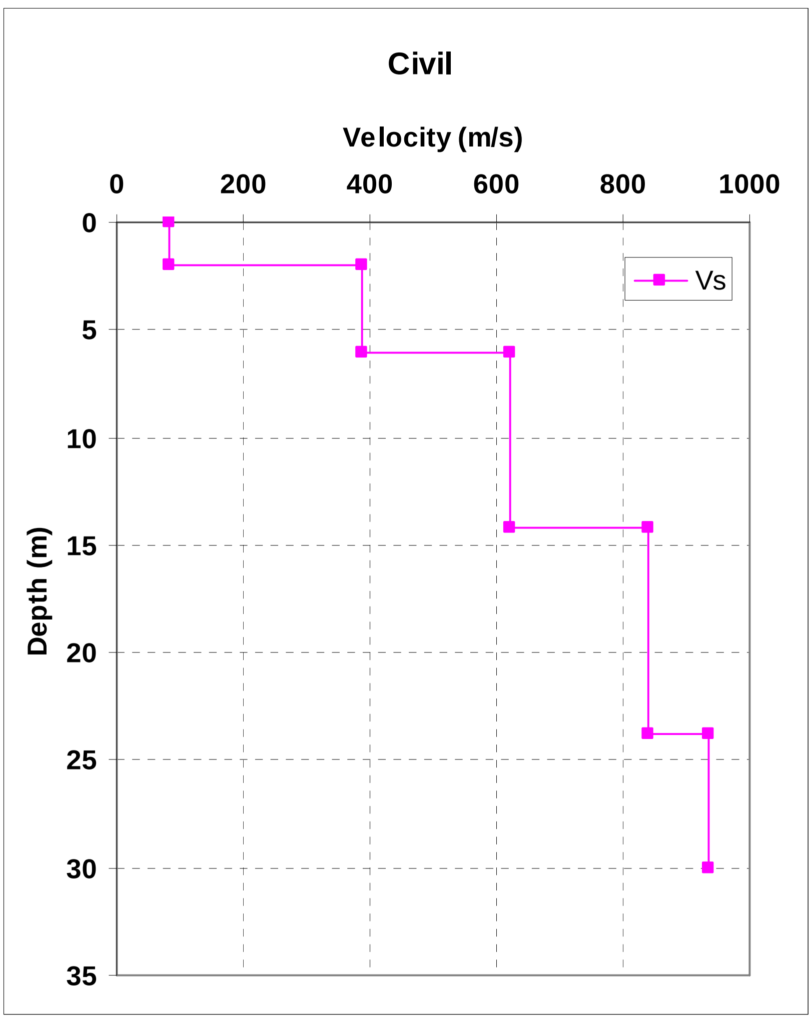

Civil	
Velocity Profile	
h	Vs
(m)	(m/s)
2.0	83.5
4.1	388.7
8.1	620.2
9.6	839.4
6.2	935.5
Vs30 (NEHRP) =	457.1
Soil Type =	C

Figure 4.10 SASW Velocity Profile for Civil Site (from Pérez, 2005)

4.2.2 *Data from Odum et al. (In preparation)*

During the summer of 2003 the United States Geological Survey (USGS) carried out several geophysical tests in collaboration with the Puerto Rico Seismic Network and the Puerto Rico Strong Motion Program. These tests consisted of seismic refraction and refraction microtremor (ReMi) tests. This section presents a summary of the results by Odum et al. (in preparation).

Odum et al. (in preparation) carried out geophysical tests at three sites in the Mayagüez area, including: El Seco Park, UPRM track field, and the Candelaria. The results for these three sites are presented below.

El Seco Park Site:

According to Odum et al. although six shear wave velocity layers were identified, they believed that only three primary geologic units were represented over the interpreted 30 m depth. They interpreted the first two layers (0 m to 1.5 m, Vs=230 m/s and 1.5 m to 3.0 m, Vs =648 m/s) as artificial fill layers where the uppermost layer is composed of compacted soil and the lower unit is likely composed of large boulder-sized and smaller rock pieces. Beneath the fill layers they interpreted a section of unconsolidated alluvial and near-shore marine material (Qal) (3.0 m to 8.0 m, Vs=150 m/s and 8.0 m to 20.0 m, Vs=172 m/s). They believed that the slight velocity increase at 8.0 m may represent an older, more consolidated unit and/or a change in lithology character. They also interpreted the lower layer (20.0 m to 30.0 m depth, Vs=340 m/s) to be weathered Ky bedrock. The calculated Vs30 for this site was 212 m/s, which is NEHRP soil type S_D (stiff soil). Figure 4.11 presents the compressional wave and shear wave velocity profiles obtained from seismic refraction and ReMi tests along with a table with the interpreted thickness and velocity for each layer found at this site.

Velocity Profile	Profile Values

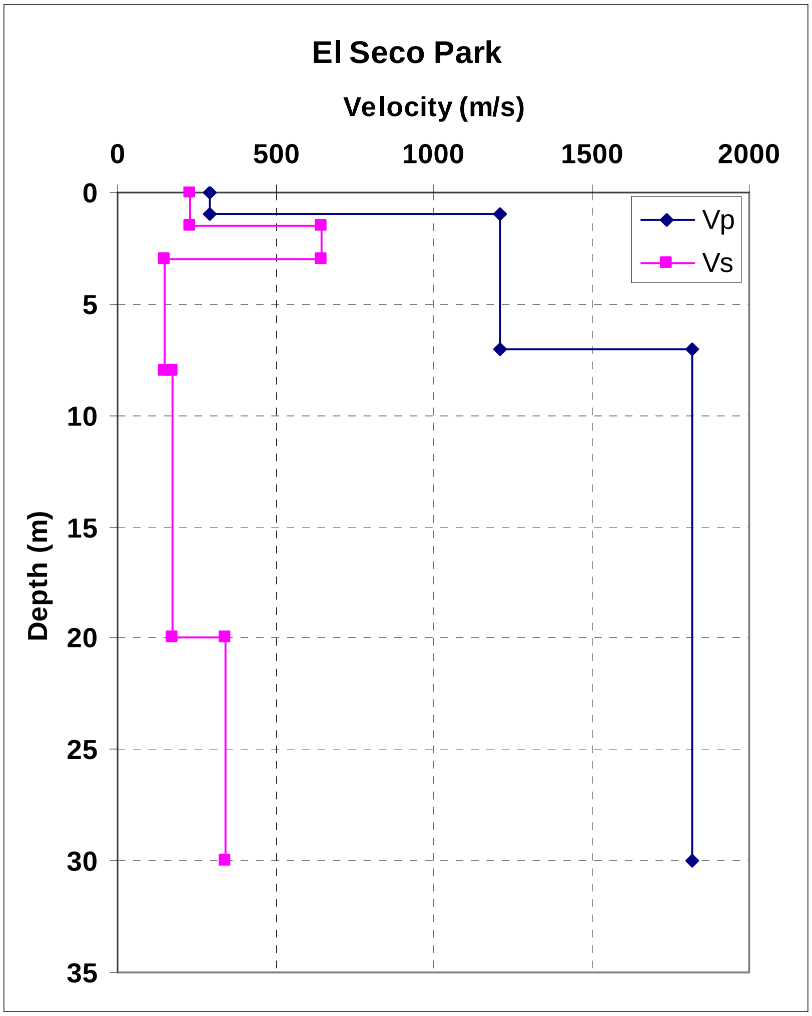

El Seco Park	
Vp	
h(m)	Velocity (m/s)
1	290
6	1210
23	1820
Vs	
h(m)	Velocity (m/s)
1.5	230
1.5	648
5	150
12	172
10	340
Vs30 (NEHRP) =	212
Soil Type =	D

Figure 4.11 Velocity Profiles for El Seco Park Site from Odum et al. (in preparation)

<u>*UPRM Track Site:*</u>

Odum et al. identified three distinct velocity layers for this site. They found a layer from the surface to 2.5 m depth, Vs=230 m/s, which they believed it consists of modified soil and artificial fill along with possibly a thin veneer of unconsolidated material (Qal). The velocity from 2.5 m to 16.5 m depth, Vs=140 m/s, was interpreted as saprolite derived from the weathering of the Yauco Formation (Ky). Their interpretation was based on a 30 m deep borehole drilled by Jaca & Sierra (Sierra del Llano, C.R., 2002) located a few hundred meters from the tested site, which indicates 29 m of saprolite beneath 1 m of artificial fill. From the SPT data a distinct physical property change in the bedrock occurred at approximately 16.0 m depth which they correlated with the dramatic increase in shear-wave velocity (Vs=140 m/s to Vs= 2400 m/s) that they interpret at approximately the same depth. The calculated Vs30 velocity for this site was 200 m/s, which is NEHRP soil type S_D. Figure 4.12, presents the compressional wave and shear wave velocity profiles obtained from seismic refraction and ReMi tests along with a table with the interpreted thickness and velocities for each layer found at this site.

Velocity Profile	Profile Values

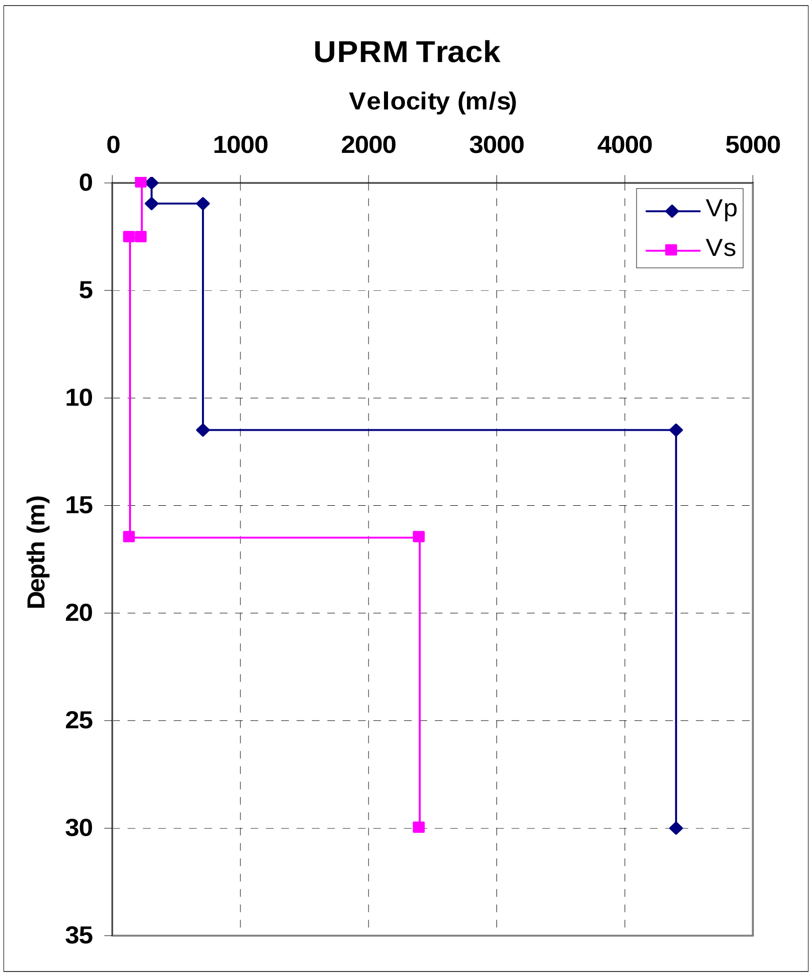

UPRM Track	
Vp	
h(m)	Velocity (m/s)
1.0	300
10.5	700
19.5	4400
Vs	
h(m)	Velocity (m/s)
2.5	230.0
14	140.0
13.5	2400.0
Vs30 (NEHRP) =	257.5
Soil Type =	D

Figure 4.12 Velocity Profiles for UPRM Track Site from Odum et al. (in preparation)

<u>*Candelaria Site:*</u>

Odum et al. identified two velocity layers in the upper three meters of this site. They interpreted the shear wave velocity from 0 m to 2 m, Vs=200 m/s, to be artificial fill. This layer overlies a 1 m thick layer, Vs=325 m/s, which they speculated to be another fill placed into what was probably a swamp area. Beneath the fill they found a 15 m thick, Vs=145 m/s, layer interpreted to be Qal. From 18 m to 30 m depth is a layer (Vs=355 m/s) which they interpreted to be saprolite (weathered Upper Cretaceous bedrock -Ky). The calculated Vs30 velocity for this site was 200 m/s, which is NEHRP soil type S_D. Figure 4.13, presents the compressional wave and shear wave velocity profiles obtained from seismic refraction and ReMi tests along with a table with the interpreted thickness and velocities for each layer found at this site.

Velocity Profile

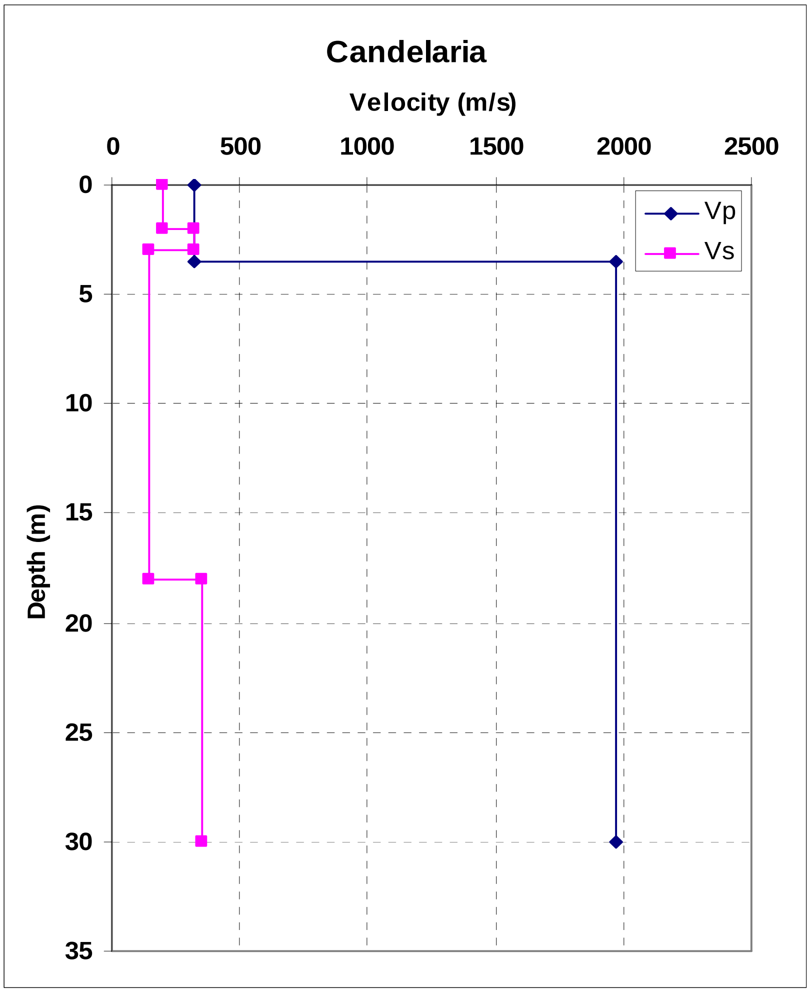

Profile Values

Candelaria	
Vp	
h(m)	Velocity (m/s)
3.5	300
26.5	700
Vs	
h(m)	Velocity (m/s)
2	200
1	325
15	145
12	355
Vs30 (NEHRP) =	200
Soil Type =	D

Figure 4.13 Velocity Profiles for Candelaria Site from Odum et al. (in preparation)

4.2.3 *Downhole Jaca & Sierra (2002)*

On 2002, the geotechnical company Jaca & Sierra conducted a series of geotechnical explorations to six seismic stations of the Puerto Rico Strong Motion Program. One of the geotechnical explorations was performed at the station located in the

University of Puerto Rico at Mayagüez. For this study, test borings and downhole seismic (DS) test were performed in order to obtain the compressional and shear wave velocity profiles of the soil. As reported by Jaca & Sierra, the borehole was drilled to a total depth of 26 m. For the DS test, the source energy was generated by impacting a wooden plank on the ground with a 16 lb sledgehammer. The shear wave velocities obtained from the DS test at the Mayagüez site ranged from 128 to 1963 m/s. The calculated Vs30 velocity for this site was 313 m/s, which is NEHRP soil type S_D. Figure 4.14, presents the shear wave velocity profiles obtained from DS test along with a table with the interpreted thickness and velocities for each layer found at this site.

Velocity Profile

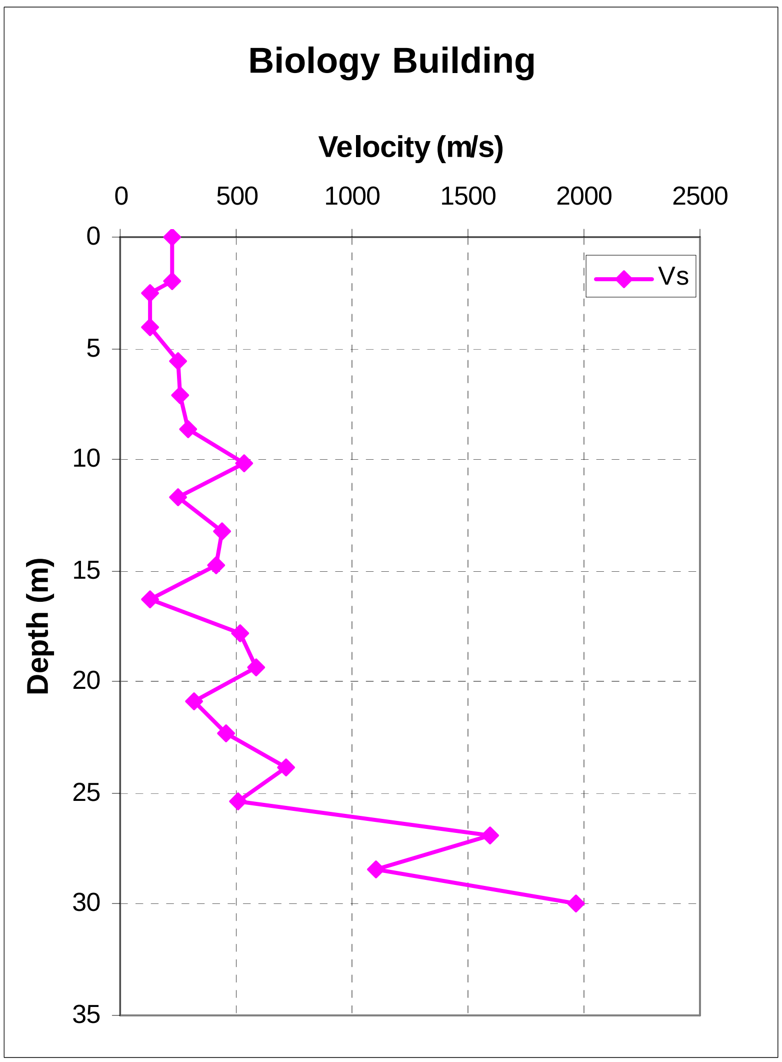

Profile Values

Biology Building	
Vs	
h(m)	Velocity (m/s)
0	222.5
1.9	222.5
2.5	131.1
4.1	128.0
5.6	253.0
7.1	256.0
8.6	295.7
10.2	533.4
11.7	249.9
13.2	435.9
14.7	414.5
16.3	128.0
17.8	515.1
19.3	588.3
20.8	323.1
22.4	457.2
23.9	713.2
25.4	512.1
26.9	1594.1
28.5	1106.4
30.0	1962.9
Vs30 (NEHRP) =	313
Soil Type =	D

Figure 4.14 Shear Wave Velocity results for Biology Building Site from Jaca & Sierra (Sierra del Llano, C.R., 2002)

4.3 *Geophysical Testing for this Study*

Seismic refraction tests were carried out as part of this research. The background theory of this method was presented in Chapter 2. This section describes the equipment, the data reduction process, and the results obtained.

4.3.1 *Equipment and Field Test Setup*

The equipment used to perform the seismic refraction tests consisted of a Geometrics ES-2401 seismograph recording system with support cables and geophones property of the Department of Geology at the University of Puerto Rico, Mayagüez Campus. Geophones with a natural frequency of 4.5 Hz were used to record the time of arrival of compressional waves generated by the energy source. The survey line consisted of 24 geophones at three meter spacing. The cable was laid out along the ground in a straight line. The energy source was aligned with the geophones, usually at the same distance as the geophone spacing at both ends of the survey line. This test arrangement is also known as the In-line spread. Figure 4.15 shows the refraction survey equipment and layout used in this study.

Figure 4.15 Equipment and Field Test Setup

Two different types of energy sources were used during the tests. The first energy source consisted of a twelve pound sledgehammer striking a steel plate placed on the ground. The second energy source used consisted of a downhole percussion firing rod, loaded with percussion black powder blanks of 300 grains, which was buried about one meter before it was detonated as shown in Figure 4.16. The energy produced by the sledgehammer source was found to be relatively low, and the registered data was influenced by ambient noise, hence time of arrival of the compressional waves was often not clear or well defined. In order to reduce the influence of the ambient noise the data from sledgehammer strikes were stacked at least six times. As the first arrival time of the compressional waves is the same on each shot, the stacking method allowed discerning between the first arrival time and the ambient noise on the record. Due to the high energy produced by the downhole percussion rod, only one shot was required for most of the field studies. Data was collected placing the energy source on both sides of the refraction line in order to obtain the soil profile at each site. The sample interval was 0.2 ms with a total record length of 409 ms.

Figure 4.16 Downhole Percussion Firing Rod

4.3.2 *Data Reduction Procedure*

Analyses of seismic refraction data were performed by Carmen Y. Lugo and Wilmel Varela under the supervision of Dr. Eugenio Asencio of the University of Puerto Rico, Mayagüez Campus. Field files of the compressional wave data were processed using the commercial processing software developed by SeisImager (SeisImager Software, 2000). The general procedure used to process the field data was to: (i) convert the raw data from the seismograph into time-distance data, (ii) bandpass filter the records and obtain first-break picks, (iii) apply time-term inversion methods to obtain velocity profiles. A detailed description of the field data processing is provided below:

1. First, the raw data (SEG2 files) was extracted from the seismograph to Pickwin95 software (SeisImager Software, 2000). This software reads and displays the refraction data as time-distance curves. In order to remove the ambient noise to obtain better data a high-cut filter, usually 512 Hz, or a low-cut filter, usually 38 Hz, were used. After the application of the filters the first arrivals of the compressional wave (P-wave) were fitted by straight lines. This technique was used because the final goal was not to obtain the specific geometric details of the subsurface interface, but rather in the generalities of the profile such as the velocity, thickness, and dip which would affect the velocity estimates. An example of the first arrival picks of the compressional wave is shown in Figure 4.17 which was used as an input file for the time-term inversion method.
2. After first-break picks were obtained, the data was imported into Plotrefa software (SeisImager Software, 2000). This software uses the output of Pickwin95 as an input and through the application of an interpretation technique (time-term inversion) a layer velocity profile was obtained. Once the travel-time vs. distance was displayed, soil layers were assigned in the model (see Figure 4.18) and the time-term inversion was performed to obtain the site P-wave velocity profile. The time-term technique used by the program is a linear least-squares approach to determine the best discrete-layer solution to the data. This method use the Snell's law described in Chapter 2.

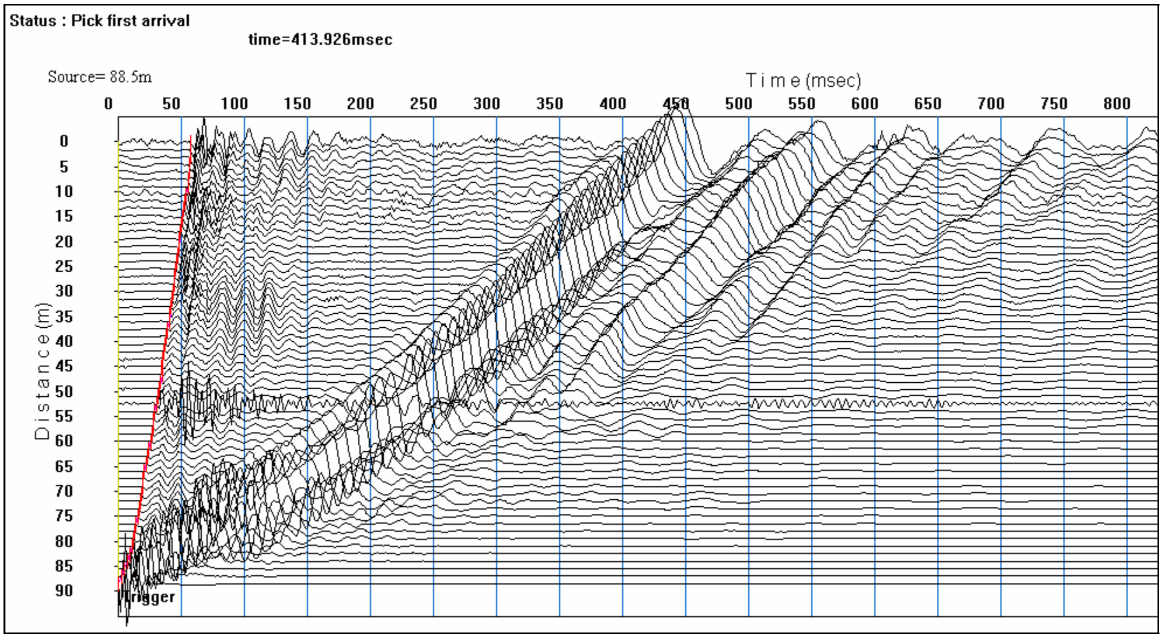

Figure 4.17 Field Seismogram opened on Pickwin95

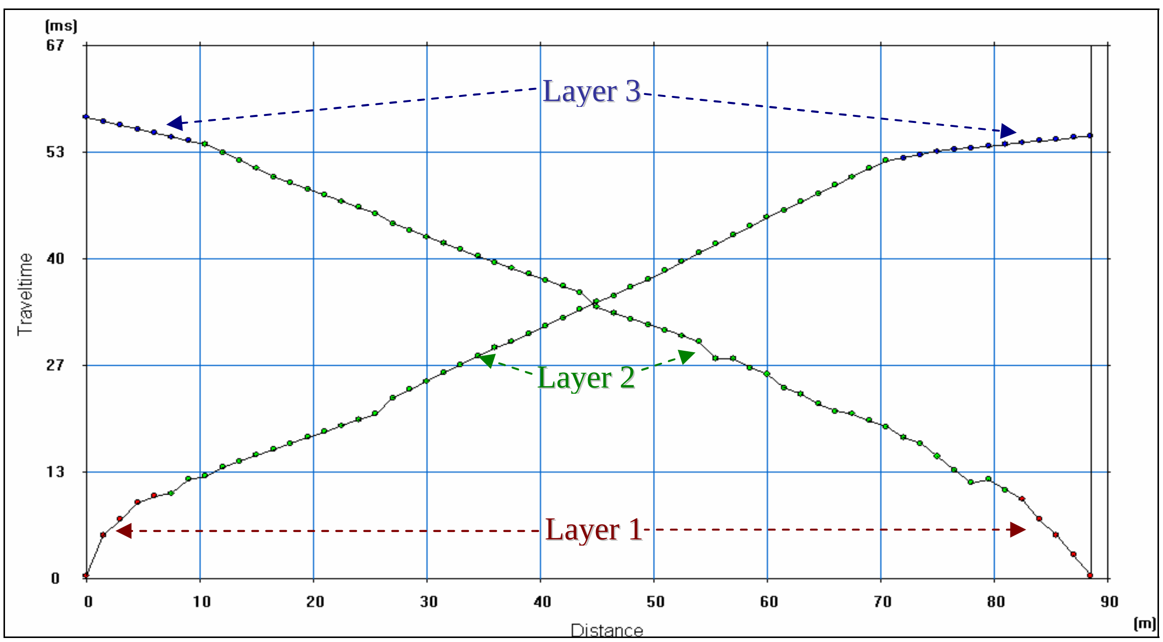

Figure 4.18 Assignment of Soil Layers or Interpretation of Seismic Data

3. In an attempt to correlate compressional wave (P-wave) velocities to shear wave (S-wave) velocities the Poisson's ratio was used. As stated in seismic and geophysics literature shear wave velocities can be estimated from compressional wave velocities using the following relation:

$$V_s = \frac{V_p}{\sqrt{\frac{1-\nu}{0.5-\nu}}} \qquad \textbf{Eq. 4-1}$$

Where:

V_s = shear wave velocity

V_p = compressional wave velocity

ν = Poisson's ratio

Based on Burger (1992) for geophysical explorations of shallow subsurface on soils and unconsolidated materials the S-wave velocity profile can be estimated as the 40 percent of the P-wave value. However, this is a generalized assumption which includes a large variety of soils. Therefore, typical values of Poisson's ratio for soils and rocks were adapted from Kulhawy (1983), Trautmann and Kulhawy (1987), and Coduto (2001). Table 4.2 was generated using the Poisson's ratio values obtained from these references:

Table 4.2 Typical Values of Poisson's Ratio for Soils and Rocks

Soil or Rock Type	Poisson's Ratio (ν)
Saturated Clay	0.50
Partially Saturated Clay	0.30-0.40
Loose Sand	0.20-0.40
Medium Dense Sand	0.25-0.40
Dense Sand	0.30-0.45
Silty Sand	0.20-0.40
Sand and Gravel	0.15-0.35
Sandstone	0.25-0.30
Granite	0.23-0.27

In order to estimate Poisson's ratio value for the layers defined by compressional waves on each site, available boring log data from nearby areas were meticulously examined. Boring log data, combined with compressional wave velocities and geologic maps, allowed to define the soil characterization of each layer profile and thus the selection of the Poisson's ratio value according to the soil type.

Using the above procedure, shear wave velocity profiles were estimated from compressional wave velocities. Results are presented in the following section.

4.3.3 *Results*

Seismic refraction explorations were performed at six locations in the Mayagüez area. Available boring log data and geologic maps were the basis to selecting the locations of the refraction surveys. Sites were chosen at locations where limited or no geotechnical data was available, or places where the conditions were considered favorable for liquefaction occurrence. Figure 4.19 presents a map of Mayagüez showing the location of the tested sites overlapped by the geological map. It is shown that all the locations are founded mostly over Quaternary Alluvium (Qal) deposits even though the UPRM and Matadero sites are near Yauco Formation (Ky) and Sábana Grande Formation (Ksg) respectively. The Quaternary Alluvium (Qal) consists of sand, silt and gravels, and includes rock falls and landslide deposits. The Yauco Formation (Ky) consists of calcareous volcanoclastic sandstone, siltstone, claystone, limestone, breccia, and conglomerate. The Sábana Grande Formation (Ksg) consists of massive breccia, conglomerate sandstone, siltstone, claystone and limestone. Table 4.3 provides the specific geographic coordinates for each of the tested sites.

Table 4.3 Tested Sites Coordinates

Sites	Geographic Coordinates
Abonos Super A	18º16’00.0”N - 67º09’45.0”W
El Mani	18º14’53.1”N - 67º10’29.6”W
El Seco Park	18º13’09.6”N - 67º09’34.2”W
UPRM	18º12’25.6”N - 67º08’24.6”W
Candelaria	18º11’42.0”N - 67º09’02.0”W
Matadero	18º09’49.4”N - 67º09’30.7”W

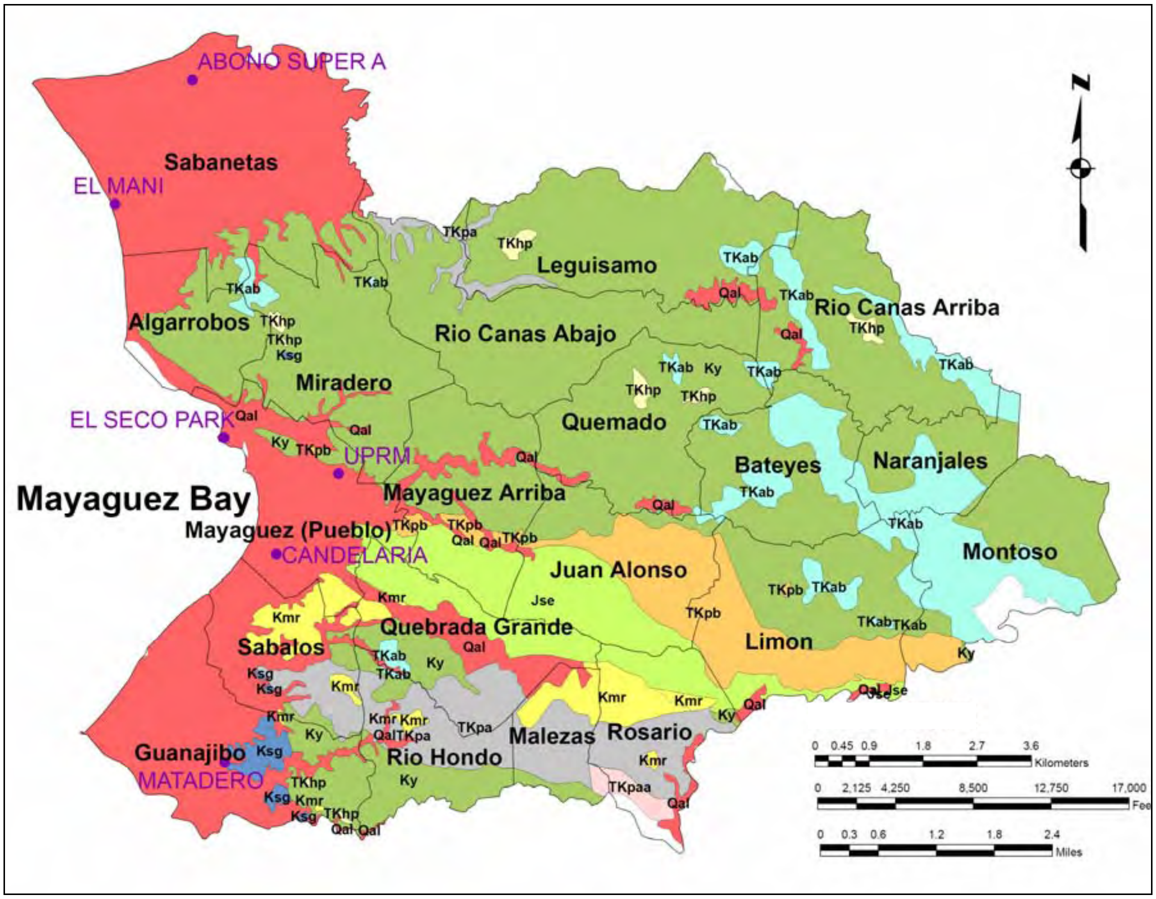

Figure 4.19 Location of Seismic Refraction Explorations

At each site the geophysical testing field work was completed following the procedure discussed previously and shear and compressional wave velocities profile were generated for each site following the data reduction process described in 4.3.2. Results for the six sites are presented below.

Abono Super A Site:

The Abono Super A site is located in the north part of the Añasco Valley at the west side of the PR-2 highway. The test was performed in a flat surface ground in front of the Abono Super A factory. Figure 4.20 shows an aerial view of the site obtained from Google Earth© (2006). This site is considered as a flat terrain and is mainly used as a cultivation field. The Añasco Valley is located on the Barrio Sabanetas which according to the geologic map is mostly founded on alluvial soils. Macari (1994) mentioned on his report that these alluvial deposits may extend to depth in excess of 100 ft.

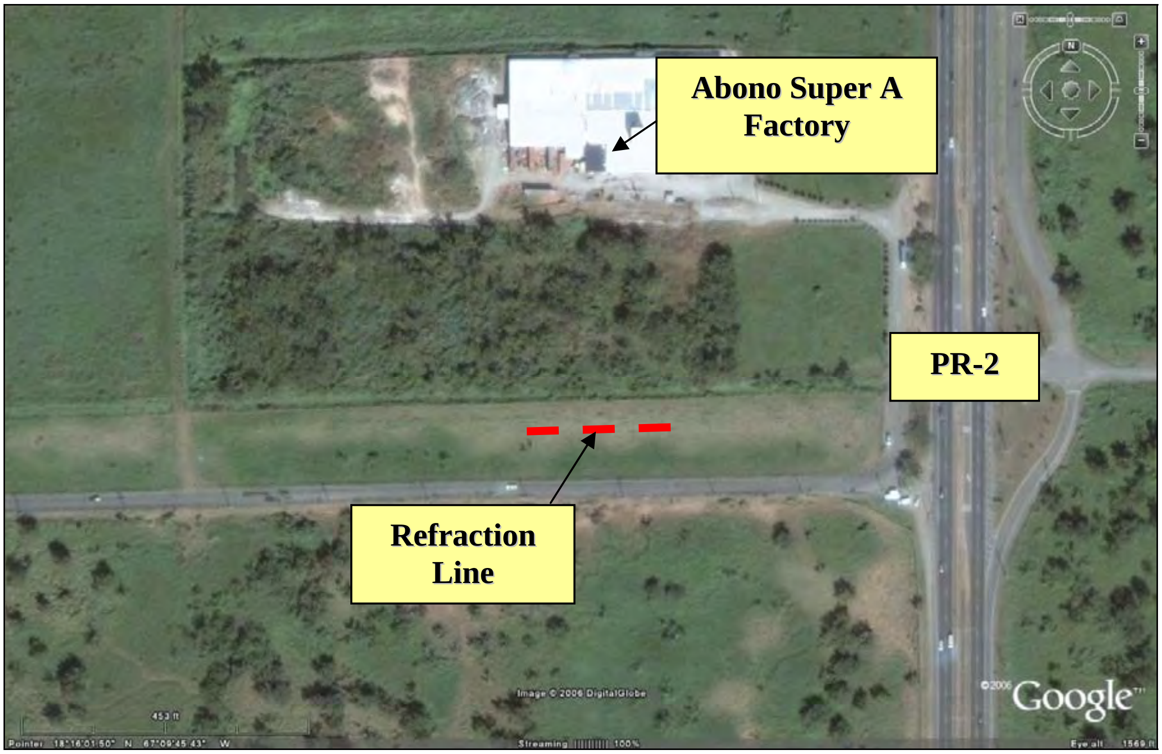

Figure 4.20 Aerial View of Abono Super A Site

After performing the required analysis, compressional wave and shear wave velocity profiles shown on Figure 4.21 were obtained. Figure 4.21 also contains a table that lists the thickness, shear wave, and compressional wave velocities of the layers found on this site. To define the soil characterization for this site the report MYWS047 was selected, specifically the boring log performed by Jaca & Sierra Testing Laboratories, in combination with the site geology. From the analysis a compacted material, apparently unsaturated silty clay, was estimated for the first 5 meters deep from the surface. For this layer a shear wave velocity of 259 m/s was estimated. Below this, it is believed that the same material with some sand, 8 meter thick, was found but in saturated conditions with an estimated shear wave velocity of 197 m/s. Then, a third layer, 11 meters thick, consisting of a saturated sandy clay was estimated with a shear wave velocity of 348 m/s. In order to obtain an average shear wave velocity (Vs30) it was assumed that the same material extends up to 30 meter below the ground surface. For this site Vs30 was 276 m/s which is classified as soil type S_D according to NEHRP and UBC-97.

Velocity Profile

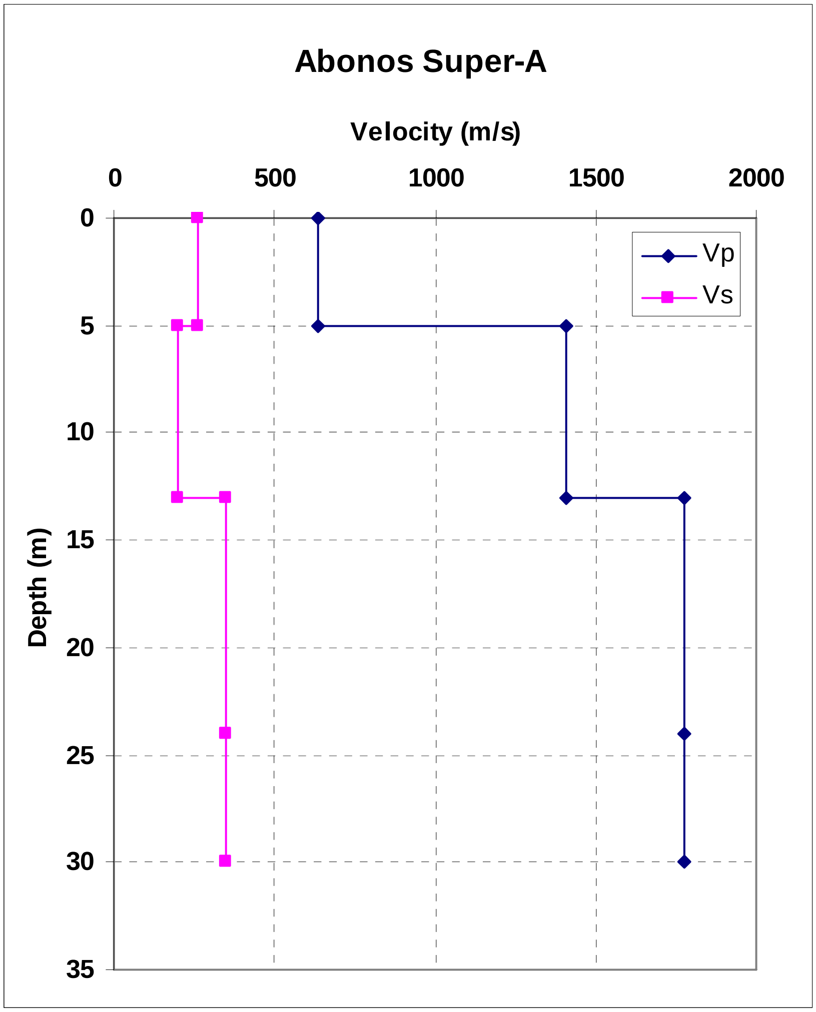

Profile Values

	Velocity (m/s)	
h (m)	Vp	Vs
5	636	259.6
8	1410	197.4
11	1777	348.5
6	1777	348.5
Vs30 (NEHRP) =		276.4
Soil Type =		D

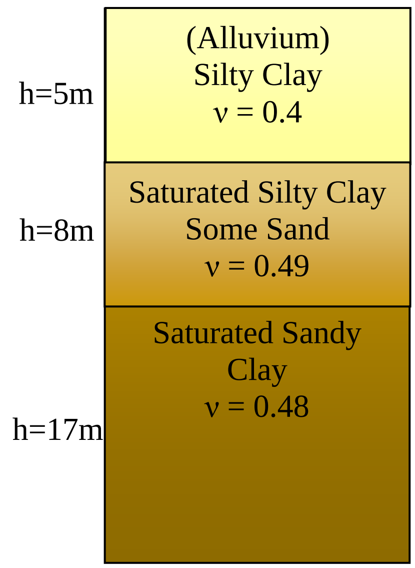

Figure 4.21 Velocity Profile for Abono Super A Site

El Maní Site:

El Maní site is also located in the Barrio Sabanetas but adjacent to the Mayagüez coast. The test was performed in a flat surface ground in front of the Maní baseball field. Figure 4.22 shows an aerial view of the site obtained from Google Earth© (2006). This site is considered as lowland, flat terrain, founded over alluvial and Holocene beach deposits that consist of rounded, moderately to well sort sands, and minor gravel.

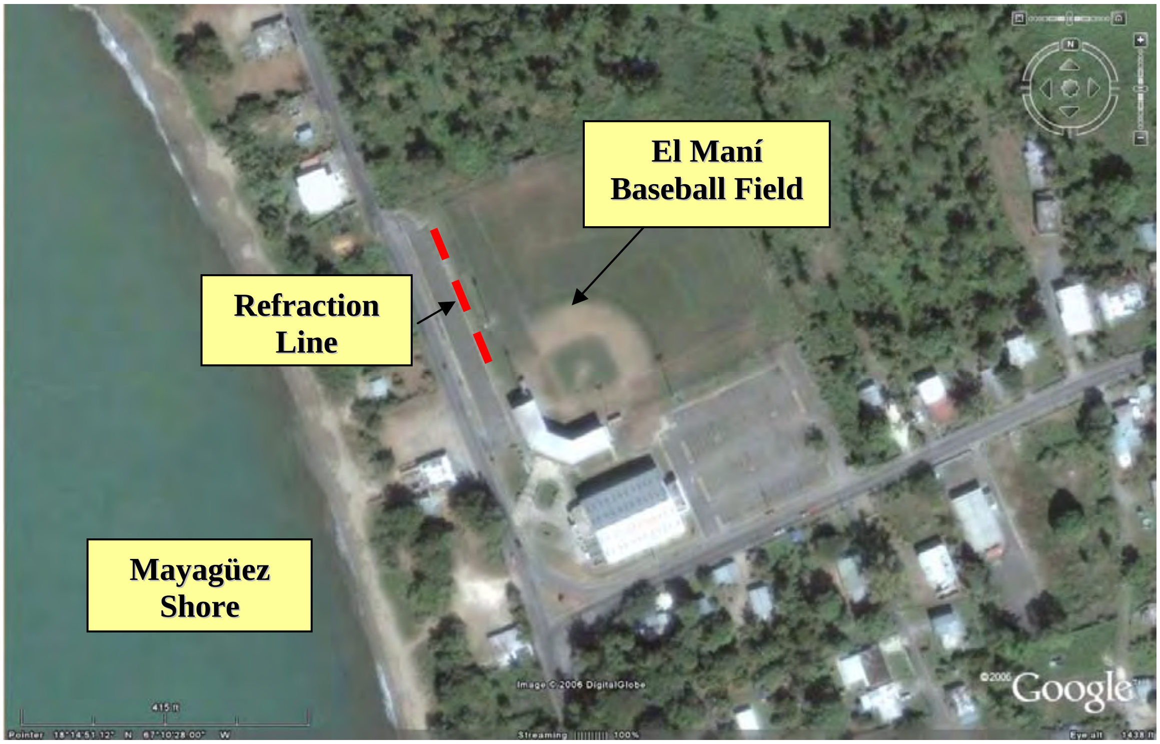

Figure 4.22 Aerial View of El Maní Site

Figure 4.23 shows the compressional wave and shear wave velocity profiles obtained for El Maní site. Additionally, a table that lists the thickness, shear wave, and compressional wave velocities for each layer is also shown on this figure. To define the soil characterization for this site the report MYWS054 was selected, specifically the boring log performed by Western Soil Inc., in combination with the site geology. From the analysis apparently a stiff to very stiff silty clay, was estimated for the first 4 meters deep from the surface. For this layer a shear wave velocity of 300 m/s was estimated. Below this, it is believed that a layer of saturated hard clay with rock fragments, 11 meter thick, was found with an estimated shear wave velocity of 219 m/s. Then, a third layer, 15 meters thick, consisting of saturated hard clayey silt with rock fragments was estimated with a shear wave velocity of 386 m/s. For this site Vs30 was 293 m/s which is classified as soil type S_D according to NEHRP and UBC-97.

Velocity Profile	Profile Values

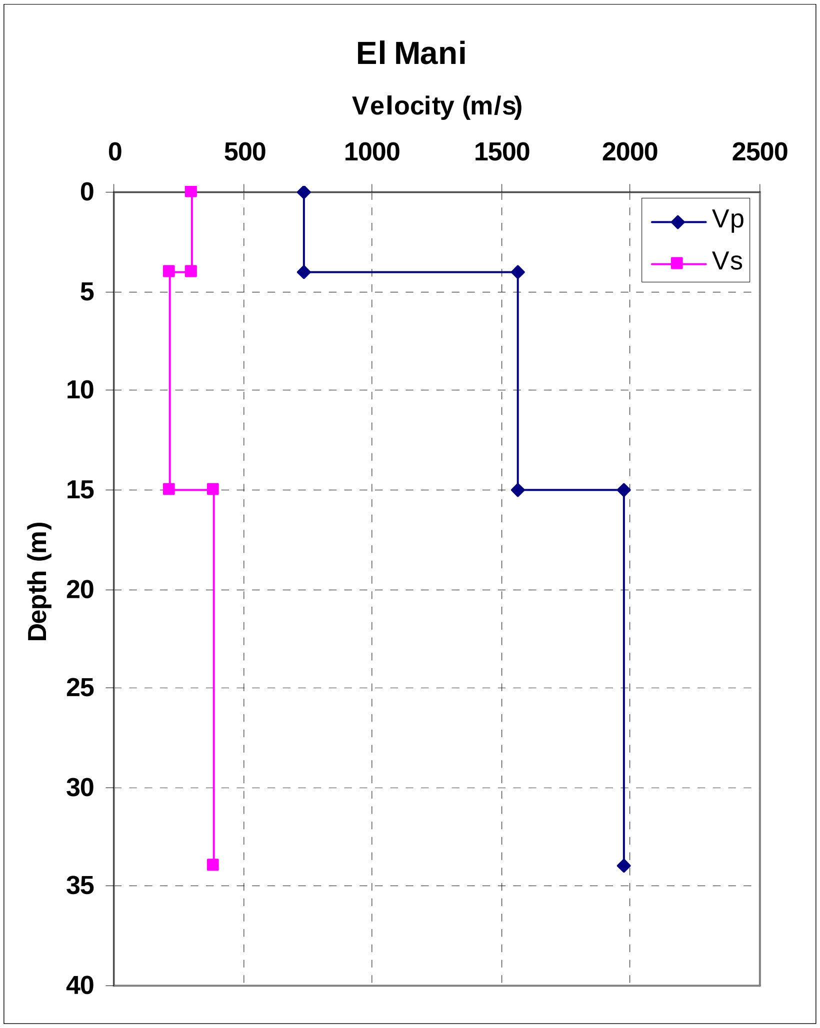

h (m)	Velocity (m/s) Vp	Vs
4	737	300.9
11	1566	219.3
15	1971	386.5
Vs30 (NEHRP) =		293.4
Soil Type =		D

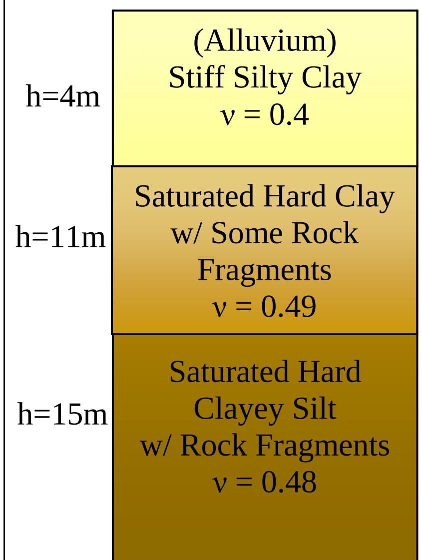

Figure 4.23 Velocity Profile for El Maní Site

El Seco Park Site:

El Seco Park site is located in the Barrio Mayagüez (Pueblo) in a neighborhood known as El Seco. This site located on the north end of the Mayagüez Bay coast, a few miles south of the El Maní site. The test was performed in a flat surface ground inside of the El Seco baseball field. Figure 4.24 shows an aerial view of the site obtained from Google Earth© (2006). As El Maní site, this site is considered a flat terrain founded over alluvial and Holocene beach deposits that consist of rounded, moderately to well sort sands, and minor gravel.

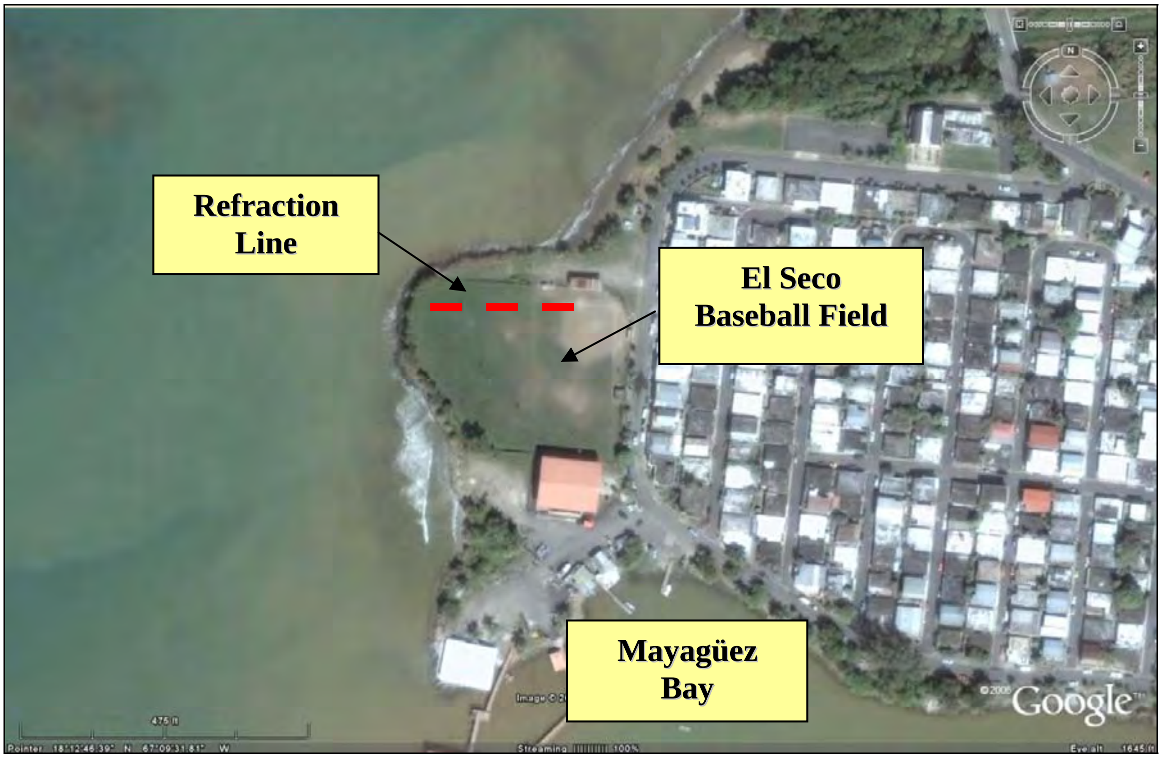

Figure 4.24 Aerial View of El Seco Park Site

Figure 4.25 shows the compressional wave and shear wave velocity profiles obtained for El Seco Park site. Additionally, a table that lists the thickness, shear wave, and compressional wave velocities for each layer is also shown on this figure. To define the soil characterization for this site the reports MYWS049 and MYWS006 were selected, specifically the boring log performed by Western Soil, Inc., in combination with the site geology. From the analysis apparently sand and gravel with rock fragments was estimated for the first 2 meters deep from the surface. For this layer a shear wave velocity of 259 m/s was estimated. Below this fill, it is believed that a layer of saturated stiff silty clay, 21 meter thick, was found with an estimated shear wave velocity of 223 m/s. Then, a third layer, 7 meters thick, consisting of saturated hard silty clay was estimated with a shear wave velocity of 450 m/s. For this site Vs30 was 256 m/s which is classified as soil type S_D according to NEHRP and UBC-97.

Velocity Profile	Profile Values

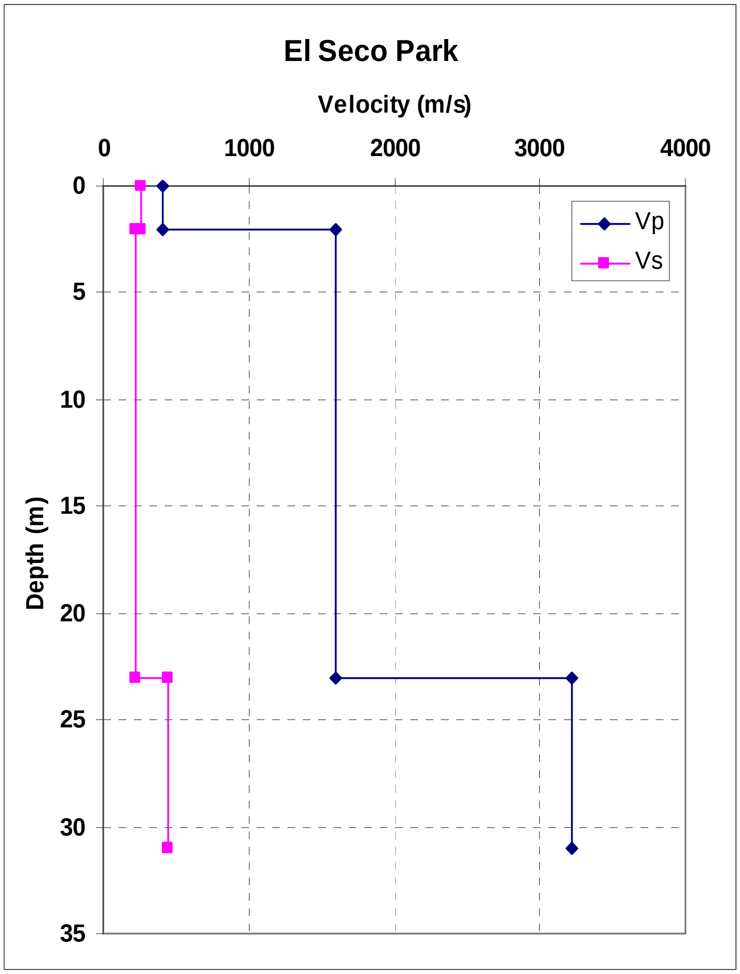

	Velocity (m/s)	
h (m)	Vp	Vs
2	404	259.2
21	1596	223.5
7	3214	450.1
Vs30 (NEHRP) =		255.9
Soil Type =		D

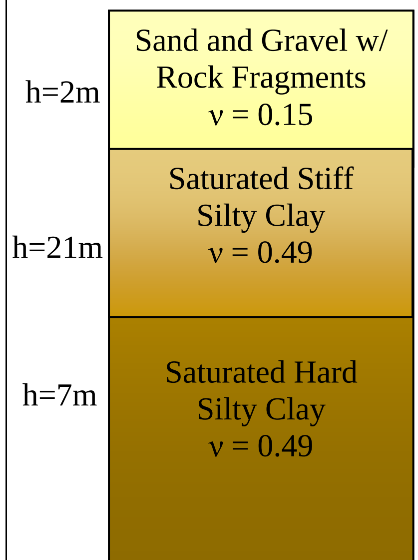

Figure 4.25 Velocity Profile for El Seco Site

<u>UPRM Track Site:</u>

The UPRM Track site is located in the barrio Mayagüez (Pueblo), outside of the coastal area. The test was also performed in a flat surface ground inside UPRM Track field. Figure 4.26 shows an aerial view of the site obtained from USGS database located on the internet (www.usgs.gov) which was also included on the GIS Database developed for this project. This site is located on an alluvial valley, considered a flat terrain and founded over alluvial deposits.

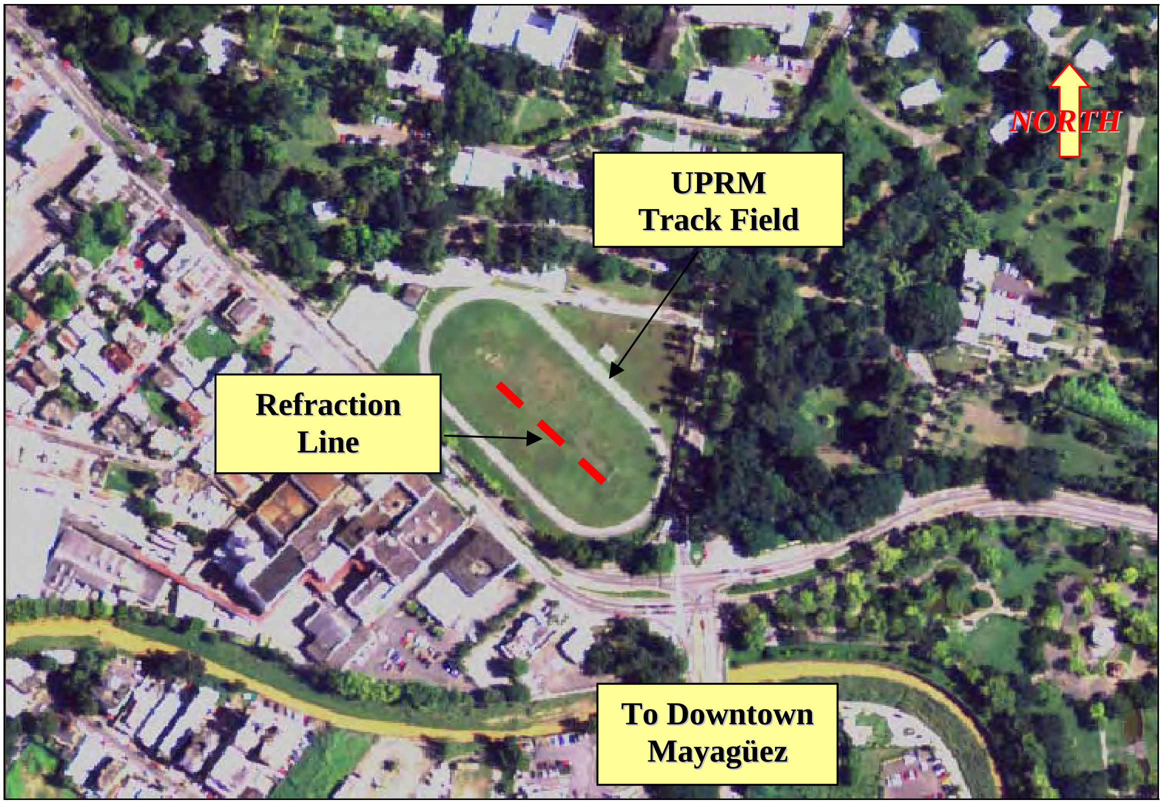

Figure 4.26 Aerial View of UPRM Site

Figure 4.27 shows the compressional wave and shear wave velocity profiles obtained for UPRM Track site. Additionally, a table that lists the thickness, shear wave, and compressional wave velocities for each layer is also shown on this figure. To define the soil characterization for this site the report MYJS115 was selected, specifically the boring log performed by Jaca & Sierra Testing Laboratories, in combination with the site geology. From the analysis, saturated sandy clay was estimated for the first 11 meters deep from the surface. For this layer a shear wave velocity of 86 m/s was estimated. Below this, it is believed that a layer of silty sand with highly weathered rock fragments, 19 meters thick, was found with an estimated shear wave velocity of 2102 m/s. For this site Vs30 was 220 m/s which is classified as soil type S_D according to NEHRP and UBC-97.

Velocity Profile	Profile Values

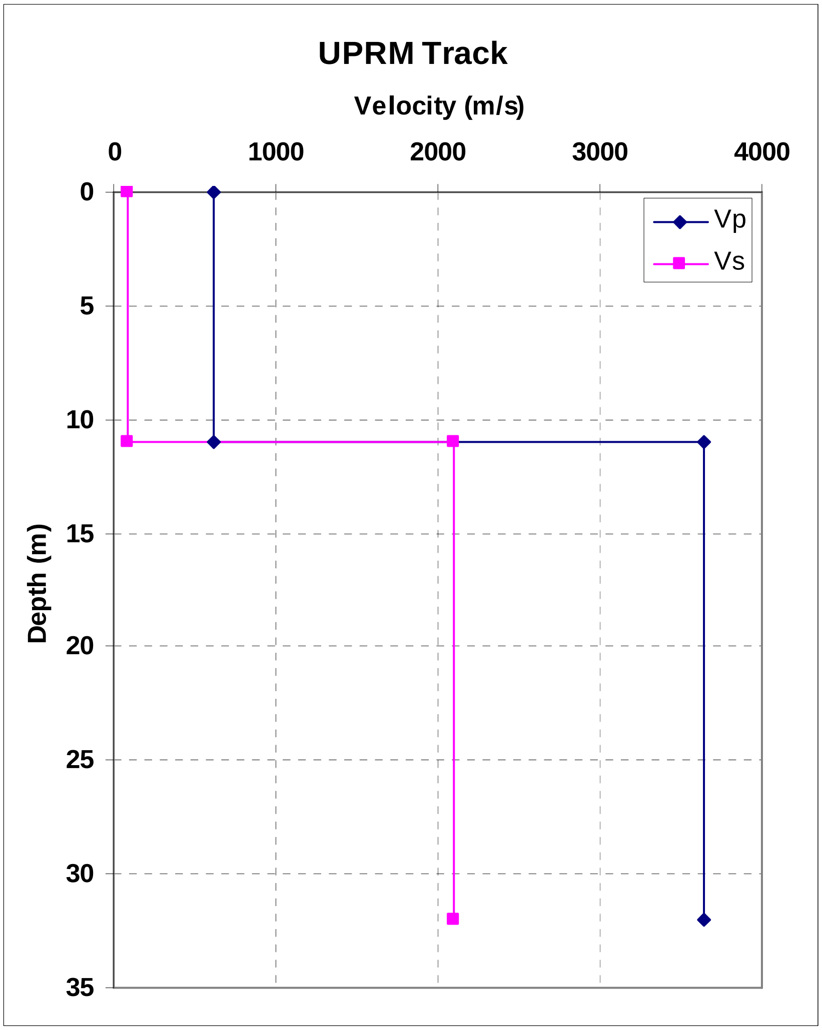

	Velocity (m/s)	
h (m)	Vp	Vs
11	618	86.5
19	3640	2101.6
Vs30 (NEHRP) =		220.3
Soil Type =		D

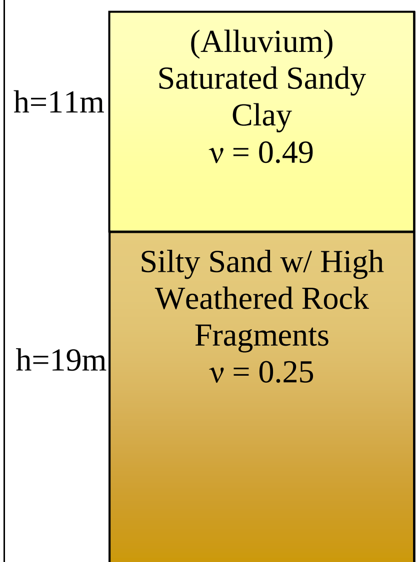

Figure 4.27 Velocity Profile for UPRM Track Site

Candelaria Site:

The Candelaria site is also located in the barrio Mayagüez (Pueblo) in a neighborhood called Candelaria. The test was performed in a flat surface ground on a vacant lot besides the PR-2. Figure 4.28 shows an aerial view of the site obtained from USGS database located on the internet (www.usgs.gov) which was also included on the GIS Database developed for this project. This site is considered a flat terrain founded over alluvial deposits that consist of rounded, moderately to well sort sands, and minor gravel.

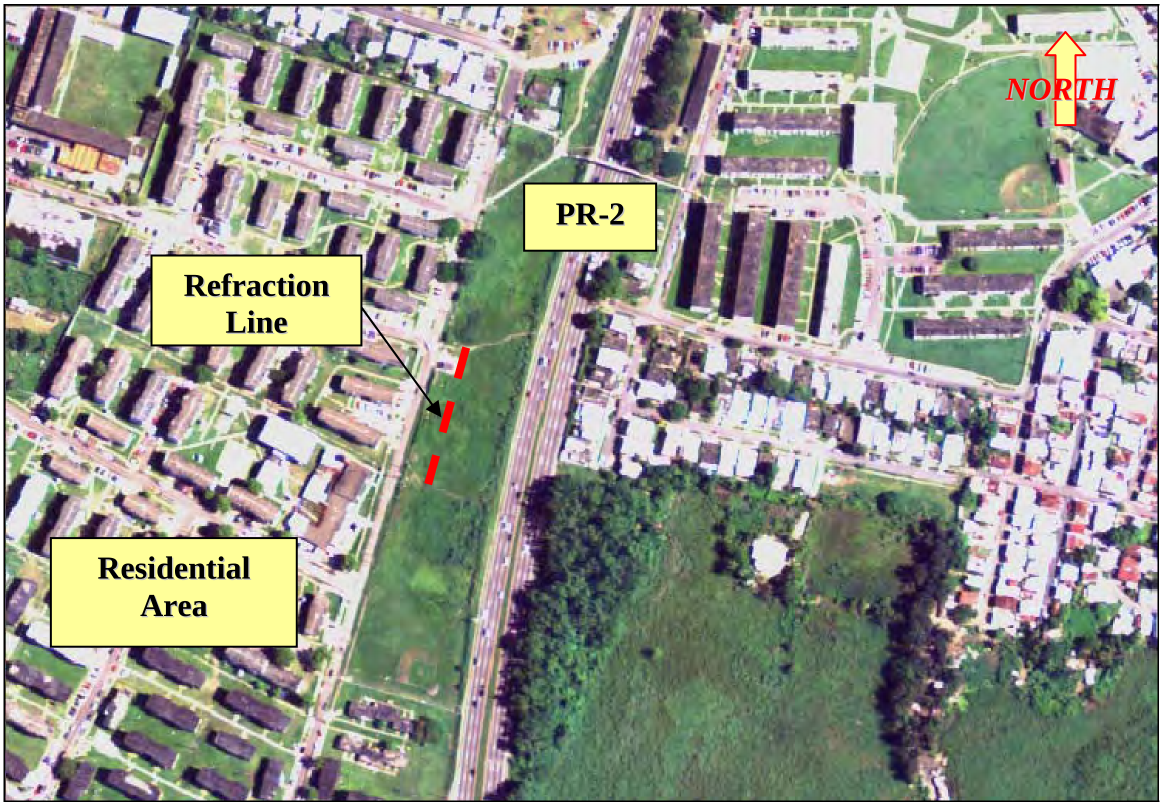

Figure 4.28 Aerial View of the Candelaria Site

Figure 4.29 shows the compressional wave and shear wave velocity profiles obtained for Candelaria site. Additionally, a table that lists the thickness, shear wave, and compressional wave velocities for each layer is also shown on this figure. To define the soil characterization for this site the report MYWS033 was selected, specifically the boring log performed by Western Soil Inc., in combination with the site geology. From the analysis apparently a sand and gravel layer was estimated for the first 4 meters deep from the surface. For this layer a shear wave velocity of 181 m/s was estimated. Below this, it is believed that a layer of saturated stiff silty clay, 10 meters thick, was found with an estimated shear wave velocity of 224 m/s. The traffic noise in the area was responsible for the data degradation which limited the imaging depth at the site to 14 meters. In order to obtain an average shear wave velocity (Vs30) it was assumed that the same material extends up to 30 meter below the ground surface. For this site Vs30 was 217 m/s which is classified as soil type S_D according to NEHRP and UBC-97.

Velocity Profile	Profile Values

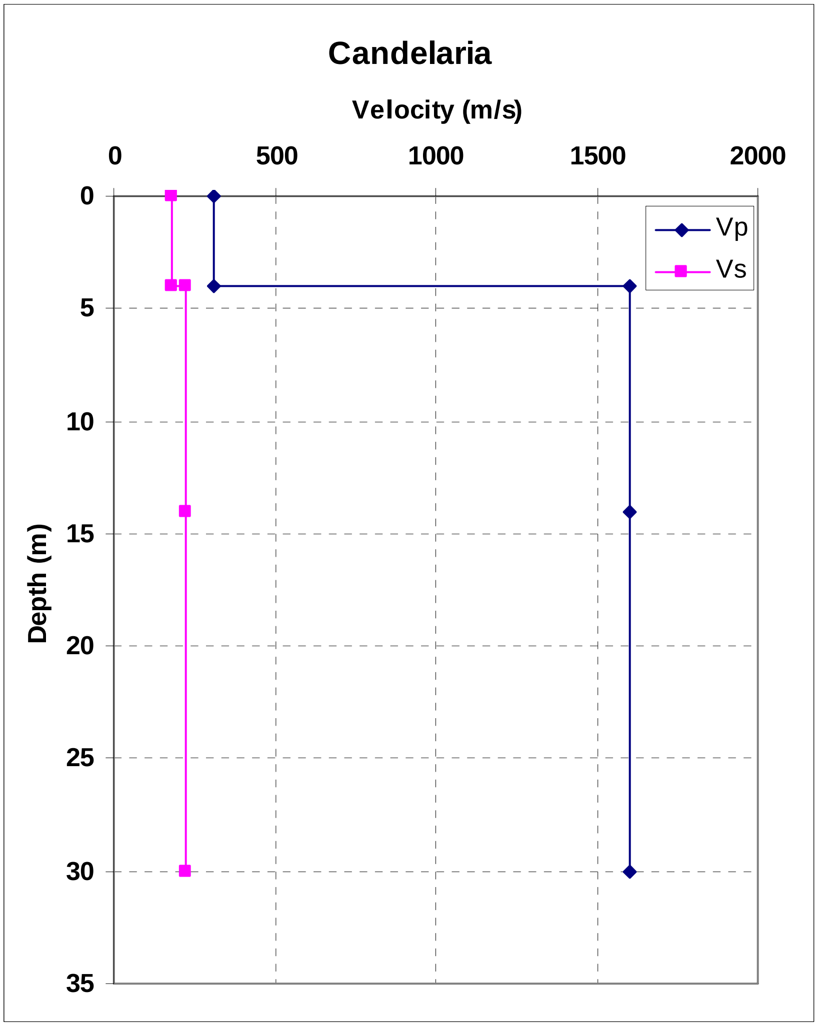

	Velocity (m/s)	
h (m)	Vp	Vs
4	313	180.7
10	1601	224.2
16	1601	224.2
Vs30 (NEHRP) =		217.2
Soil Type =		D

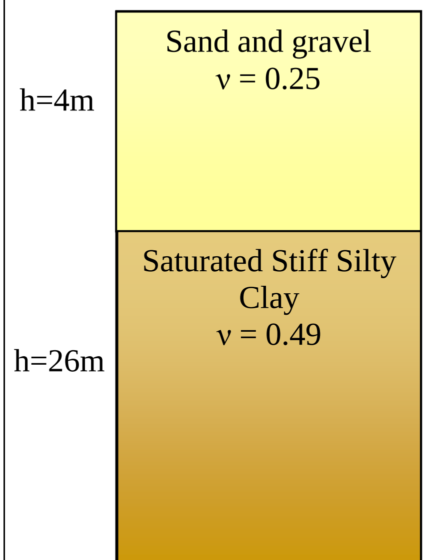

Figure 4.29 Velocity Profile for Candelaria Site

Matadero Regional Site:

The Matadero Regional site is located in the Barrio Guanajibo located on the south part of Mayagüez. The test was performed in a relatively flat surface ground on the backyard of the Matadero Regional Office. Figure 4.30 shows an aerial view of the site taken from Google Earth© (2006). This site is considered as a flat terrain founded over Quaternary alluvium and mangrove and swamp deposits.

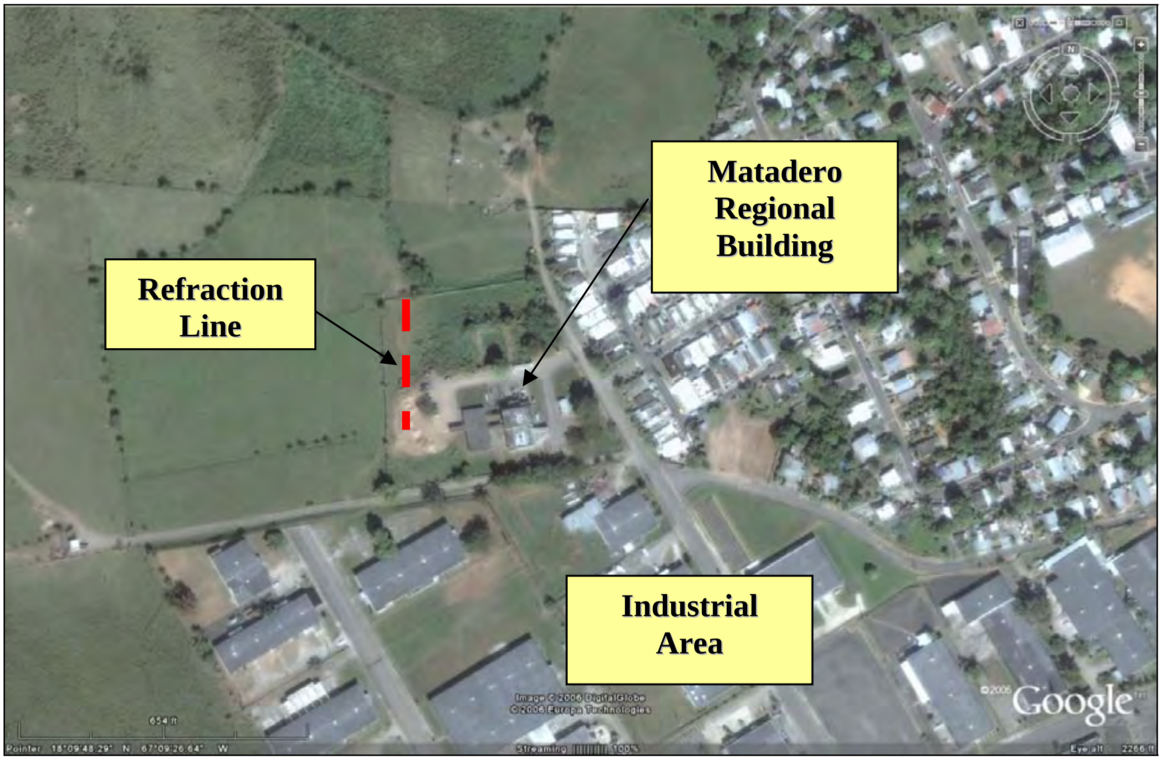

Figure 4.30 Aerial View of the Matadero Regional Site

Figure 4.31 shows the compressional wave and shear wave velocity profiles obtained for Matadero Regional site. Additionally, a table that lists the thickness, shear wave, and compressional wave velocities for each layer is also shown on this figure. To define the soil characterization for this site the report MYPM081 was selected, specifically the boring log performed by Ponce I&M Engineering Laboratory Inc., in combination with the site geology. From the analysis, a silty clay with trace sand layer was estimated for the first 5 meters deep from the surface. For this layer a shear wave velocity of 240 m/s was estimated. Below this, it is believed that a layer of saturated very stiff silty clay with weathered rock fragments, 18 meter thick, was found with an estimated shear wave velocity of 464 m/s. In order to obtain an average shear wave velocity (Vs30) it was assumed that the same material extends up to 30 meter below the ground surface. For this site Vs30 was 402 m/s which is classified as soil type S_C according to NEHRP and UBC-97.

Velocity Profile	Profile Values

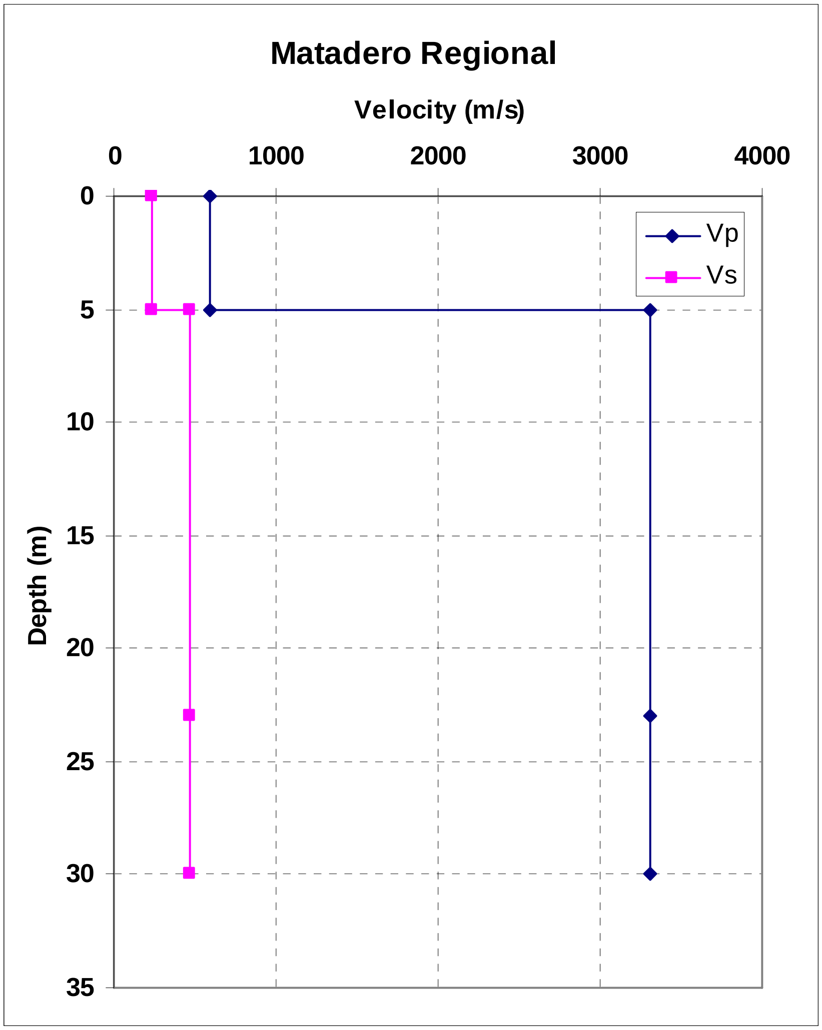

	Velocity (m/s)	
h (m)	Vp	Vs
5	589	240.5
18	3311	463.6
7	3311	463.6
Vs30 (NEHRP) =		401.5
Soil Type =		C

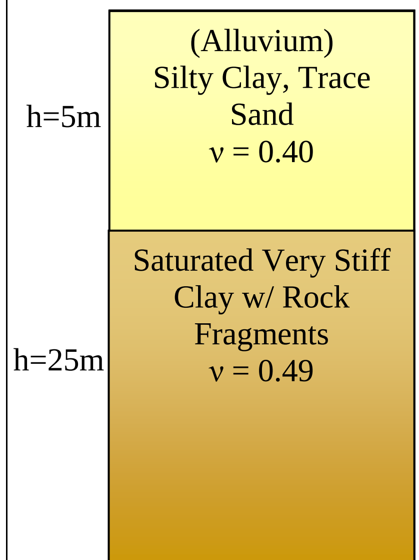

Figure 4.31 Velocity Profile for the Matadero Regional Site

4.4 *Comparison of Results*

This section presents a comparison of the results of geophysical tests carried out for this study with results from Odum et al. (in preparation) and Pérez (2005). Comparison was done only for common sites that were no more than a few hundred meters from each other. Three of the six sites tested in this study were close enough to those tested by Odum et al. (in preparation). Three sites of Pérez (2005) were close enough to the sites tested herein to include them in this comparison.

Table 4.4 presents a summary of the calculated average shear wave velocity (Vs30) results from the three studies and shows values obtained from the different geophysical methods used, i.e., refraction, SASW and ReMi. This table shows that the average shear wave velocity values obtained from each method as well as the NEHRP site were consistent between the three studies. The percent of difference between seismic refraction and the other geophysical methods (SASW and ReMi) ranged from 5.1% to 33.6%. Even though, there was a difference in the average shear wave velocity values obtained, there was no difference in the soil type classification. The differences in velocity values can be attributed to many factors. Although, the geology of the tested sites is generally composed of alluvium deposits (Qal) overlaying the Yauco formation (Ky) or Sábana Grande formation (Ksg) there is a large lateral variation of soil characteristics from site to site even at short distances. Therefore, often the results from geophysical testing of nearby sites could be quite different. Also, the variability in soil properties could be influenced by the instrumentation array, i.e. north-south vs. east-west direction. In addition, each geophysical method has advantages, limitations, and inherent differences. Furthermore, the acquired data for each method is subjected to differences related to individual interpretation.

Table 4.4 Comparisons of Refraction Results with Other Geophysical Techniques

	Refraction (This Study)		**SASW Pérez (2005)**		**ReMi Odum et al. (In Preparation)**		**Average**		**% Difference of Refraction with**	
Site	**Vs**	**Soil Type**	**Vs**	**Soil Type**	**Vs**	**Soil Type**	**Vs**	**Soil Type**	**SASW**	**ReMi**
Abonos	276.4	D	196.9	D	---	---	236.7	D	33.5	---
El Maní Park	293.4	D	273.8	D	---	---	283.6	D	6.9	---
El Seco Park	255.9	D	243.8	D	212.0	D	237.2	D	5.1	18.5
UPRM	220.3	D	---	---	257.5	D	238.9	D	---	15.6
Candelaria	217.2	D	---	---	200.0	D	208.6	D	---	8.3

CHAPTER 5 Geotechnical Database for Mayagüez Area

5.1 *Introduction*

This chapter presents an overview of the geotechnical database design and layout. A brief summary of the content is also presented. Readers interested in a detailed review of the database content should access the database provided in the enclosed DVD.

5.2 *Background*

A large amount of information included in the database was gathered by a preceding M.E. thesis by Llavona (2004). This thesis entailed the collection of geotechnical data for Mayagüez and the preparation of NEHRP soil classification maps. The geotechnical database presented in this research extended the work by Llavona (2004) by adding additional layers to the database, including geophysical testing, wetlands, flood zones, groundwater wells, etc. The data was digitalized using ArcView GIS 3.2© (Environmental Systems Research Institute, 1996) and ESRI® ArcMap 9.0 (Environmental Systems Research Institute, 2004).

The information was positioned in the map considering UTM NAD 27 Zone 19 projected coordinates. After the geotechnical database was finished, a user interface was developed using the computer program DemoShield® 7.5 (Install Shield Software Corporation, 2002). This interface permits the user to access the database directly from the DVD where it is located, avoiding loss of information. The interface (see Figure 5.1) will run automatically after the DVD is inserted.

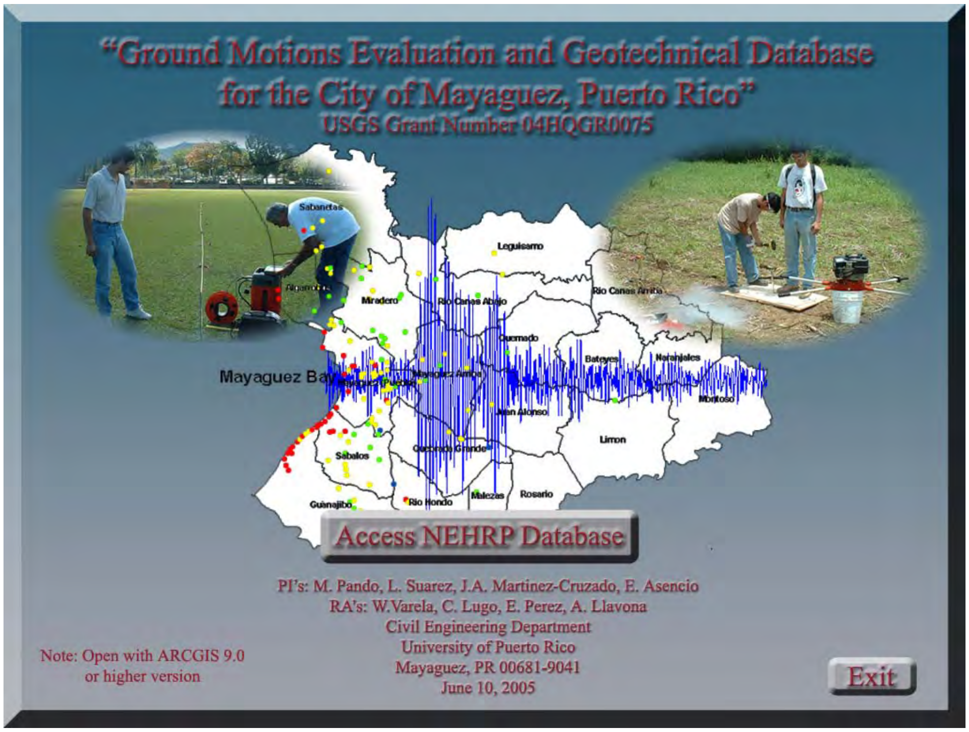

Figure 5.1 Interface Developed to Access NEHRP Database

5.3 *Accessing the Database with ArcMap 9.0/ GIS*

To access the database the user must click the "Access NEHRP Database" button that appears on the interface screen. This action will open the database automatically on the program ArcMap 9.0 (or higher version). It is important to note that the computer must have this program installed. The database is set to open by default showing all Mayagüez counties and points representing the locations of geotechnical collected and classified according to NEHRP class type. The NEHRP classification map shown is based on work done by Llavona (2004) where a peak ground acceleration of 0.34g was used. Lower peak ground acceleration values may result in change of class type and some S_F sites that can change to S_E site classification as they may become non-liquefiable at lower cyclic stresses (due to a lower PGA). Figure 5.2 shows the initial screen of the geotechnical database.

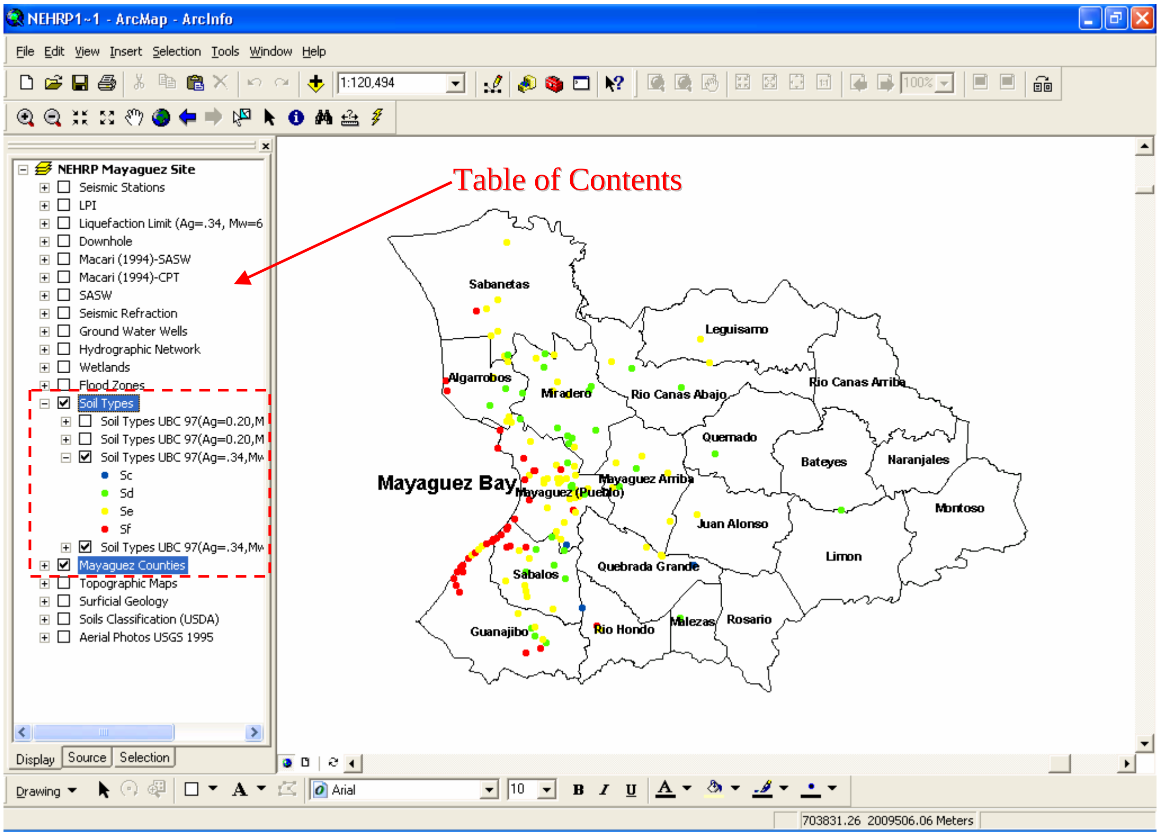

Figure 5.2 Initial View of Geotechnical Database

The first step recommended to start working with the NEHRP database is to set the tools that will help the user to perform the most common tasks. In addition to the Main menu and the Standard toolbar, it is recommended to have active other toolbar options like, Draw, Layout, and Tools. To do this, the user needs to select these applications from the toolbars list in the View menu (See Figure 5.3). A check mark next to the toolbar name indicates this option is active and visible. After selecting the toolbar options, the application displays the toolbar as a floating toolbar on the desktop or if the toolbar was previously turned on, it returns to its last specified position.

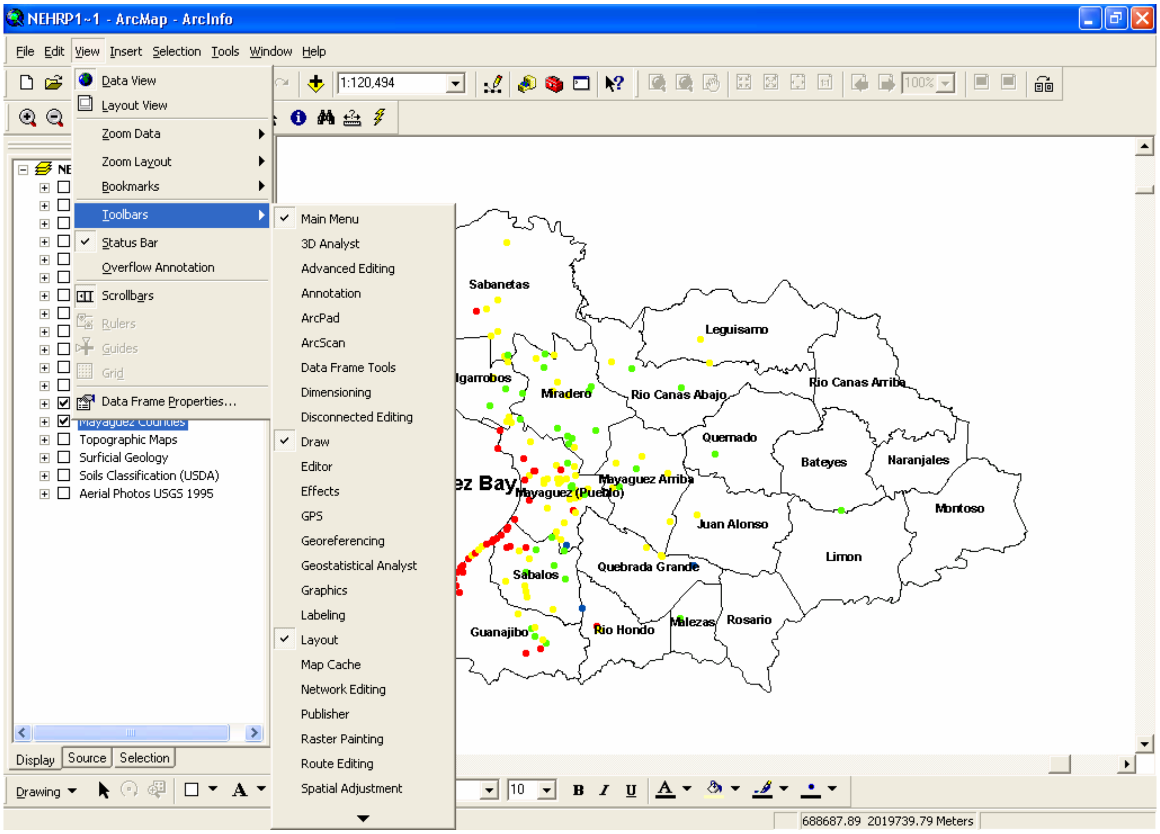

Figure 5.3 Settings Toolbars

For this database the Tools menu (see Figure 5.4) is one of the menus most frequently used by the user. The Tools menu contains the most needed features that will permit the user to access, interpret, and study the geotechnical model and database. For example, it contains the zoom in and zoom out tools, select features tool, identify tool and hyperlink tool.

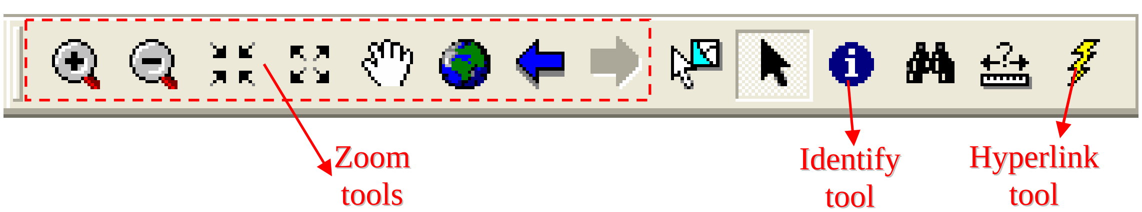

Figure 5.4 Tools Menu Features

After the user defines the tools needed to work in ArcMap 9.0, the next step is to explore or browse the data collected and stored in the geotechnical model and database. The zoom tools can be used to easily change how the user views the data in the map in order to investigate different areas and features.

Another useful feature is to use the Identify tool which can be used to access information about a feature displayed in the map. It allows the user to see the attributes or information related to the data. The Identify tool is considered an easy way to learn something about a location in a map. Usually, the information that can be accessed with the Identify tool is information stored in the input file or input table that is linked to that particular data or feature presented in the map. Examples of attributes for a point on the map are its coordinates. As soon as the user clicks the Identify tool, the Identify Results window opens (see Figure 5.5) and when the user clicks a location in the map the Identify Results dialog box will display the data for that location.

The default option is to show the information of the topmost layer in the table of contents for the location. If more than one feature was identified, the user can click any of the features in the left panel of the Identify Results window to see the attributes of that feature. If the user can use the Layers dropdown list at the top of the Identify Results dialog box to choose from several other options in addition to the topmost layer: Visible layers, Selectable layers, All layers, or any other specific layer in the map. The Identify tool will act on whatever is chosen in the Layers dropdown list.

The hyperlink tool is used for accessing documents stored in the database. To do this, the user must select the hyperlink tool on the Tools menu. Once the user selects the hyperlink tool option, blue dots (see Figure 5.6) will appear in the map for all the points that contain additional data in the form of a linked document. When the user selects or clicks over a specific blue dot the linked document or file associated with this point will be opened. The file will be launched using the application for which that file type is currently associated, for example a pdf file will likely open through Acrobat Reader.

Once the user is familiar with the basic tools required to work with the ArcMap 9.0 program, he or she can readily explore the NEHRP database and all the information contained in it. This will allow the user determine which are the geotechnical conditions present at a specific site, this in turn could aid with the engineering design or decision making related to further investigations required.

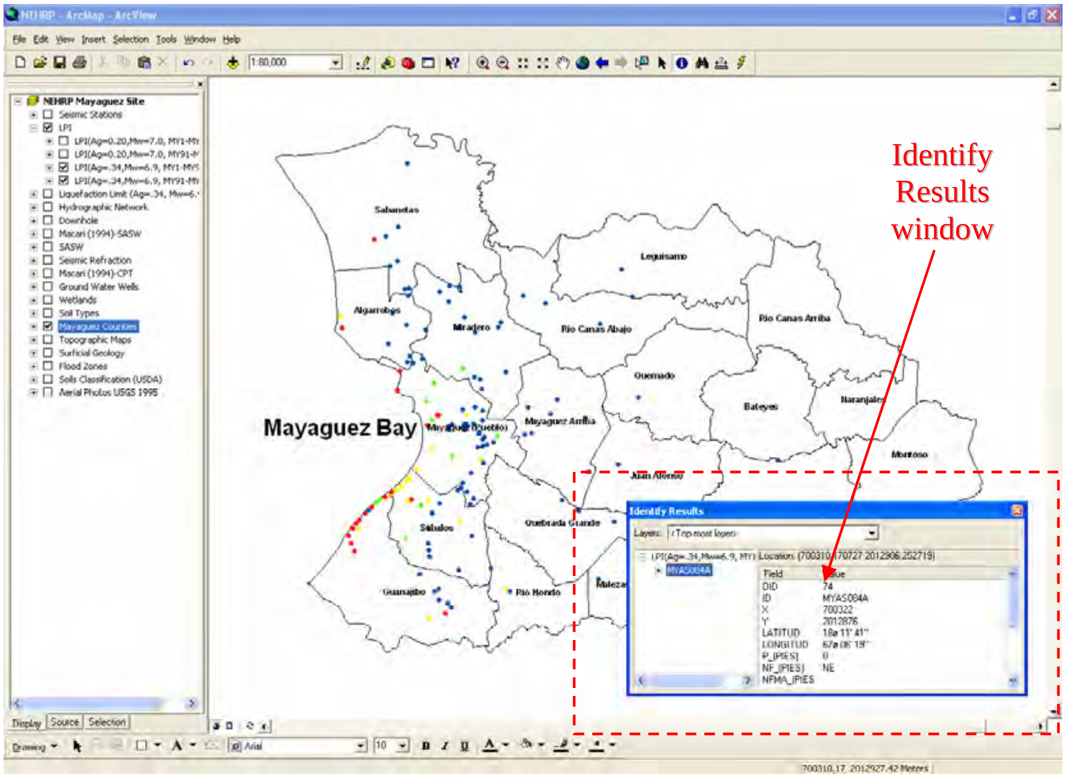

Figure 5.5 Identify Results Window

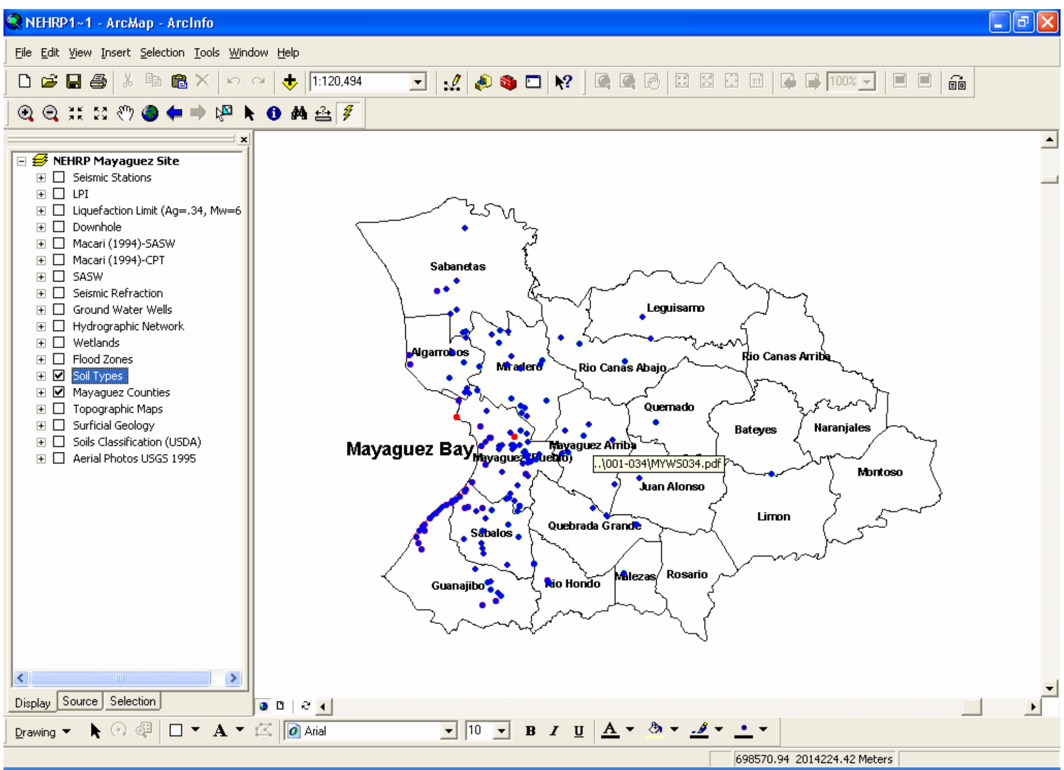

Figure 5.6 Hyperlink Tool Selected

5.4 *Description of the Geotechnical Database Content*

This section presents a general overview of the content of the database. More detailed information is available by directly accessing the database enclosed. The geotechnical model includes nineteen layers that contain specific data for the Mayagüez area. The layers presented in the geotechnical model are the following:

- Seismic Stations: This layer presents the location of the PRSMP seismic stations in the Mayagüez area. There are eight stations on the area. All stations are controlled by the Puerto Rico Strong Motion Program. This layer is presented on Figure 5.7.

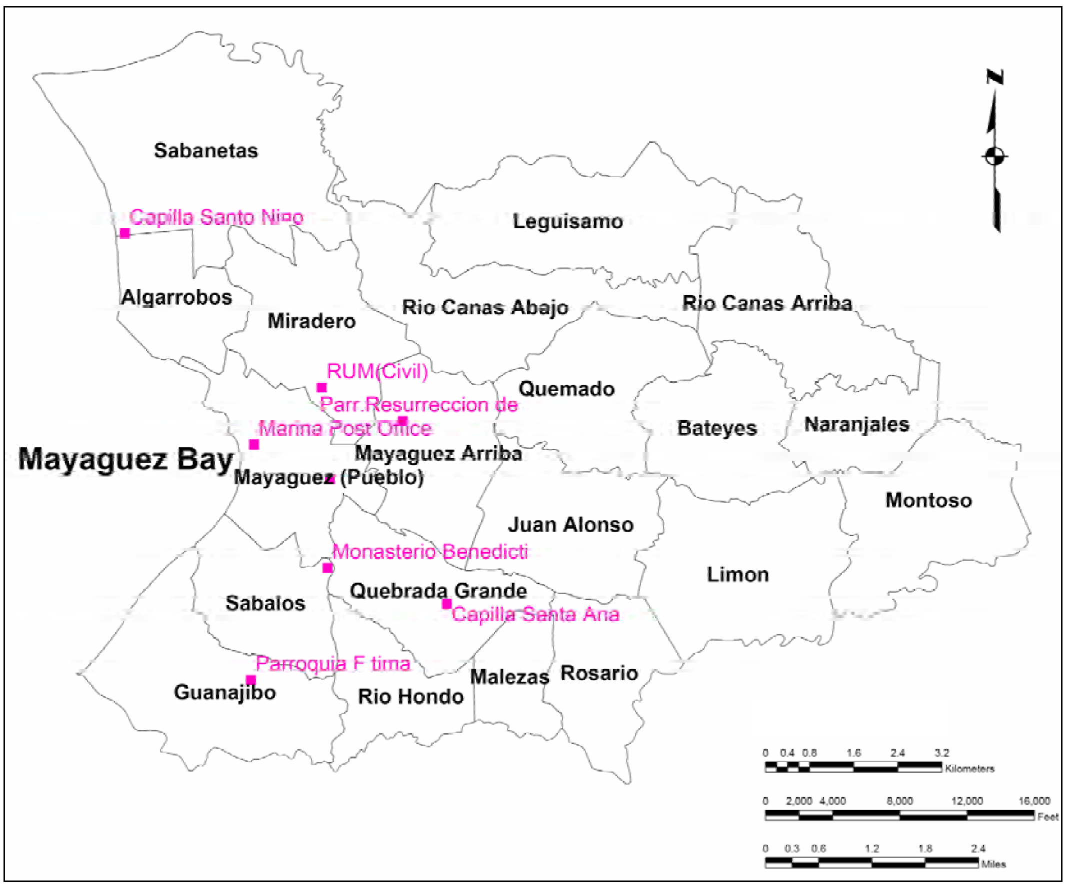

Figure 5.7 Location of Mayagüez Seismic Stations

- LPI: This layer contains four sub layers that classify the sites by its Liquefaction Potential Index. The soil studies (mainly in the form of SPT- Standard Penetration Test) collected from different agencies were classified using the Revised Simplified Method (Youd et al., 2001). The first two layers consider a peak ground acceleration (Ag) of 0.2g and an earthquake magnitude of M=7.0. They are divided according to its study number, from 1 to 90 and from 91 to 147; this layer is shown on Figure 5.8. The following layers consider a peak ground acceleration (Ag) of 0.34g and an earthquake magnitude of M=6.9. These layers are also divided according to the study number. This layer is presented on Figure 5.9. All soil studies were analyzed using the program LicuadoPR (Sosa and Pando, 2004). All points have hyperlinks to the LicuadoPR results file.

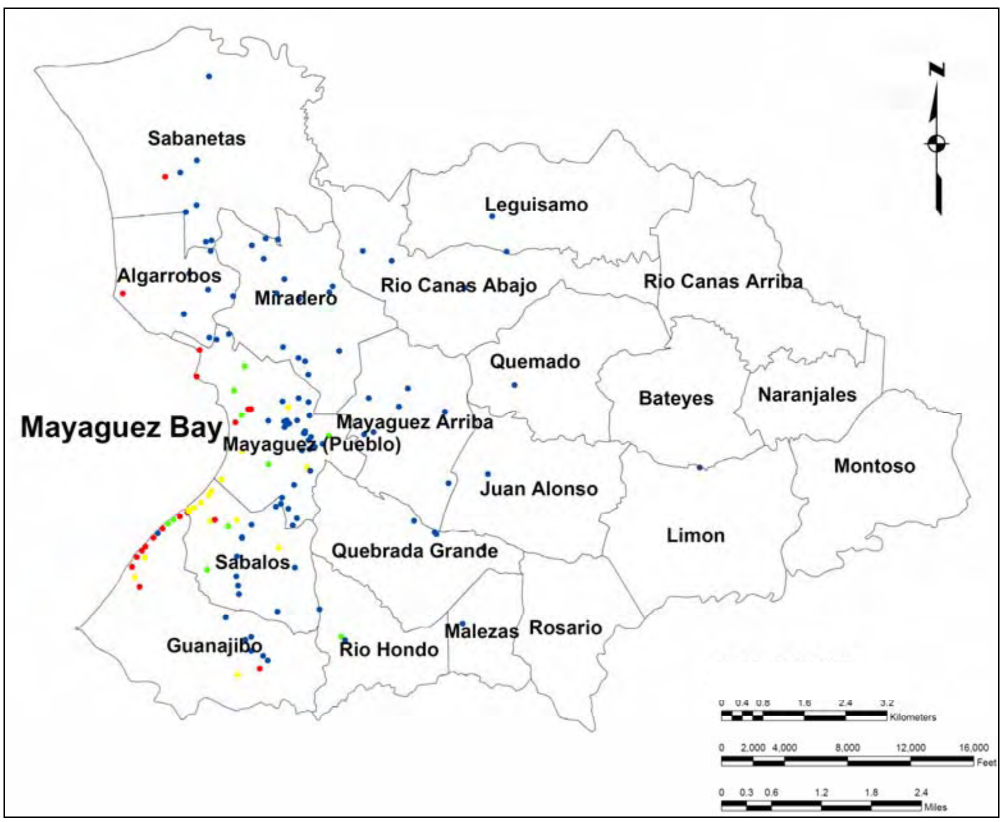

Figure 5.8 LPI Layer for Ag=0.2 and Mw=7.0

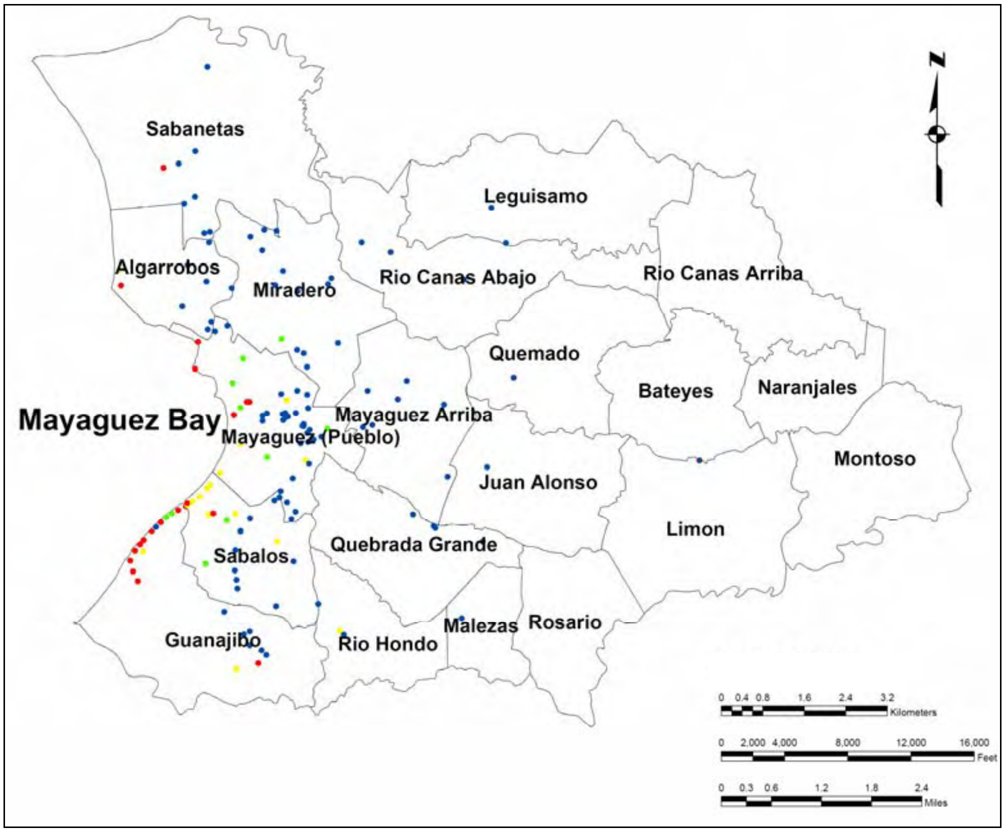

Figure 5.9 LPI Layer for Ag=0.34 and Mw=6.9

- <u>Liquefaction Limit</u>: This limit defines and identifies all the Mayagüez zones that have a high liquefaction potential. These zones were established by Llavona (2004). This layer is presented on Figure 5.10.

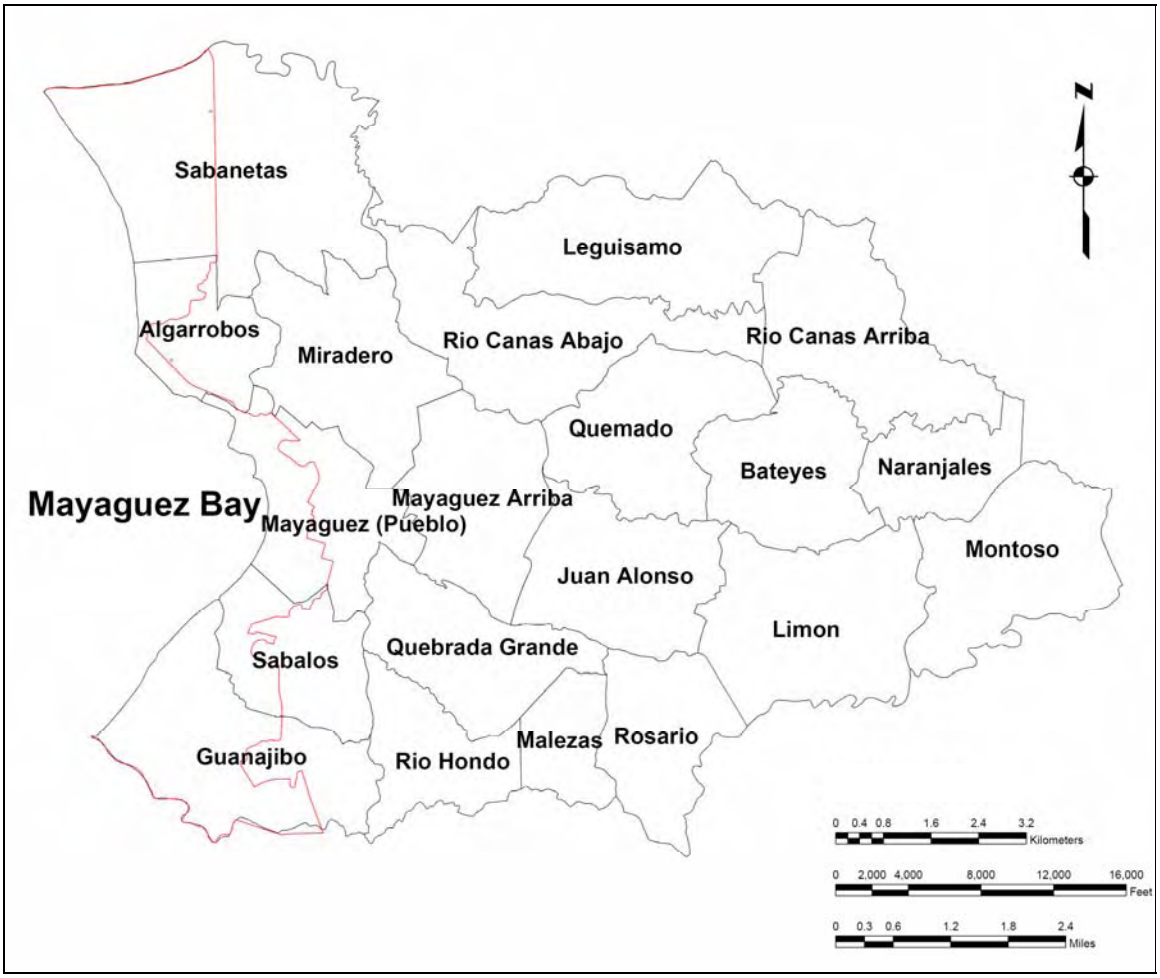

Figure 5.10 Liquefaction Limit Developed by Llavona (2004)

- <u>Downhole Study</u>: This layer shows the location of a downhole study made for the Puerto Rico Strong Motion Program by the Jaca & Sierra Company (Sierra del Llano, C.R., 2002). This layer contains a hyperlink to a document that presents the Shear Wave Velocity Profile obtained with the test. This layer is presented on Figure 5.11.

Figure 5.11 Downhole Study Performed by Jaca & Sierra (Sierra del Llano, C.R., 2002)

- SASW (Macari, 1994): This layer shows the location of eight "Spectral Analysis of Surface Waves" (SASW) studies made by Macari in 1994. This layer contains hyperlinks, for all the locations, to a document that presents the Shear Wave Velocity Profile obtained with the tests. This layer is presented on Figure 5.12.

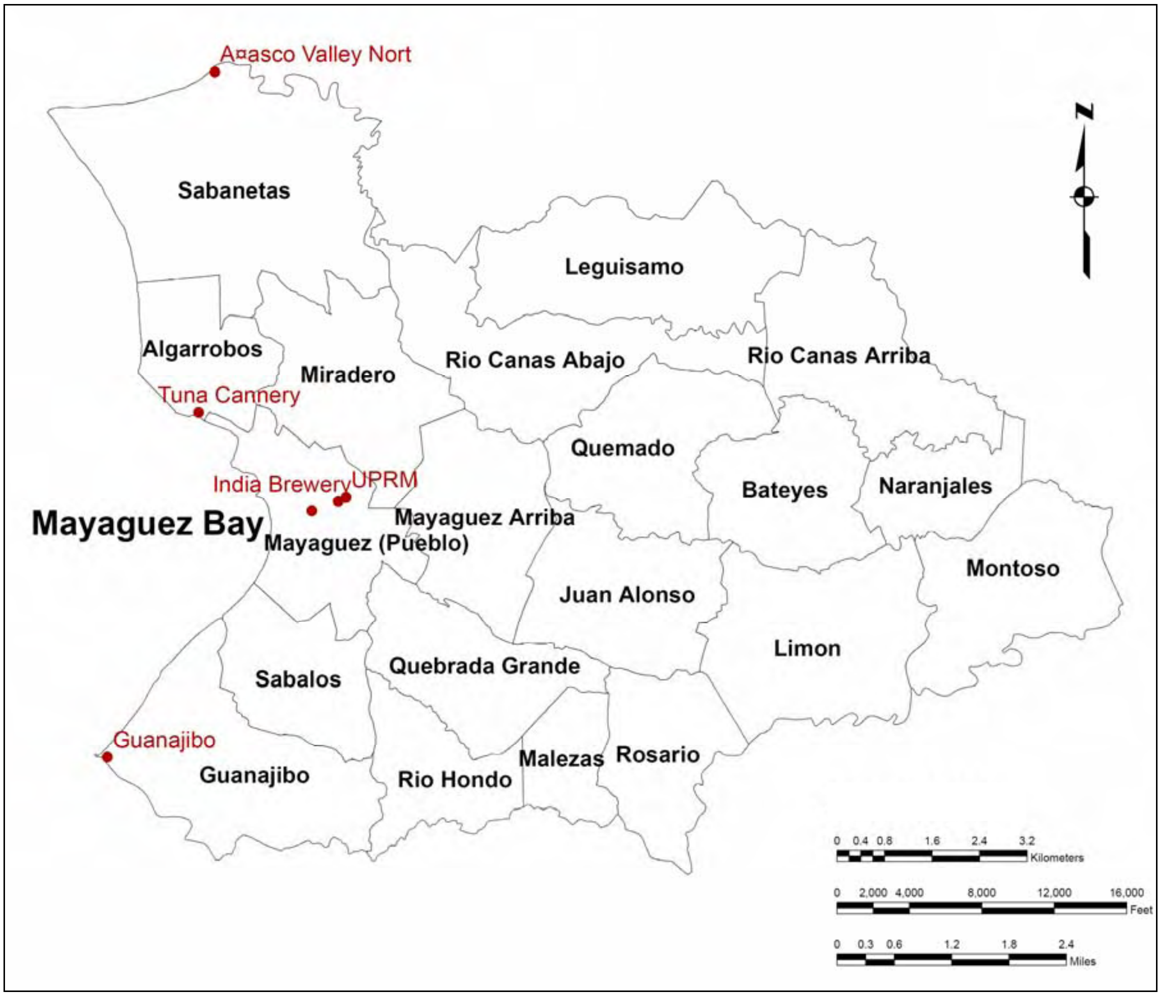

Figure 5.12 Location of SASW Test Performed by Macari (1994)

- <u>CPT (Macari, 1994)</u>: This layer shows the location of three Cone Penetration Test (CPT) soundings made by Macari in 1994. This layer contains hyperlinks, for all the locations, to a document that presents the results of the piezocone data analysis obtained with the tests. This layer is presented on Figure 5.13.

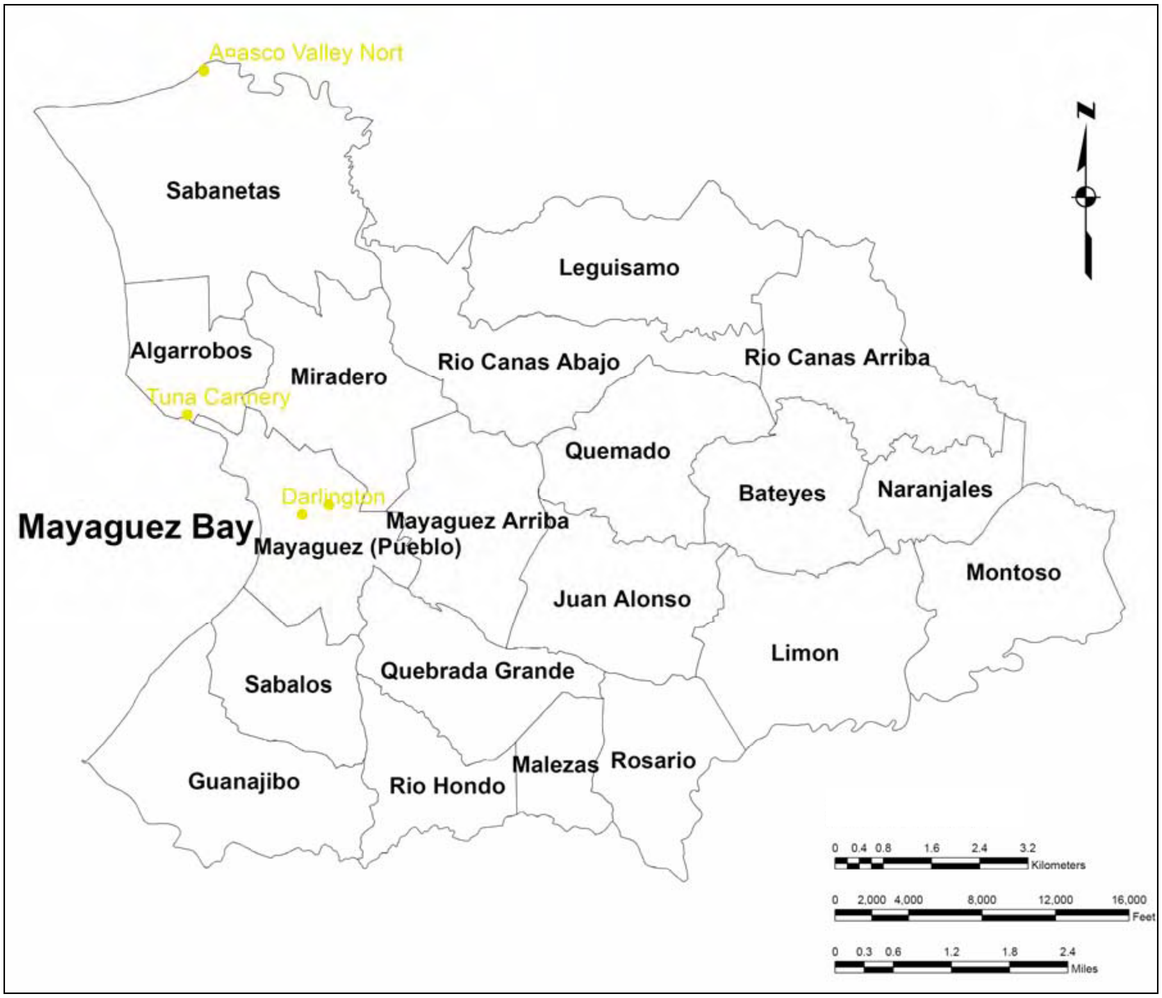

Figure 5.13 Location of CPT Test Performed by Macari (1994)

- SASW (Pérez, 2005): This layer shows the location of ten "Spectral Analysis of Surface Waves" (SASW) studies performed by Pérez in 2005. This layer contains hyperlinks, for all the locations, to a document that presents the Shear Wave Velocity Profile obtained from the tests. This layer is presented on Figure 5.14.

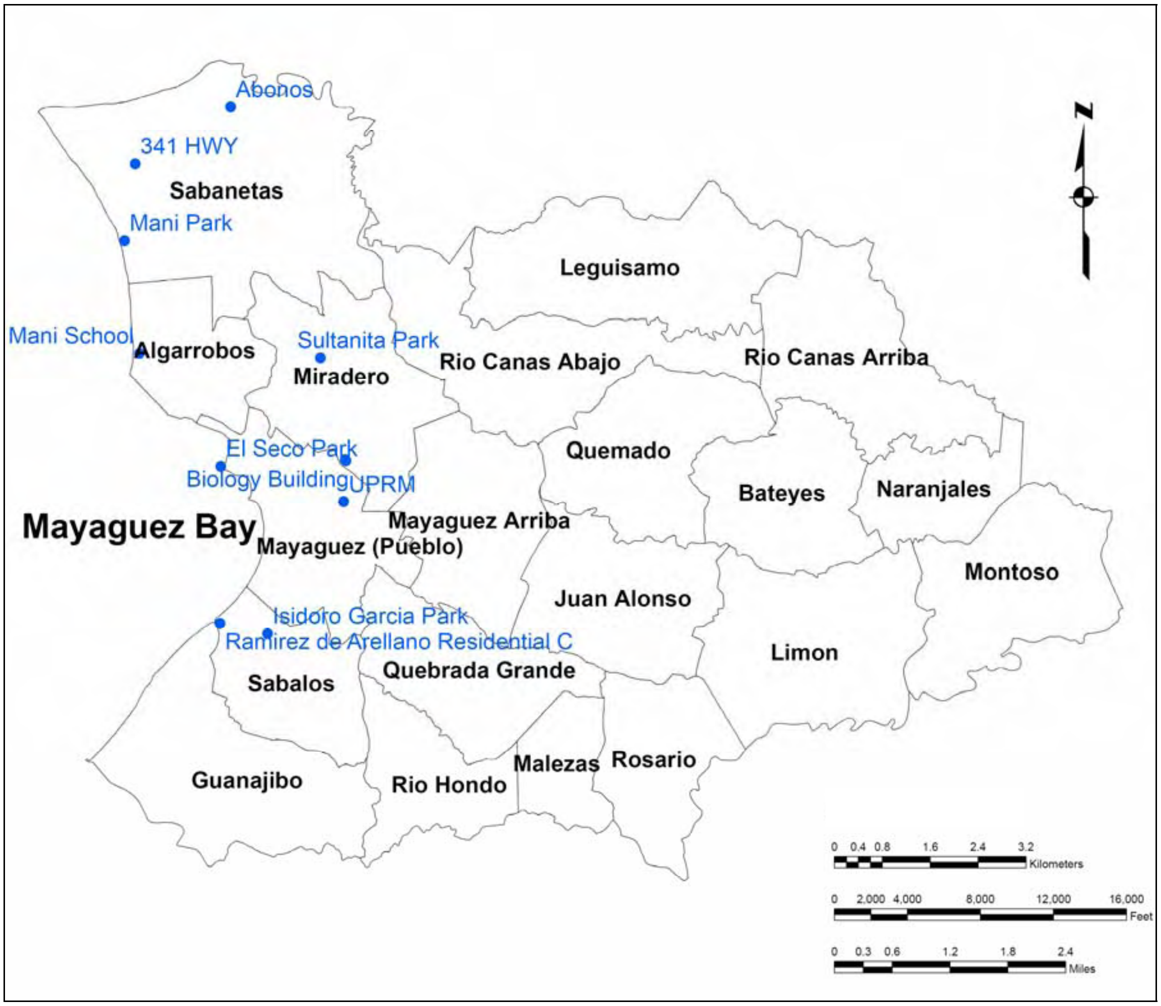

Figure 5.14 Location of SASW Test Performed by Pérez (2005)

- Seismic Refraction test for this thesis: This layer shows the location of six seismic refraction studies made for this project carried out by Lugo and Varela in 2004 and complemented with data from Odum et al. in 2004 for another USGS project. This layer contains hyperlinks, for all the locations, to a document that presents the Velocity Profile obtained with the tests. This layer is presented on Figure 5.15.

Figure 5.15 Location of Seismic Refraction Test (this thesis)

- Ground Water Wells: This layer shows the location of the USGS ground water wells located within the Mayagüez area. All locations are linked to an EXCEL spreadsheet that contains general information for all the wells. On these spreadsheets each well has a link (Site Number) to an internet site, managed by the USGS. In the website link the user can access available historical data. This layer is presented on Figure 5.16.

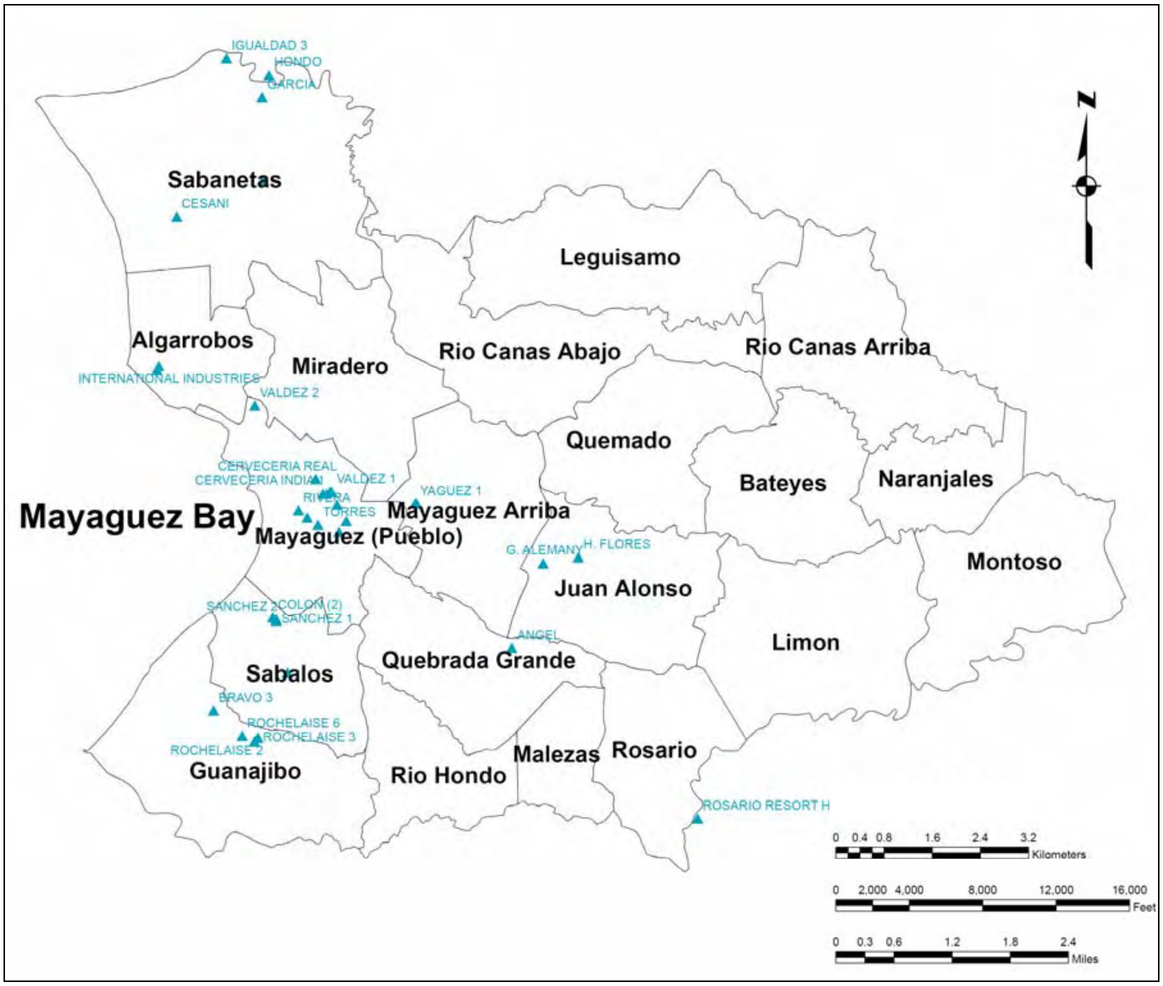

Figure 5.16 Groundwater Wells in Mayagüez

- Hydrographic Network: This layer presents the hydrographic network for the Mayagüez area. This layer can be used to identify sites with high values of ground water levels which can influence the liquefaction susceptibility of the site if it is characterized as a sandy soil site. This layer is presented on Figure 5.17.

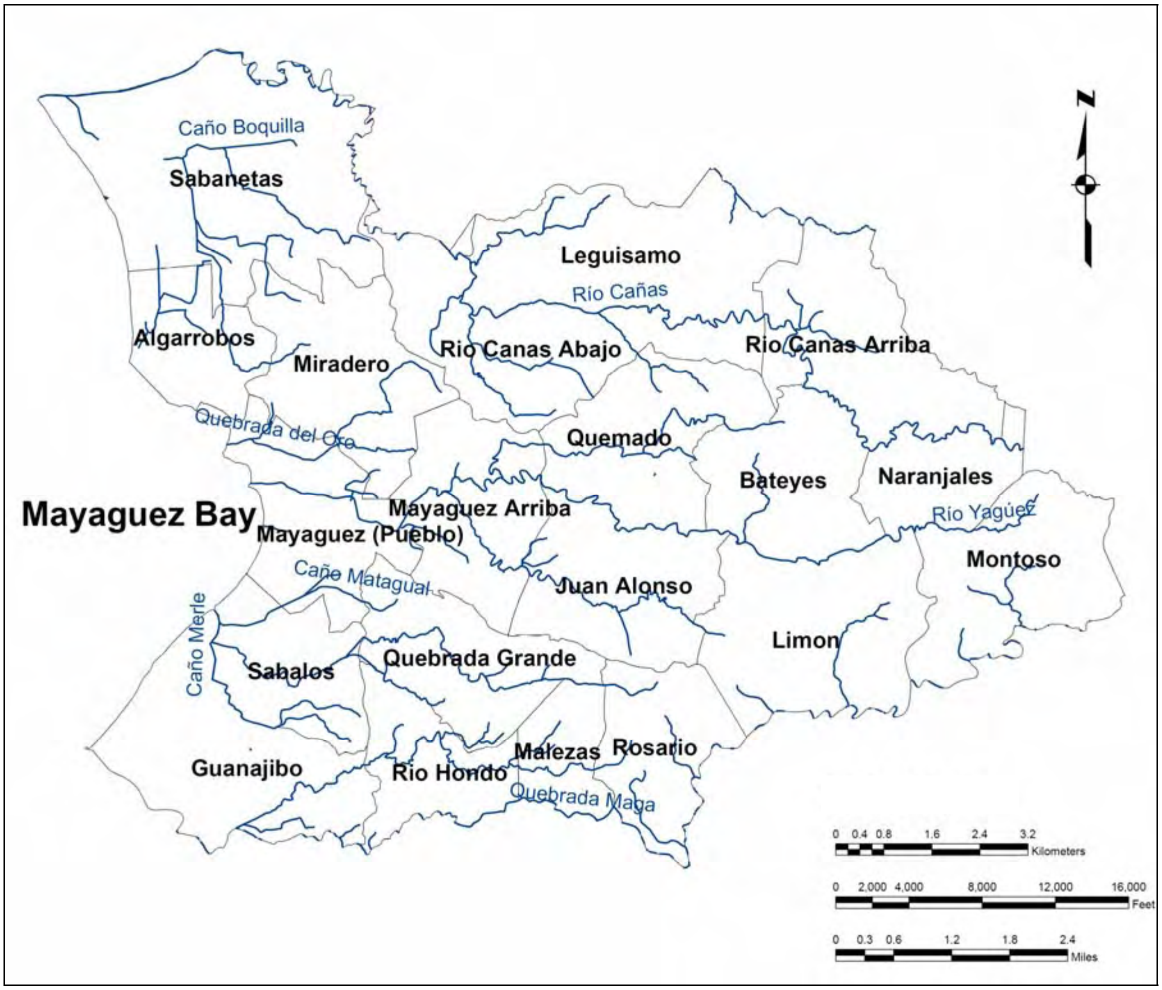

Figure 5.17 Mayagüez Hydrographic Network

- Wetlands: This layer presents the wetlands located in the Mayagüez area. This layer can be used to identify sites with high ground water levels which can influence the liquefaction susceptibility of the site if it is characterized as a sandy soil site. This layer is presented on Figure 5.18.

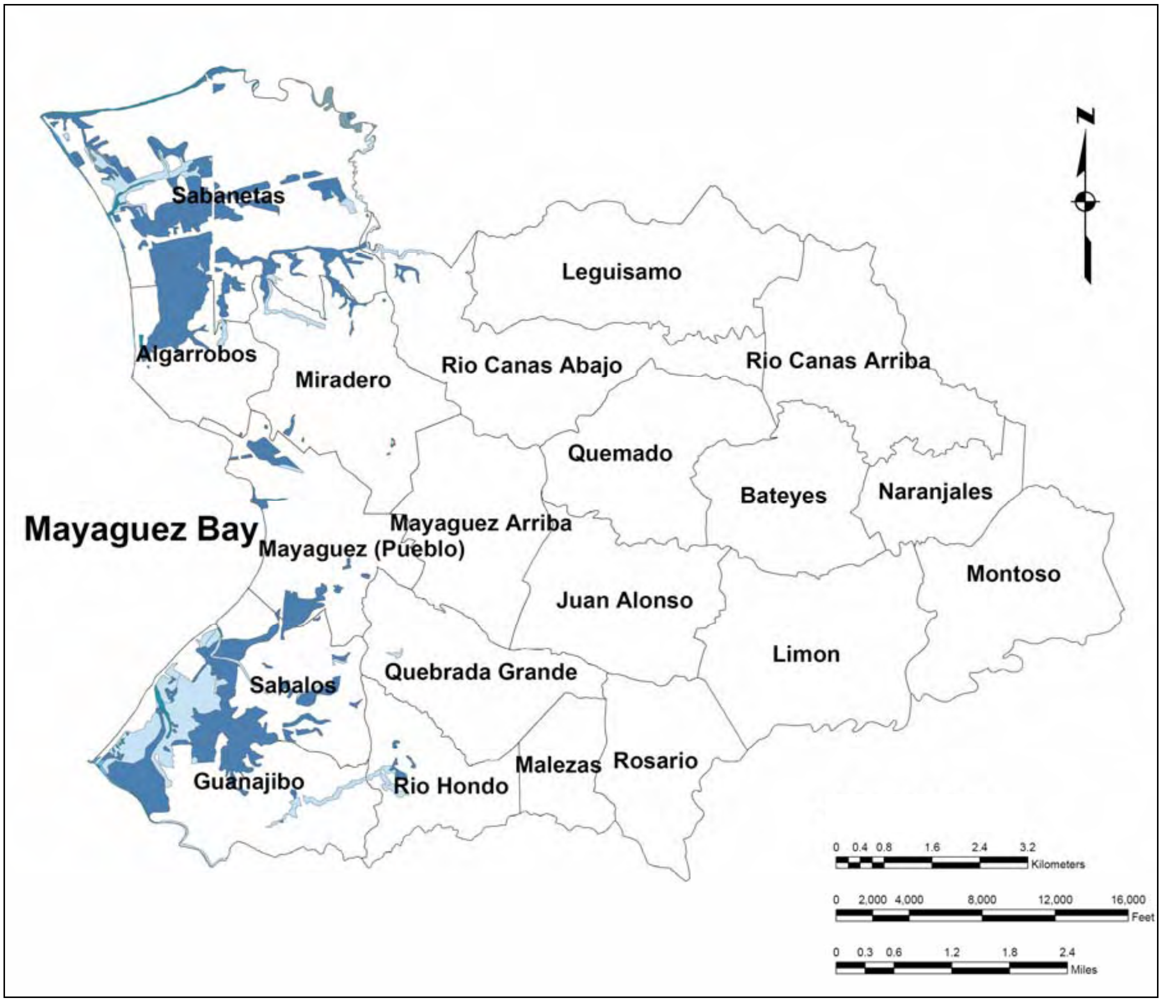

Figure 5.18 Wetlands in the Mayagüez Area

- <u>Flood Zones</u>: This layer presents the flood zones of the Mayagüez area based on data from the "Junta de Planificación" agency. This layer can be used to identify sites with high ground water levels which can influence the liquefaction susceptibility of the site if it is characterized as a sandy soil site. This layer is presented on Figure 5.19.

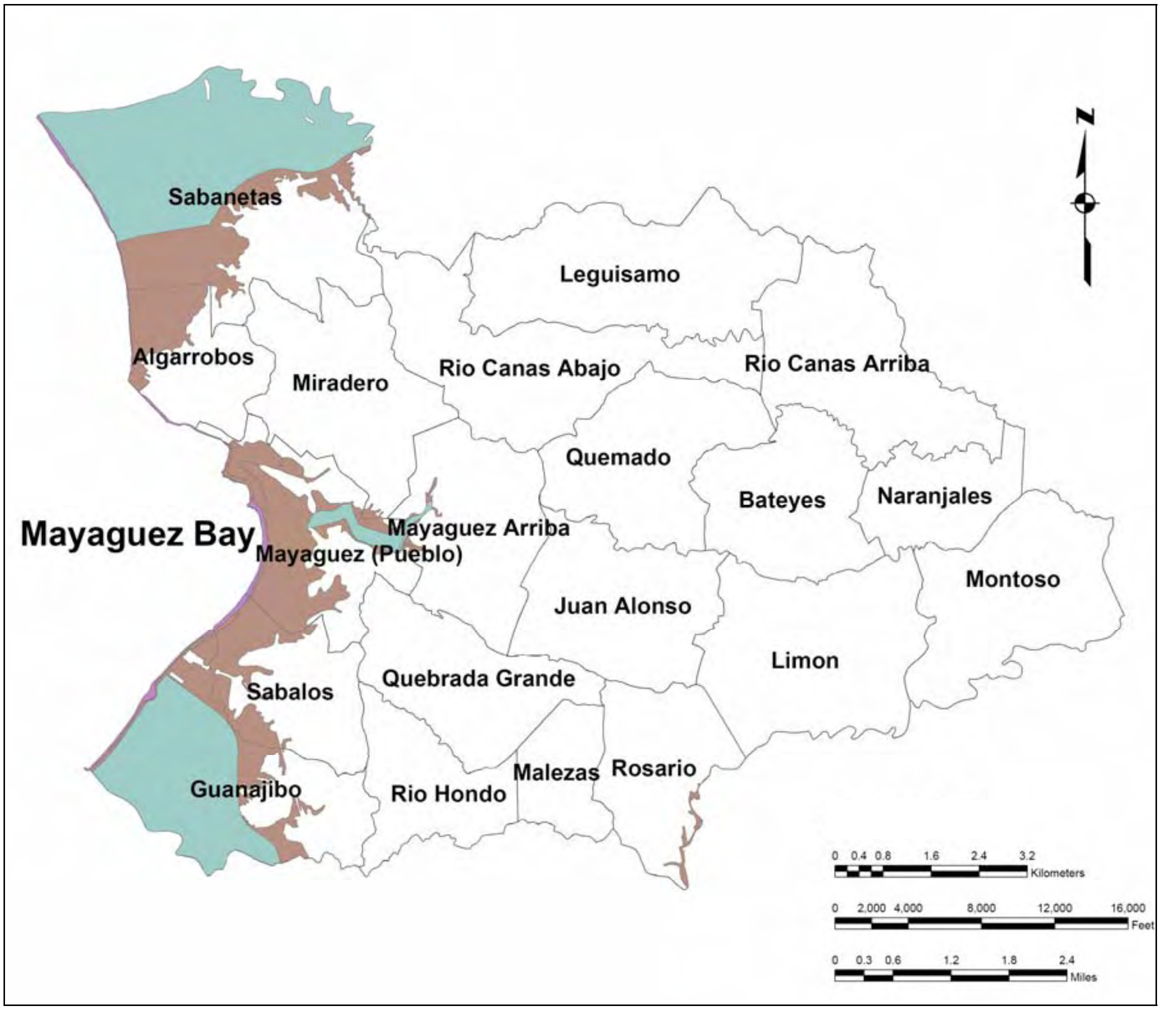

Figure 5.19 Mayagüez Flood Zones

- Soil Types: This layer contains four sub layers that classify the sites by soil type according to the 1997 Uniform Building Code Provisions. The soil studies (mainly available in the form of SPT- Standard Penetration Tests) collected from different agencies were classified using the Shear Wave Velocity and the N value obtained from the SPT. The first two layers (Figure 5.20) consider peak ground acceleration (Ag) of 0.2g and are divided according to its study number, from 1 to 90 and from 91 to 147. The following layers (Figure 5.21) consider peak ground acceleration (Ag) of 0.34g and are also divided according to the study number. Lower peak ground acceleration values may result in change of class type and some S_F sites that can change to S_E site classification as they may become non-liquefiable at lower cyclic stresses (due to a lower PGA). All soil studies were analyzed using the program LicuadoPR (Sosa and Pando, 2004) and all points have hyperlinks to the LicuadoPR results file.

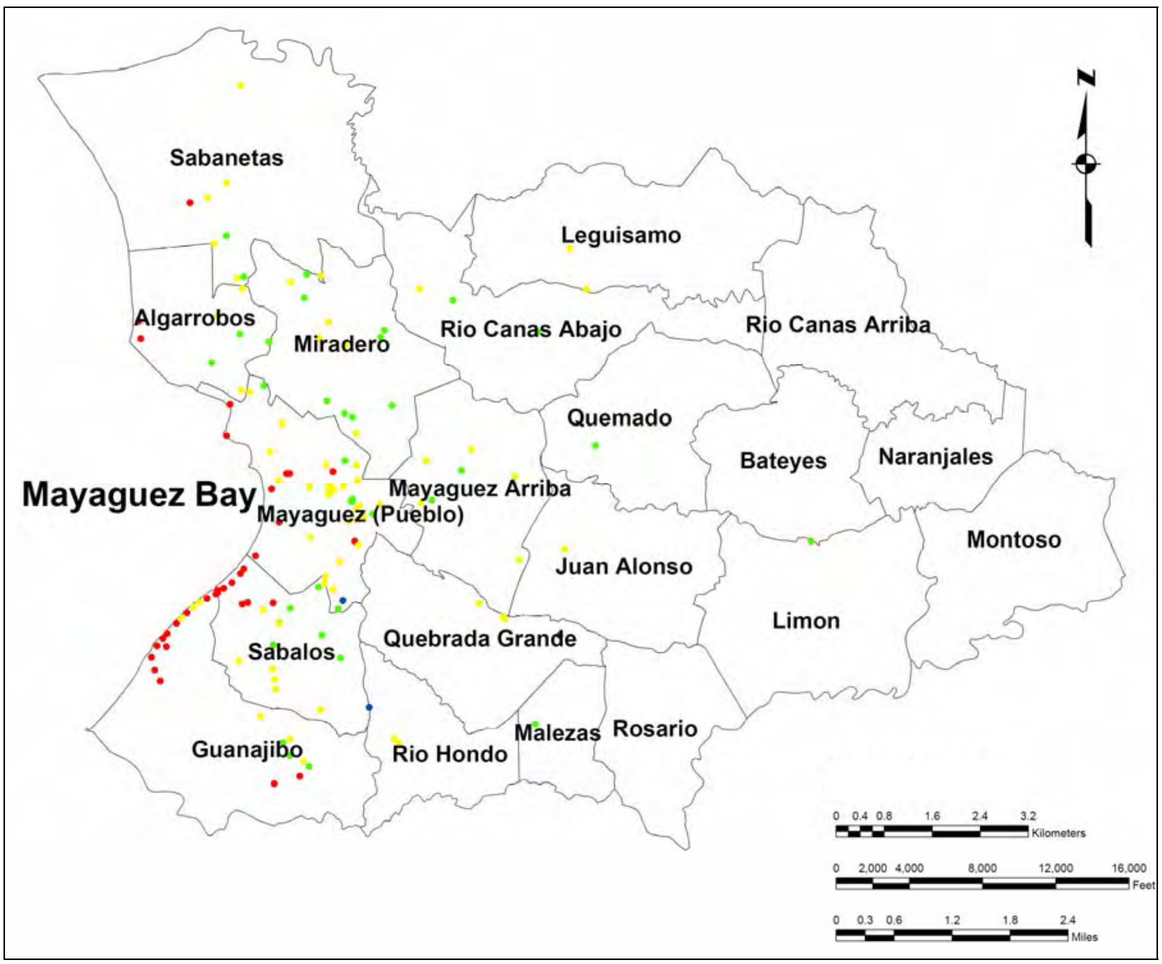

Figure 5.20 Soil Types According to UBC 97 Code (Ag=0.2, Mw=7.0)

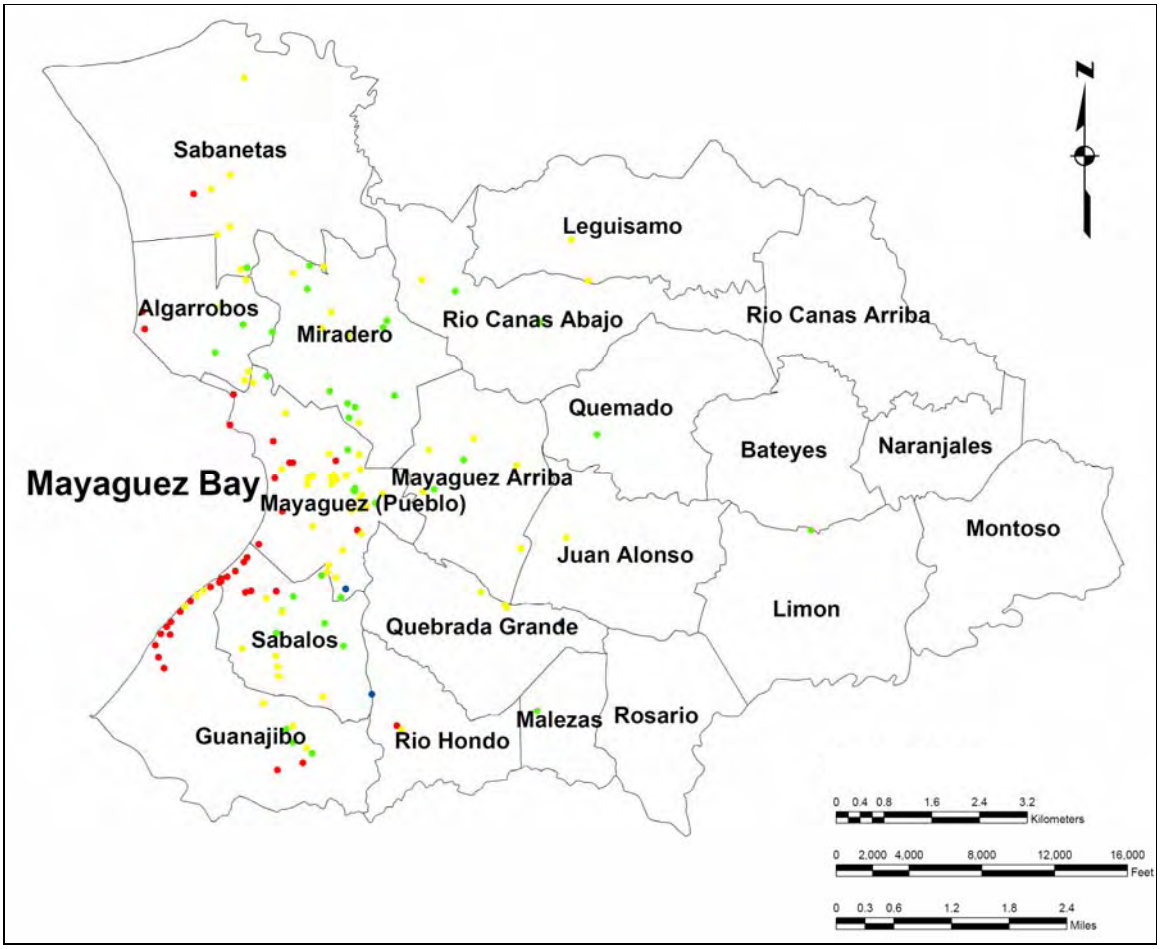

Figure 5.21 Soil Types According to UBC 97 Code (Ag=0.34, Mw=6.9)

- Mayagüez Counties: This layer (Figure 5.22) presents the counties that compose the municipality of Mayagüez. This layer will help the user to establish a relation between the location of the site and the characteristics of a specific area. For example, identify Mayagüez (Pueblo) as a highly populated zone.

Figure 5.22 Mayagüez Counties (Barrios)

- Topographic Maps: This layer presents the topographic information for the Mayagüez area, in terms of contour lines providing values of elevation above sea level. This layer can help the user identify liquefaction susceptible zones located mainly in low laying areas like the coastal areas. This layer is presented on Figure 5.23.

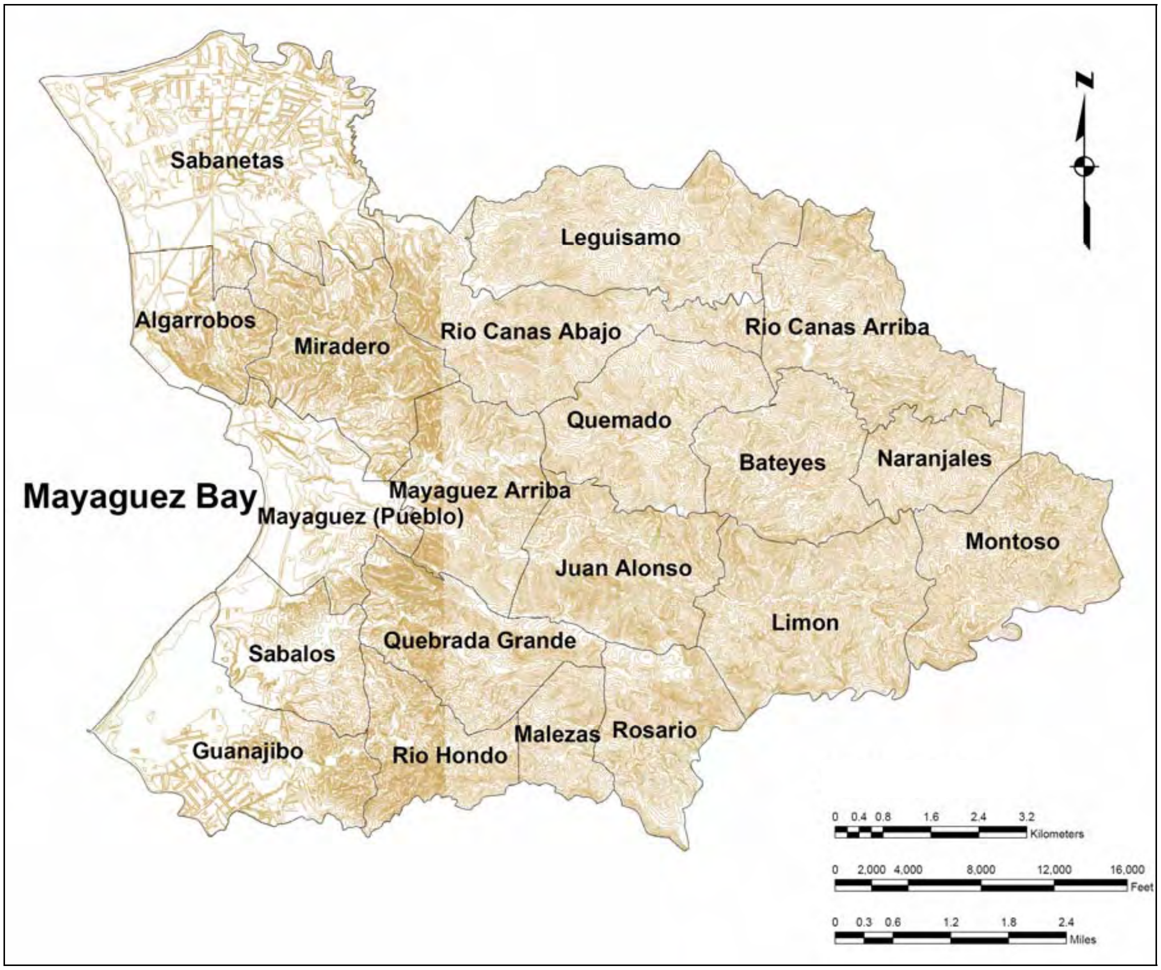

Figure 5.23 Mayagüez Topographic Map

- Surficial Geology: This layer (Figure 5.24) shows the different types of geologic formations that compose the Mayagüez area. With this layer the user can determine the geologic characteristics of a specific site within Mayagüez. This layer can be used to help assess the liquefaction susceptibility of a site based on its geologic conditions. For example, sites located within alluvial deposits of Holocene age will be considered susceptible to liquefaction if other conditions are present.

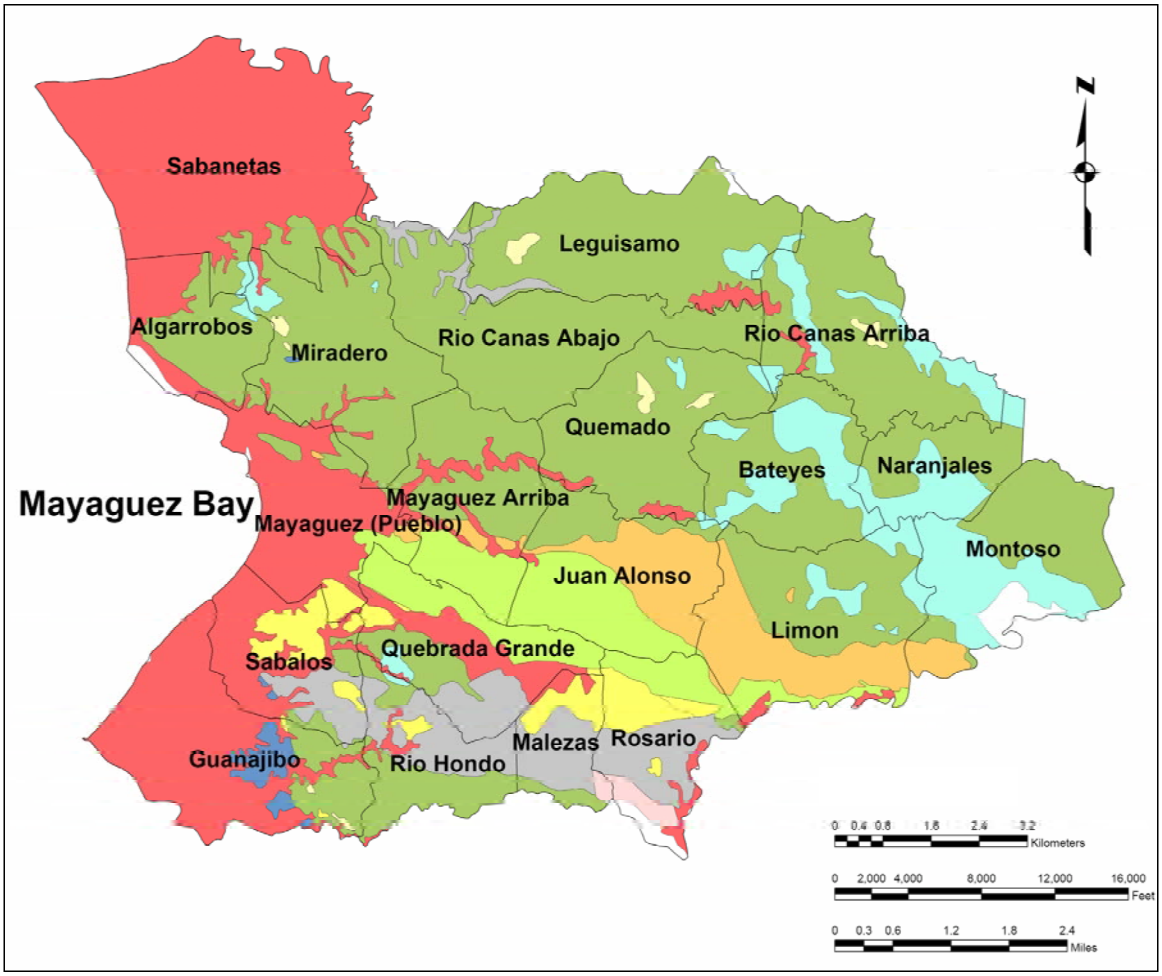

Figure 5.24 Mayagüez Surficial Geology

- <u>Soils Classification (USDA)</u>: This layer shows the soil types within the Mayagüez area, based on the USDA specifications. The USDA soil classification is primarily based on agricultural considerations such as soil chemistry and moisture content. Nevertheless it provides useful information that complements the other layers. The database includes a description of each soil type. This layer is presented on Figure 5.25.

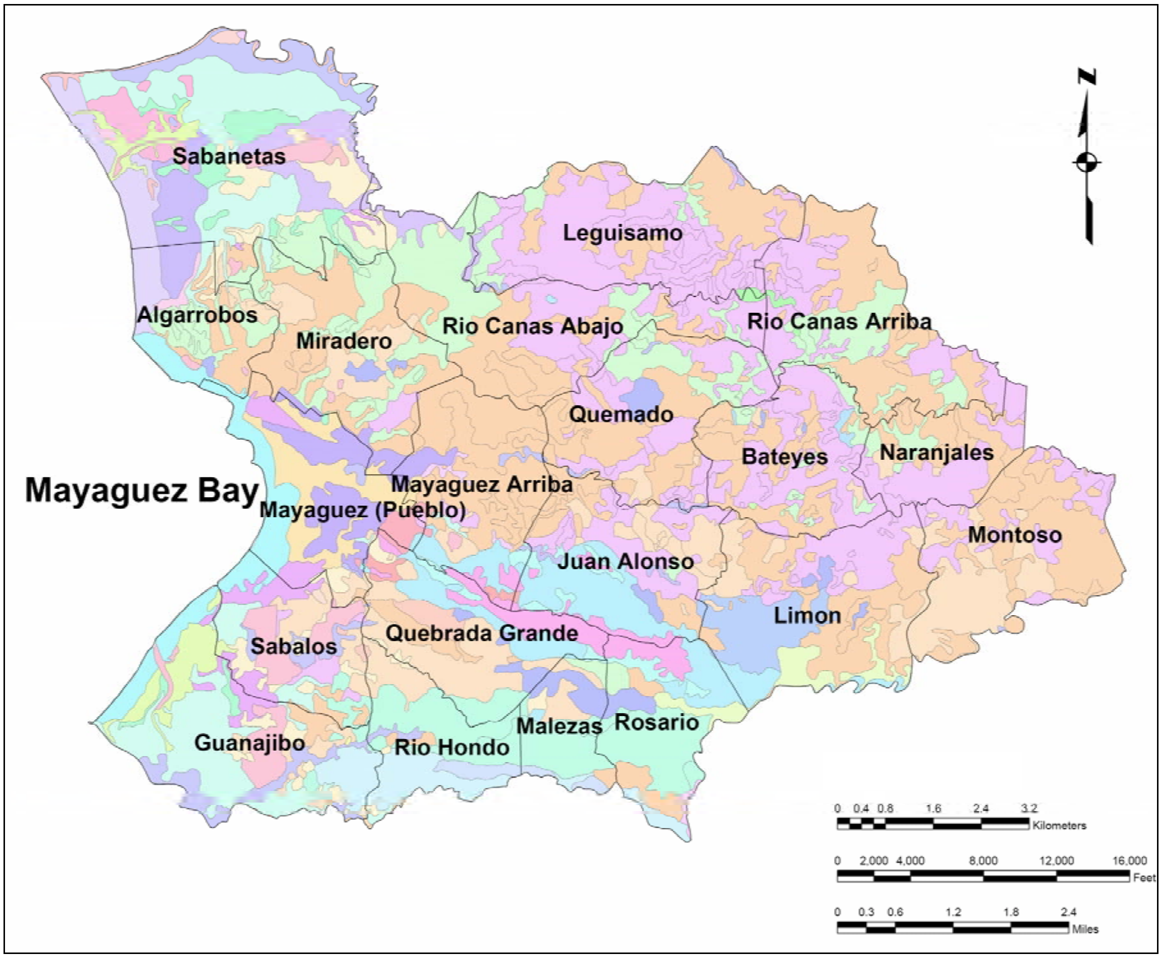

Figure 5.25 Mayagüez USDA Soil Classification

- <u>Aerial Photos USGS 1995</u>: This layer is included to provide the user with visual information of the type of structures and infrastructures that are within the study area. This layer is presented on Figure 5.26.

Figure 5.26 Aerial Photos USGS 1995

- Aerial Photos USGS 2004: This layer complements the 1995 air photos and provides an idea of the construction activity within 1995 and 2004. This layer is presented on Figure 5.27.

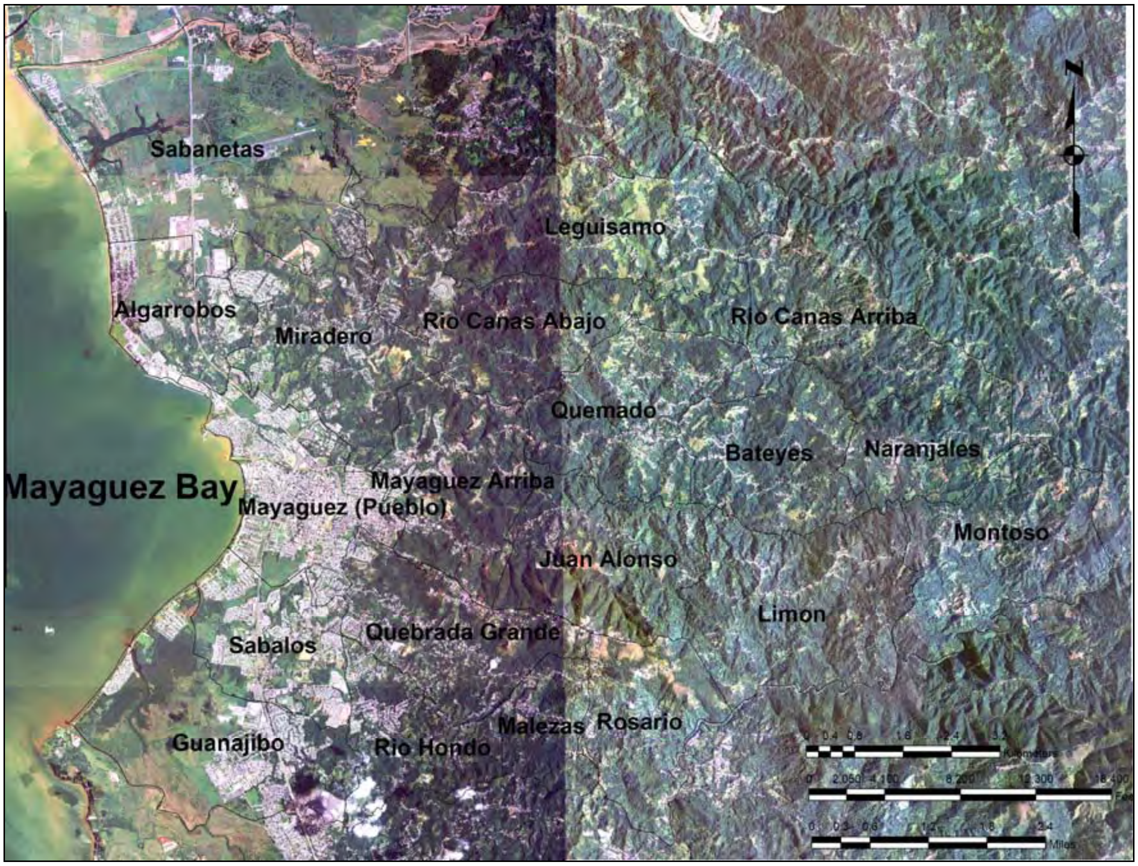

Figure 5.27 Aerial Photos USGS 2004

CHAPTER 6 Conclusions

A detailed geotechnical model (database) of the Mayagüez city was developed using existing geotechnical data gathered from local consulting firms, research papers and reports, and government agencies and complemented with seismic refraction fieldwork. The geotechnical database consisted of a graphical interface developed in the computer program ArcMap© 9.0. The layered model includes an extensive database which allows the users to browse through and append additional information, when available, by means of an easy and effective approach. The importance of the development of this database relies in the fact that it can be used as a planning tool for structural and geotechnical engineers for design purposes and for liquefaction potential screenings. The developed database can also be used for future seismic studies that require inclusion of local site effects.

The database was complemented with geophysical testing which includes Seismic Refraction fieldwork from this study, Spectral Analysis of Surface Waves (SASW) from Pérez (2005), and Seismic Refraction and Refraction Microtremor (ReMi) analyses by Odum et al. (in preparation). Seismic refraction tests were performed at six locations in the Mayagüez area. The seismic refraction results were used to determine the average shear wave velocity (Vs30) for each site. After the geophysical analyses were completed, sites were classified according to the rock and soil classification scheme defined by NEHRP (2000). Five of the six sites tested were classified as soil profile type S_D and only one was classified as type S_C. Average shear wave velocity values obtained in this study compared well with those obtained by Pérez (2005) and Odum et al. (in preparation). The results obtained from each method were consistent despite the inherent differences in the applied methods and actual site location. Even though, there was some degree of difference in the average shear wave velocity values, no differences were found in terms of the NEHRP soil classification determined for each site.

This study hopes to contribute to better and safer seismic design in the Mayaguez area. This is believed to be mainly through facilitating access to comprehensive geotechnical and geophysical data for this region. However this study highlighted the importance to expand the level of available data. Important knowledge gaps still remaining are depth to bedrock, soil period maps, bedrock/soil contact characteristics, dynamic properties, among other areas that require further research.

REFERENCES

Arroyo, E.N., 1991, "*Liquefaction Analysis Potential on Some Site on the Mayagüez Area Based on Geotechnical Reports,*" Reporte sometido al Departamento de Geología de la Universidad de Puerto Rico, Recinto de Mayagüez.

Asencio, E., 1980, "*Western Puerto Rico Seismicity,*" USGS Open File Report 80-192.

Building Seismic Safety Council (BSSC), 2001, "*2000 Edition, NEHRP Recommended Provisions for Seismic Regulations for New Buildings and Other Structures,*" FEMA -368, Part 1 (Provisions): developed for the Federal Emergency Management Agency, Washington, D.C.

Burger, H. R., 1992, "*Exploration Geophysics of the Shallow Subsurface,*" Prentice Hall.

Capacete, J.L. and Herrera, A., 1972, "*The 1918 Earthquake; An Engineering Study,*" CIAA. Vol 22 No.1, Puerto Rico.

Coduto, D.P., 2001, "*Foundation Design: Principles and Practices,*" 2nd Ed., Prentice Hall, Inc., New Jersey.

Colón-Dieppa, E., and Quiñonez-Martínez, F., 1985, "*A Reconnaissance of the Water Resources of the Central Guanajibo Valley, Puerto Rico,*" Puerto Rico.

Clinton, J.F., Cua, G., Huérfano, C.V., von Hillebrandt-Andrade, C.G., and Martínez-Cruzado, J. , 2006, "*The Current State of Seismic Monitoring in Puerto Rico,*" SSA Seismological Research Letters, Vol. 77 No 5, 532-543.

Curet, A.F., 1986, "*Geologic Map of the Mayagüez and Rosario Quadrangles, Puerto Rico,*" Map I-1657, US Geological Survey.

Dames and Moore, 1999, "*Probabilistic Seismic Hazard Analysis of Puerto Rico and Recommended Revisions to the Seismic Coefficients of the ANSI/ASCE 7-95 Standard,*" Puerto Rico Earthquake Commission, 47 pp.

Dobry, R., Borcherdt, R.D., Crouse, C.B., Idriss, I.M., Joyner, W.B., Martin, G.R., Power, M.S., Rinne, E.E., and Seed, R.B., 2000, "*New Sites Coefficients and Site Classification System used in Recent Building Codes Provisions,*" Earthquake Spectra 16(1), 41-68.

EG&G Geometrics, "*Exploration Seismograph Operator's Manual,*" January 1992.

Environmental Systems Research Institute, Inc. 1996, "*ArcView GIS,*" 380 New York Street, Redlands, CA 92373-8100.

Environmental Systems Research Institute, Inc. 2004, *"Arc GIS Desktop,"* 380 New York Street, Redlands, CA 92373-8100.

Gelabert, P.A., 1968, *"Engineering Geology of Highway Number 2 Between Aguadilla and Mayagüez, P.R.,"* Boletín de la Academia de Artes y Ciencias de Puerto Rico, Tomo IV-Num. 2, San Juan.

Green, R.A., Cameron, W.I., 2003, *"The Influence of Ground Motion Characteristics on Site Response Coefficients,"* 2003 Pacific Conference Earthquake Engineering Paper #90, Department of Civil and Environmental Engineering, University of Michigan, Ann Arbor, MI, USA.

.

Hayashi, K., and Takahashi, T., 2001, *"High Resolution Seismic Refraction Method Using Surface and Borehole Data for Site Characterization of Rocks,"* International Journal of Rock Mechanics and Mining Sciences, Vol. 38.

Hengesh, J.V., and Bachhuber, J.L., 1999, "*Seismic Hazard Zonation of Greater San Juan Area Northern Puerto Rico Coastal Plain,"* Final Technical Report.

Idriss, I.M., 1990, *"Response of Soft Soil Sites During Earthquakes,"* Volume 2, Proceedings: H. Bolton Seed Memorial Symposium, (J.M. Duncan, ed.), University of California, Berkeley, 273 – 289.

Install Shield Software Corporation, 2002, "*DemoShield 7.5*," 900 National Parkway, Suite 125, Schaumburg, Illinois 60173.

International Conference of Building Officials, 1997, *"1997 Uniform Building Code Volume 2: Structural Engineering Design Provisions"*.

Irizarry Padilla, J., 1999, *"Design Earthquakes and Design Spectra for Puerto Rico's Main Cities Based on World Wide Strong Motion Records,"* M.S. Thesis, University of Puerto Rico RUM.

Iwasaki, T., Tokida, K., Tatsuoka, F., Watanabe, S., Yasuda, S., and Sato, H., 1982, *"Microzonation for Soil Liquefaction Potential using the Simplified Model,"* Proceedings of the 3rd International Earthquake Microzonation Conference, Seattle, Washington, pp. 1319-1330.

Koester, J.P., Sharp, M.K., and Hynes, M.E., 2000, *"Technical Bases for Regulatory Guide for Soil Liquefaction,"* USACE NUREG/CR-5741.

Kulhawy, F.H., Trautmann, C.H., Beech, J.F., O'Rourke, T.D., McGuire, W., Wood, W.A., and Capano, C., 1983, *"Transmission Line Structure Foundations for Uplift-Compression Loading,"* Report No. EL-2870, Electric Power Research Institute, Palo Alto, CA.

Llavona, A., 2004, *“Clasificacion de Suelos (UBC-97) del Municipio de Mayagüez,”* Master’s thesis, University of Puerto Rico RUM.

Macari, E.J., 1994, *“A Field Study in Support of the Assessment for Liquefaction and Soil Amplification in Western Puerto Rico,”* Final Document presented to the Puerto Rico Earthquake Safety Commission.

Macari, E.J., 1997, *“Earthquake Hazard Assessment of Western Puerto Rico”*.

Macari, E.J., Hoyos, and L.R., Divakarla, P.K., 2004, *“A Study of Earthquake Induced Liquefaction Potential In Western Puerto Rico Using GIS Technology”*.

Mattson, P.H., 1960, *“Geology of the Mayagüez Area, Puerto Rico,”* Bulletin of the Geological Society of America, Vol. 71, pp. 319-362.

McCann, W. R., 1987, *“Historic Earthquakes and the Earthquake Hazard of Puerto Rico,”* Proceedings of Conference XXXVI, A Workshop on Assessment of Geologic Hazards and Risk in Puerto Rico, May 14-16, 1986, U.S. Department of the Interior Geological Survey, Open File Report, 87-008.

McCann, W.R., 1993, *“Seismic Hazard Map for Puerto Rico,”* Report to the Seismic Safety Commission of Puerto Rico.

McGuiness, C.L., 1946, *“Records of Wells in Puerto Rico,”* U.S. Geological Survey, Study prepared for the Aqueduct and Sewer Service.

Mercado, A., and McCann, W.R., 1998, *“Numerical Simulation of the 1918 Puerto Rico Tsunami,”* Natural Hazards 18, 57-76.

Molinelli, J., 1985, “*Earthquake Vulnerability Study for the Metropolitan Area of San Juan, Puerto Rico,”* Department of Natural Resources, Puerto Rico.

Molinelli, J., 1988, *“Earthquake Vulnerability Study for the Areas of Ponce, Arecibo and Aguadilla, Puerto Rico,”* Department of Natural Resources, Puerto Rico.

Moya, J.C., and McCann, W.R., 1992, *“Earthquake Vulnerability Study of the Mayagüez Area, Western Puerto Rico,”* Presented at “Comisión de Seguridad Contra Terremotos” (Dr. Leandro Rodríguez, president), 43p.

Mueller, C.S., Frankel, A.D., Petersen, M.D., and Leyendecker, E.V., 2004, *“Documentation for 2003 USGS Seismic Hazard Maps for Puerto Rico and the U.S. Virgin Islands,”* U.S. Geological Survey, Golden, CO., Open File Report 03-379.

National Research Council, 1985, *“Liquefaction of Soils during Earthquakes,”* National Academy Press, Washington, D.C.

Odum, J., Williams, R., Stephenson, W., von Hillebrandt, C., Asencio, E., and Cameron, A., *"Near-Surface S- and P-wave Velocities of Geological Formations within Urban Areas and PRSN Stations, Puerto Rico,"* USGS Open File Report, (in preparation).

Pacheco, J.F., and Sykes, L.R., 1992, *"Seismic Moment Catalog of Large Earthquakes, 1900 to 1989,"* Bulleting of the Seismological Society of America 82, 1306-1349.

Pérez, E., 2005 *"Ground Response Spectra at Surface for Mayagüez considering in-situ Soil Dynamic Properties,"* Master's thesis, University of Puerto Rico RUM.

Prentice, C.S., Mann, P., and Burr, G., 2000, *"Prehistoric Earthquakes Associated with a Late Quaternary Fault in the Lajas Valley, Southwestern Puerto Rico,"* Transactions of the American Geophysical Union 81, F 1182 (abstract).

Prentice, C.S., and Mann, P., 2005, *"Paleoseismic Study of the South Lajas Fault: First Documentation of an Onshore Holocene Fault in Puerto Rico,"* Active Tectonics and Seismic Hazards of Puerto Rico, the Virgin Islands, and Offshore Areas, Geoplogical Society of America Special Paper 385, 215-222.

Red Sísmica de Puerto Rico, 2004, *"Terremoto de 1918"*.
http://rmsismo.upr.edu

Redpath, B., 1973, *"Seismic Refraction Exploration for Engineering Site Investigations,"* USACE Technical Report E-73-4.

Reid, H.F., and Taber, S., 1919, *"The Porto Rico Earthquakes of October – November, 1918,"* The Bulletin of the Seismological Society of America. Vol IX. p. 95-127.

Rodríguez-Martínez, J., Santiago-Rivera, L., Guzmán-Ríos, S., Gómez-Gómez, F., and Oliveras-Feliciano, M.L., 2004, *"Surface-Water, Water-Quality, and Ground-Water Assessment of the Municipio of Mayagüez, Puerto Rico, 1999-2002," USGS* Water-Resources Investigations Report 03-4317.

Rodríguez, C.E., and Capacete, J.L., 1988, *"Liquefaction Potential in Puerto Rico,"* Dimensión, Año 2, Vol. 8.

Seed, H.B., and Idriss, I.M., 1971, *"Simplified Procedure for Evaluating Liquefaction Potential,"* Journal of Soils and Foundations Division, ASCE 97(SM9), pp.1249-1272.

Seed, H.B., and Idriss, I.M., 1982, *"Ground Motions and Soil Liquefaction during Earthquakes,"* Earthquake Engineering Research Institute Monograph, Oakland, California.

Sierra del Llano, C.R., 2002, *"On the Geotechnical Exploration Performed at Six Seismic Stations Sites for the Downhole and Direct Seismic Investigation Project, Puerto Rico,"* Jaca & Sierra Testing Laboratories.

Sladen, J.A., Hollander, D', R.D. & Krahn,J., 1985, *"The liquefaction of sands, a collapse surface approach,"* Canadian Geotechnical Journal 22, 564-578.

Sosa, E., and Pando, M., 2004, *"LiquadoPR: Programa para Estimar la Susceptibilidad de Licuación Utilizando las Recomendaciones de NCEER Reporte GEO-03-001,"* Programa de Movimientos Fuertes de Puerto Rico, Universidad de Puerto Rico, Mayagüez, 50 p.

Soske, J.L., 1959, *"The blind Zone Problem in Engineering Geophysics,"* Geophysics 24, 359-365.

Stokoe, K. H., Rix, G. J., and Nazarian, S.,1989, *"In Situ Testing with Surface Waves,"* Proceedings of the 12th International Conference on Soil Mechanics and Foundation Engineering, Rio de Janeiro, Brazil, pp. 331-334.

Sykes, L., McCann, W. R., and Kafka, A., 1982, *"Motion of Caribbean Plate during last Seven Million Years and Implications for Earlier Cenozoic Movements," J. Geophys. Res.* 87, 10656-10676.

Trautmann, C.H., and Kulhawy, F.H., 1987, *"CUFAD-A Computer Program for Compress and Uplift Foundation Analysis and Design,"* Report EL-4540-CMM, Vol. 16, Electrical Power and Research Institute.

Tuttle, M.P., Dyer-Williams, K., Schweig, E.S., Prentice, C., Moya J.C., and Tucker, K.B., 2003, *"Liquefaction Induced by Historic and Prehistoric Earthquakes in Western Puerto Rico,"* Seismological Research Letters.

United States Department of Agriculture Soil Conservation Service, University of Puerto Rico College of Agricultural Sciences, 1969, *"Soil Survey of Mayagüez Area of Western Puerto Rico"*.

USACE, 1995, *"Geophysical Exploration for Engineering and Environmental Investigation," Engineering* Manual EM 1110-1-1802, Washington, DC.

US Census Bureau, Census 2000 Summary File 1, July 2000. http://www.census.gov/population/estimates/puerto-rico/prmunnet.txt

USGS, 2000, *"A Digital Liquefaction Susceptibility Map for the HAZUS Earthquake Loss Estimation of the San Juan Metropolitan Area, Puerto Rico: final document prepared for The Puerto Rico Planning Board,"*.

USGS, 2002, "Water Resources Data for Puerto Rico and the US Virgin Islands,".

Youd, T.L., Idriss, I.M., Andrus, R.D., Arango, I., Castro, G., Christian, J.T., Dobry, R., Liam Finn, W.D., Harder, L.F., Hynes, M.E., Ishihara, K., Koester, J.P., Liao, S.S.C., Marcuson III, W.F., Martin, G.R., Mitchell, J.K., Moriwaki, Y., Power, M.S., Robertson, P.K., Seed, R.B., and Stokoe II, K.H., 2001, *"Liquefaction Resistance of Soils: Summary Report From The 1996 NCEER And 1998 NCEER/NSF Workshops On Evaluation Of Liquefaction Resistance Of Soils,"* Journal of Geotechnical and Geoenviromental Engineering, 817-833.

Youd, T. L., and Perkins, D. M., 1978, *"Mapping of Liquefaction induced Ground Failure Potential," J. Geotech. Engrg. Div.*, ASCE, 104(4), 433–446.

Youd, T.L., 1998, *"Screening Guide for Rapid Assessment of Liquefaction Hazard at Highway Bridge Sites," Technical* ReportMCEER-98-0005, Multidisciplinary Center for Earthquake Engineering Research, State University of New York at Buffalo, Buffalo, NY.

Appendix A

Hydrogeologic Terranes for the City of Mayagüez Developed by Rodríguez-Martínez et al. (2004)

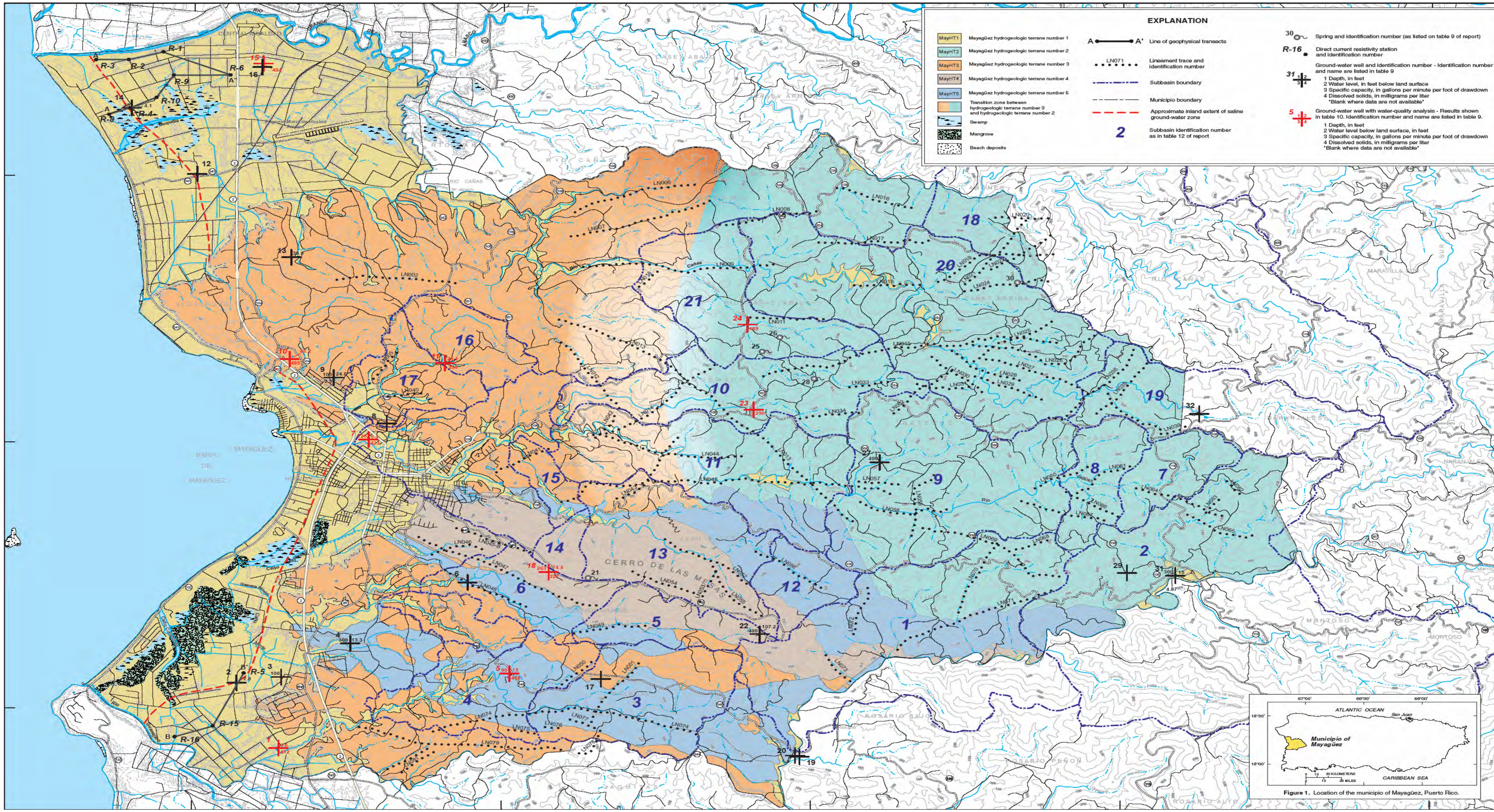

Figure 1. Location of the municipio of Mayagüez, Puerto Rico.